MECHANISM DESIGN FOR FIRST-MILE RIDESHARING

By

ZHEYONG BIAN

A dissertation submitted to the

School of Graduate Studies

Rutgers, The State University of New Jersey

In partial fulfillment of the requirements

For the degree of

Doctor of Philosophy

Graduate Program in Civil and Environmental Engineering

Written under the direction of

Dr. Xiang Liu

And approved by

_____

_____

_____

_____

New Brunswick, New Jersey

October 2020

ABSTRACT OF THE DISSERTATION

MECHANISM DESIGN FOR FIRST-MILE RIDESHARING

By ZHEYONG BIAN

Dissertation Director:

Dr. Xiang Liu

Americans take 11 billion trips annually on public transportation, a 40 percent increase since 1995 (American Public Transportation Association 2016). The $61 billion American public transportation industry faces an ongoing challenge of transit hub accessibility – how travelers get to nearby transit hubs. This challenge is also known as the "*first-mile*" bottleneck. In the United States, many transit riders either drive their own vehicles or take taxis or other emerging mobility services (e.g. Uber and Lyft) to nearby transit hubs. However, uncoordinated traveling does not fully utilize the empty seats in a car. This increases traffic congestion, fuel consumption, emissions, and parking demands. Ridesharing is an effective transportation mode to provide first-mile accessibility to public transit and low-cost, environment-friendly and sustainable mobility service. A key issue is to incentivize passengers for ridesharing participation. This dissertation addresses this problem using Mechanism Design Theory. "Mechanism design" is a field in economics and game theory that designs economic incentives toward desired states by reconciling players' objectives and has been applied in transportation research fields recently.

This dissertation accounts for passengers' personalized requirements for inconvenience attributes in optimizing the vehicle-passenger matching and vehicle routing as well as designing incentive prices for both scheduled and on-demand first-mile ridesharing services. The basic problem studied in the dissertation is that if the designed incentive is able to compensate for the inconvenience cost caused by ridesharing considering passengers' personalized requirements. This dissertation considers multiple incentive objectives to achieve the ultimate goal of maximizing the total social welfare. These incentive objective includes 1) promoting passengers' collaboration to participate in the service (i.e. individual rationality), 2) incentivizing passengers to truthfully report their personalized information (e.g. the maximum willing-to-pay price bidden for the service and personalized requirements on inconvenience attributes) (i.e. incentive compatibility), and 3) incentivizing the service provider to be financially sustainable. In order to obtain the mechanism results for large-scale problems for both scheduled and on-demand service, I develop a novel heuristic algorithm called Solution Pooling Approach (SPA) to optimize the vehicle-passenger matching and vehicle routing plan as well as to calculate the prices. It is proved that SPA is able to sustain the properties of "individual rationality" and "incentive compatibility". Based on the experimental results, I find that SPA is much more efficient in solving large-scale problems compared with the commercial solver (e.g. Branch and Bound) and traditional heuristic algorithms (e.g. hybrid simulated annealing and tabu search) from the literature.

ACKNOWLEDGMENTS

I would like to express my heartiest gratitude and sincere thanks to my advisor, my thesis committee members, funding agencies and industrial collaborators, my friends and lab mates, and my family for supporting me throught my PhD study.

First and foremost, I am extremely grateful to my advisor Dr. Xiang Liu. As a supervisor thoughtout my PhD study, you have provided me with valuable guidance, encouragement, and endless support, as well as many precious opportunities to work on important research topics that are academically challenging and also useful for the transportation engineering. Your talent, vision, passion and wisdom for research and education motivates me to uplift my limit to achieve more. It is a great honor and fortune that I can study, do research, and work under your supervision.

I would like to thank my PhD dissertation committee, Dr. Jie Gong, Dr. Peter J. Jin, and Dr. Jingjin Yu. It is so kind of you to share your tremendous experience and knowledge with me and support me throughout my graduate studies. Your valuable and insightful comments and crucial remarks helped me significantly improve the quality of the dissertation.

I also want to acknolwdge Federal Railroad Administration of the U.S. Department of Transportation, New Jersey Department of Transportation, New Jersey Transit as funding agencies and industrial collaborators in supporting my research.

In addition, I sincerely appreciate my colleagues and the staff at Rutgers University. I am grateful to Dr. Yun Bai, Dr. Zhipeng Zhang, Dr. Kang Zhou, etc., for the

encouragement and support of my graduate studies and also Gina Cullari for your generous help.

Finally, I would like to express my deepest gratitude to my mother (Chunyan Jiang), grandfather (Shouming Jiang) and grandmother (Zhuqing Gu), my dear friends (Bijun Wang, Qi Zhou, Changsheng Huang, etc.) and all other relatives and friends who always love and support me.

TABLE OF CONTENTS

LIST OF TABLES

LIST OF ILLUSTRATIONS

CHAPTER 1 INTRODUCTION

1.1 Background

Americans take 11 billion trips annually on public transportation, a 40 percent increase since 1995 (American Public Transportation Association 2016). The $61 billion American public transportation industry faces an ongoing challenge of transit hub accessibility – how travelers get to nearby transit hubs. This challenge is also known as the "*first-mile*" bottleneck. Several studies have found that travelers' choice of public transportation is significantly affected by the accessibility to transit hubs (Krygsman et al. 2004, Rietveld 2000). In the United States, many transit riders either drive their own vehicles or take taxis or other emerging mobility services (e.g. Uber and Lyft) to nearby transit hubs. However, uncoordinated traveling does not fully utilize the empty seats in a car. This increases traffic congestion, emissions, and parking demands.

Ridesharing is a potential solution to address first- or last-mile transit accessibility, and to provide low-cost, environment-friendly and sustainable mobility service (Furuhata et al. 2013, Cici et al. 2014, Kuhr et al. 2017). There are various types of ridesharing services. Furuhata et al. (2013) classified ridesharing into three categories, carpooling/vanpooling, long-distance ride-match, and dynamic real-time ridesharing based on target markets. Furuhata et al. (2013) indicated that carpooling usually targets on commuters and that users can schedule the service. Long-distance ride-match provides intercity or interstate trips. This service usually requires passengers to schedule the service in advance. Real-time dynamic ridesharing provides an automated process of ride-matching between drivers and passengers on very short notice or even en-route. Thus,

based on the user type, ridesharing can be categorized as scheduled and on-demand services. For scheduled service, passengers send requests early enough (e.g. at least 30 minutes) before they need the service. The system can pre-optimize the matching and routing plan and pre-determine the prices before the service is approaching. For on-demand service, passengers send spontaneous requests when they need the service. The system needs to optimize the matching and routing plan and determine the prices in real time, so that vehicles can be dispatched to serve passengers within a very short time. Ridesharing can also be categorized as targeted and untargeted services. Targeted ridesharing provides the service for specific type of passengers (e.g. commuters, transit riders, etc.). Passengers taking targeted ridesharing service usually have the same destinations (e.g. companies, transit hubs, etc.). Untargeted ridesharing provides the service for any passenger who sends a request. Passengers taking untargeted ridesharing service usually have different destinations. In this dissertation, we focus on scheduled, on-demand, and mixed scheduled and on-demand first-mile ridesharing to the transit hub accounting for its characteristics.

The prior literature has recognized the trend of integrating first-mile ridesharing with public transportation. For example, Shaheen and Chan (2016) discussed that mobile technology and public policy continue to evolve to integrate shared mobility with public transit and future automated vehicles. Masoud et al. (2017a) developed a mobile application with an innovative ride-matching algorithm as a decision support tool that suggests transit-rideshare connection. Stiglic et al. (2018)'s study showed that the integration of a ridesharing system and a public transit system can significantly enhance mobility and increase the use of public transport. Ma (2017) proposed a dynamic bi-modal vehicle dispatching and routing algorithm to address the real-time operating policy of

ridesharing (feeder) services in coordination with the presence of existing public transportation networks. In addition, there is potentially a high demand for the first-mile ridesharing service in transit-intensive metropolitan areas. For example, based on the NYC taxicab data (New York City Taxi, & Limousine Commission 2018), there were 3,122,731 taxi trips to the Pennsylvania Station in New York City in 2017. An average of 8555 taxis traveled to this station every day. Among 3,122,731 taxi trips, 2,189,467 trips (70.1%) had only one passenger per trip. Among these one-passenger trips, approximately 1,509,580 (68.95%) taxi trips are within the same pickup zone and their pickup times are within 10 minutes. These trips might potentially be combined under certain incentive mechanisms for ridesharing. Ridesharing emerges as an efficient way to better coordinate the travels in order to reduce vehicle-miles to the transit hub. Also, ridesharing service providers (e.g. Uber and Lyft) have already added public transportation to their apps, allowing for seamless transfers from their ridesharing to the public transit services for convenient multi-modal journeys (Shelton 2016, Smartrail world 2016 and 2018) in New York, Boston, Los Angeles, and other metropolitan cities around the world. This market of emerging multi-modal first-mile ridesharing service inspires us to design mechanisms to incentivize more passengers for ridesharing participation.

1.2 Methodology

Mechanism design theory (Hurwicz and Reiter 2006) is a field in economics and game theory that designs economic mechanisms or incentives toward desired objectives. The ridesharing mechanism design consists of three major elements: 1) Passengers' personalized mobility information (θ); 2) Transportation modeling function (d), and 3)

Incentive function (t) (Figure 1.1). Let P_i denote the i^{th} request, which may have one or multiple passengers. The information of each request (θ_i) includes the location (l_i), the public transit to take (DL_i, a deadline of arriving at the transit hub imposed by the public transit schedule), non-inconvenience values NIV_i (the maximum willing-to-pay price for direct transport without inconvenience), inconvenience disvalues IDV_i (reduced maximum willing-to-pay prices due to detour, extra waiting time, etc.). We say a decision rule d (passenger matching and vehicle routing) is efficient if the social welfare is maximized (Parkes et al. 2001). The social welfare for first-mile ridesharing is passengers' cumulative values and the service provider's value (Parkes et al. 2001). A passenger request's value V_i is represented by her maximum willing-to-pay price. The service provider's value can be defined as the transportation cost that needs to be covered. Let $X = d(\theta)$ represent an optimal vehicle-passenger matching and routing obtained by the efficient decision rule X = argmax $\sum_{i \in P} V_i - TC$, where TC is the service provider's transportation cost. The third element is the incentive function. Let $p_i = t_i(X, \theta)$ denote the function of incentives provided to a specific passenger request. In practice, the incentive typically takes the form of customized pricing discount. In addition, other types of incentives (e.g., free trips, bonus points, and credits) can also be used to promote ridesharing. In this research, I will **primarily focus on pricing as the main form of incentive function** due to its ease of implementation. In the future, I will consider other non-monetary incentives.

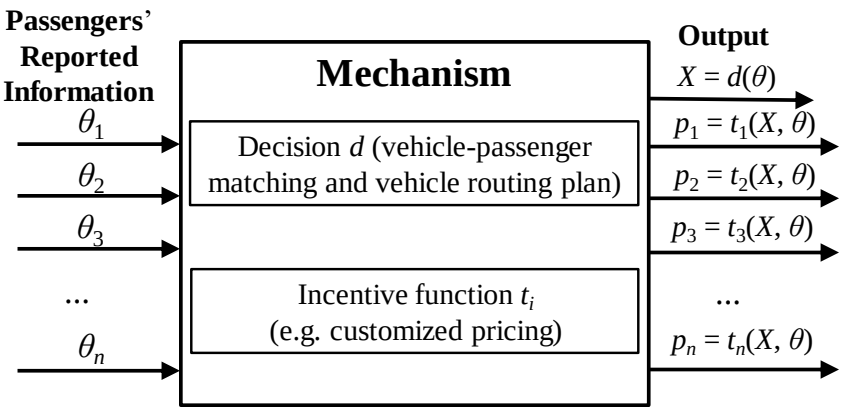

Figure 1.1. Ridesharing Mechanism Design Illustration

The proposed dissertation consists of two basic layers, which are the **transportation network modeling layer** (layer 1) and the **incentive design layer** (layer 2). The incentive design layer interacts with transportation network modeling, $p_i = t_i(X, \theta)$; thus, price "p_i" is determined by the optimization results $X = d(\theta)$, where θ is passengers' reported information regarding their individual mobility preferences and needs. The interaction between the two layers elicits the property of "customizability." For instance, if a passenger increases the service requirement (e.g., less detour), the system will adjust the matching and routing plan so that she will have higher-quality service with a higher price, and vice versa.

Layer 1- Transportation Network Modeling

The transportation network modeling layer is implemented to solve the **Vehicle Routing Problem with Time Constraints (VRPTC)** based on the input information, such as passenger locations, requested times, the kind of public transit hub and schedule, maximum willing-to-pay price for direct transport, maximum tolerable detours and extra waiting time, vehicle locations, etc.

Let P denote the locations of passenger requests, V represent the set of real-time vehicle locations, and H denote the location of transit hub(s). Let $PV = P \bigcup V$ and $PT = P \bigcup H$. Let x_{ij}^k ($k \in V, i \in PV, j \in PT$) and y_i^k ($k \in V, i \in P$) represent decision variables. If vehicle k travels from location i to location j, $x_{ij}^k = 1$, otherwise, $x_{ij}^k = 0$. If vehicle k picks up passenger(s) in request i, $y_i^k = 1$, otherwise, $y_i^k = 0$. Let X denote the collection of all decision variables, representing a vehicle-passenger matching and vehicle routing plan. For transportation network modeling, the objective function can maximize the total social welfare, which is the summation of all passengers' values minus the transportation cost that the service provider covers: $\max f(X) = \sum_{i \in P} V_i(X) - TC(X)$, where $V_i(X)$ is Passenger(s) i's value and $TC(X)$ is the service provider's transportation cost given the matching and routing plan X. The constraints include:

1) Vehicle capacity, in which the number of riders in a vehicle should not exceed its capacity: $\sum_{i \in P} y_i^k np_i \le Q_k$, for all $k \in V$, where np_i is the number of passengers in request i and Q_k is vehicle k's capacity.

2) Passenger deadlines: the matching and routing plan should ensure that the vehicle can arrive at the transit hub before the deadline, which should be some time before the transit departure time (for example, arriving at the transit hub 10 minutes earlier for ticket purchase): $\sum_{i \in PV} \sum_{j \in PT} x_{ij}^k t_{ij} + \sum_{i \in P} y_i^k pt_i \le RT$, for all $k \in V$, where t_{ij} is the travel time from location i to location j and pt_i is pickup time for Passenger(s) i, and RT is the remaining time to the deadline.

3) Vehicle flow constraints: one passenger should be served by at most one vehicle, and other constraints such as flow-in and flow-out should be balanced, sub-tour should be

eliminated, etc.

Layer 2 –Incentive Design

In achieving a lower cost, long-term sustainable, and valuable first-mile ridesharing service, a special emphasis of my framework in achieving certain objectives is on (i) promoting shared trips, (ii) incentivizing truthfully reported information, (iii) incentivizing the service provider to be financially sustainable. Incentive design is used to promote cooperative behavior between passengers and the ridesharing service.

Incentive 1: Promoting shared trips. The designed pricing scheme provides incentives to promote the cooperation of passengers to share trips. The incentive (e.g. price discount) should be able to compensate for passengers' disvalues of inconvenience factors (e.g. detour and extra waiting time) caused by ridesharing. This induces the property of "**individual rationality**" – passengers' prices should not be greater than their maximum willing-to-pay prices, $U_g = V_g - p_g \geq 0$, where U_g is Passenger(s) g's non-negative utility (defined as the difference between the maximum willing-to-pay price and the actual paid price, Kamar and Horvitz 2009), V_g is Passenger(s) g's value (maximum willing-to-pay price), and p_g is the actual price.

Incentive 2: Incentivizing to truthfully report information. Passengers may manipulate the system to maximize their utility by misreporting their mobility preference information on purpose. For example, misreporting a low maximum willing-to-pay price on purpose in order to have a low price will impair the optimization of the matching and routing plan and the service provider's benefit. The designed mechanism will **incentivize the truthful solicitation** of passenger information. This induces the property of "**incentive compatibility**" – where truthfully reporting the personalized mobility preference is

passengers' optimal strategy. I give an example of incentive compatible pricing. Consider Passenger(s) g: if the price is given by $p_g = g(X_{g^-}^*) - (f(X^*) - V_g(X^*))$, and then Passenger(s) g's utility is defined as $U_g = V_g(X^*) - p_g = f(X^*) - g(X_{g^-}^*)$, where X^* is the optimal solution of the efficient decision ($X^* = d(\theta)$, when the social welfare is maximized) in the transportation network modeling layer and $f(.)$ is an objective function of the decision rule, $X_{g^-}^*$ is the optimal solution of a model (denoted as model M_g) that is independent of Passenger(s) g's report, and $g(.)$ is the objective function of the model. This can ensure that the mechanism is incentive compatible. Regardless of what Passenger(s) g reports, $g(X_{g^-}^*)$ remains constant, because $g(X_{g^-}^*)$ is independent of Passenger(s) g's report. If she misreports her information, X^* may no longer be efficient, indicating that the social welfare $f(X^*)$ will suffer from a decrease caused by her misreporting. Thus, her utility $U_g = f(X^*) - g(X_{g^-}^*)$ will decrease as well. Therefore, truthful reporting is passengers' optimal strategy. Other properties can also be considered when designing the models M_g. For example, if the condition $g(X_{g^-}^*) \leq f(X^*)$ is always satisfied, the mechanism is also individual rational for all passengers.

Incentive 3: Incentivizing the service provider to be financially sustainable. The designed mechanism needs to incentivize the service provider to continually provide the service without a financial deficit. The collected prices from passengers should be able to cover the service providers' transportation cost, including the fuel consumption cost, driver labor cost, etc. Mathematically, the condition $\sum_{g \in P} p_g - TC(X_0^*) \geq 0$ should be satisfied.

1.3 Contents of this Dissertation

The remaining content of the dissertation is summarized as follows

Chapter 2. This chapter reviews related work on mechanism design for ridesharing. Based on the reviewed references, I identify the knowledge gaps and introduce the intended contributions of this dissertation.

Chapter 3. This chapter designs a mechanism for the first-mile ridesharing service. The mechanism accounts for passengers' personalized requirements on different inconvenience attributes (e.g. the number of co-riders, extra in-vehicle travel time, and extra waiting time in the transit hub) of the service in determining the optimal vehicle-passenger matching and vehicle routing plan and customized pricing scheme. The proposed mechanism is proved to be individual rational, incentive compatible, and price non-negative. The three properties respectively indicate that passengers are willing to participate in the service, that honestly reporting personalized requirements is the optimal strategy, and that the service provider is guaranteed to receive revenue from the participants. A case study is proposed to interpret the mechanism and to demonstrate the generality of the personalized-requirement-based mechanism that can be adapted into different scenarios.

Chapter 4. In order to address the computational challenge of obtaining the mechanism for large-scale transportation networks, this chapter develops a novel heuristic algorithm, called the Solution Pooling Approach (SPA) for efficiently solving large-scale mechanism design problems in the first-mile ridesharing context. This chapter also extends the SPA to solve generalized mechanism design problems, analyzes specific circumstances under which SPA can sustain the game-theoretic properties, including "individual rationality" and "incentive compatibility", and identifies its limitation. For the particular

application in the first-mile ridesharing, SPA maintains the properties of "individual rationality" and "incentive compatibility". SPA is computationally efficient because it simultaneously solves vehicle-passenger matching and vehicle routing problem and calculates the prices for all individuals. Numerical experimental results show that SPA can address the complex first-mile ridesharing service mechanism design problem in a computationally viable and efficient manner.

Chapter 5. This chapter studies the mechanism design problem for on-demand first-mile ridesharing and proposes a novel mechanism, namely "Mobility-Preference-Based Mechanism with Baseline Price Control" (MPMBPC), which adapts the traditional Vickrey-Clarke-Groves (VCG) mechanism and incorporates a baseline price control component. MPMBPC is proved to satisfy several important mechanism design properties, including "individual rationality", "incentive compatibility", "price controllability", and "detour discounting reasonability". In comparison with the traditional general-purpose VCG mechanism, MPMBPC can avoid unreasonably low prices and prevent carriers' deficits. A computationally efficient heuristic algorithm called Solution Pooling Approach (SPA) is developed to solve large-scale ridesharing mechanism design problems. Numerical examples are developed to demonstrate that SPA can solve large-scale ridesharing mechanism design problems in a computationally efficient way, with satisfactory solution qualities.

Chapter 6. This chapter draws the conclusions of the dissertation and introduces the potential future work.

CHAPTER 2 LITERATURE REVIEW

2.1 Existing Work

Much prior work has focused on the optimization of vehicle-passenger matching and vehicle routing for ridesharing service. Different models and algorithms (e.g. mixed integer programming, Lagrangian column generation, genetic heuristic algorithm, particle swarm optimization) were developed for the optimization of matching and/or routing plans for scheduled services (Baldacci et al., 2004; Calvo et al., 2004; Yan and Chen, 2011; Armant and Brown, 2014; Huang et al., 2015, 2017, 2018; Chou et al., 2016; Fan et al., 2018; Jiau et al., 2018; Hou et al., 2018). In addition, optimization of dynamic ridesharing services has also been studied (Ma, 2017; Agatz et al., 2011; Wang et al., 2017; Ghoseiri et al., 2011; Jung et al., 2016; Di Febbraro et al., 2013; Masoud and Jayakrishnan, 2017a,b; Bian and Liu, 2017) using re-optimization algorithms (e.g., insertion heuristic and rolling horizon strategy) to dynamically adjust the matching and routing plan in real time, based on updated information.

While the transportation community has focused on transportation network modeling of ridesharing, economists have focused more on incentive mechanism design for promotion of passengers' and/or drivers' cooperation. There exist many mechanisms in the literature, such as supply-demand-balance mechanisms, fair cost-sharing mechanisms, optimization mechanisms, etc. The supply-demand-balance mechanism, which is widely used in taxi service (Yang et al., 2002; Zhang and Ukkusuri, 2016; Qian and Ukkusuri, 2017), adjusts the price to balance the supply and demand. Witt et al. (2015), Banerjee et al. (2015), Fang et al. (2016), Liu and Li (2017) applied and modified this pricing strategy to adapt into ridesharing service. When customers' demand exceeds supply, the price is

increased to re-balance the demand and supply, and vice versa. Ridesharing companies, such as Uber and Lyft, use this pricing framework to incentivize drivers to move to undersupplied locations (Hall et al., 2015). Fair cost-sharing mechanism fairly allocates costs among participants based on different travel attributes, such as travel distance, detour, and waiting time (Lu, 2014; Bistaffa et al., 2015; Gopalakrishnan et al., 2016; Li et al., 2016; Wang et al., 2018; Chen et al., 2018; Bian and Liu, 2018a). Optimization mechanisms optimize passengers' prices and matching and routing plan simultaneously to achieve certain objectives, such as maximizing the total profit, minimizing passengers' total travel cost, and maximizing the total saved travel mileage (Cheng et al., 2012; Biswas et al., 2017a,b; Santos and Xavier, 2015; Qian et al., 2017). These mechanisms do not consider different passengers' valuations of the service when there is a shortage of vehicle fleet size in the on-demand scenario so that not necessarily all passengers can be served within a short time.

The auction-based mechanisms, which are more related to the scope of this dissertation, aim to maximize the society's overall welfare, which is usually defined as riders' cumulative values minus the service provider's total cost (Ma et al., 2018), by incentivizing participants to truthfully report their valuations (e.g. maximum willing-to-pay price) of the service. The VCG mechanism is one widely used mechanism of this type (Vickrey, 1961; Clarke, 1971; Groves, 1973). Several researchers developed VCG-based mechanisms for scheduled ridesharing service, in which riders book the service in advance. For example, Zhao et al. (2014) developed an incentive mechanism for scheduled ridesharing service with a deficit control. Zhao et al. (2015) considered the uncertainty, whether passengers would undertake the trip after sending requests, in their mechanism for

ridesharing organization. Nguyen (2013) and Cheng et al. (2014) proposed multiple auction-based mechanisms for the last-mile ridesharing service. Zheng et al. (2019) proposed a greedy and a ranking approach to the order dispatch and pricing strategies to achieve their individual rational and truthful auction-based mechanism. Hsieh et al. (2019) proposed a driver-passenger double side auction mechanism for carpooling systems and developed a particle swarm optimization algorithm to solve the problem. Auction-based mechanisms for on-demand (dynamic) ridesharing have also been studied by several researchers. For example, Kleiner et al. (2011) proposed a parallel auction-based mechanism for real-time ridesharing service, but the mechanism is limited to a single passenger assignment per vehicle. Kamar and Horvitz (2009) determined the local VCG payments among the agents that share the same vehicle instead of all agents requesting the service. Luo (2019) proposed a two-stage approach to ridesharing assignment and auction in a crowdsourcing collaborative transportation platform. The auction-based mechanisms proposed by Zhang et al. (2017 and 2018) are truthful, budget balanced (i.e. the payment offsets the cost), computationally efficient, and individual rational (passengers are willing to participate in the service and pay the prices). Asghari et al. (2016) and Asghari and Shahabi (2017) developed driver-bidding auction-based mechanisms for real-time ridesharing. Karamanis et al. (2019) developed a passenger-driver double-side auction mechanism to dynamically determine the assignment and pricing plan of shared rides in ride-sourcing. Zhang et al. (2016), Masoud and Lloret-Batlle (2016), Lloret-Batlle et al. (2017), and Masoud et al. (2017b) developed mechanisms for peer-to-peer dynamic ridesharing to promote ridership and user permanence. Shen et al. (2016) developed an

online mechanism for ridesharing in autonomous mobility-on-demand systems. Ma et al. (2018) proposed a spatio-temporal pricing mechanism for dynamic ridesharing platforms.

All existing work is summarized in Table 2.1.

Table 2.1 Existing Work

Mechanisms	References
Optimization of vehicle-passenger matching and vehicle routing	Baldacci et al., 2004; Calvo et al., 2004; Yan and Chen, 2011; Armant and Brown, 2014; Huang et al., 2015, 2017, 2018; Chou et al., 2016; Fan et al., 2018; Jiau et al., 2018; Hou et al., 2018; Ma, 2017; Agatz et al., 2011; Wang et al., 2017; Ghoseiri et al., 2011; Jung et al., 2016; Di Febbraro et al., 2013; Masoud and Jayakrishnan, 2017a,b; Bian and Liu, 2017
Supply-demand-balance mechanisms	Witt et al., 2015; Banerjee et al., 2015; Fang et al., 2016; Liu and Li, 2017
Fair cost-sharing mechanism	Lu, 2014; Bistaffa et al., 2015; Gopalakrishnan et al., 2016; Li et al., 2016; Wang et al., 2018; Chen et al., 2018; Bian and Liu, 2018a
Pricing optimization mechanisms	Cheng et al., 2012; Biswas et al., 2017a; Santos and Xavier, 2015; Qian et al., 2017
Auction-based mechanisms	Zhao et al., 2014; Zhao et al., 2015; Nguyen, 2013; Cheng et al., 2014; Hsieh et al., 2018; Kleiner et al., 2011; Kamar and Horvitz, 2009; Zhang et al., 2017; Zhang et al., 2018;

	Asghari et al., 2016; Asghari and Shahabi, 2017; Zhang et al., 2016; Masoud and Lloret-Batlle, 2016; Lloret-Batlle et al., 2017; Masoud et al., 2017b; Shen et al., 2016; Ma et al., 2018

2.2 Knowledge gaps

To our knowledge, very little prior research addressed the incentive mechanism design for first-mile ridesharing with respect to public transit accessibility. First-mile ridesharing has four characteristics. 1) All passengers have the same destination (i.e., the transit hub); 2) Passengers may have a strict deadline for arriving at the transit hub; 3) Passengers can schedule the first-mile ridesharing service in advance if they know their transit schedules (particularly for commuters);

Very limited prior research accounted for passengers' personalized requirements on inconvenience factors (e.g. detour) caused by ridesharing in optimizing the vehicle-passenger matching and vehicle routing plan as well as designing customized incentive price simultaneously. The interactive relationship among passengers' personalized requirements, optimization of matching and routing plan, and incentive pricing scheme has not been well studied in the literature. In summary, the problem if the designed incentive is able to offset the inconvenience caused by ridesharing is rarely considered in the literature.

Existing research developed algorithms to solve small-scale or simplified mechanism design to circumvent the computational complexity. Very little research has addressed large-scale complex dynamic ridesharing mechanism design problems with

solution algorithms that is computationally efficient and can simultaneously satisfy important above-mentioned mechanism design properties (e.g. "individual rationality" and "incentive compatibility").

2.3 Intended Contributions

Based on the identified knowledge gaps, this dissertation brings the following contributions.

- This dissertation is first to account for passengers' personalized requirements for inconvenience attributes in optimizing the vehicle-passenger matching and vehicle routing as well as designing incentive prices for both scheduled and on-demand first-mile ridesharing services.

- This dissertation considers multiple incentive objectives to achieve the ultimate goal of maximizing the total social welfare in this dissertation, which is defined as the passengers' cumulative value minus the service provider's transportation cost. These incentive objective includes 1) promoting passengers' collaboration to participate the service, 2) incentivizing passengers to truthfully report their personalized information (e.g. the maximum willing-to-pay price bidden for the service and personalized requirements on inconvenience attributes), 3) incentivizing the service provider to be financial sustainable.

- In order to obtain the mechanism results for large-scale problems, I develop a novel heuristic algorithm called Solution Pooling Approach (SPA) to optimize the vehicle-passenger matching and vehicle routing plan as well as to calculate the prices for both scheduled and on-demand service. It is proved that SPA is able to sustain the properties of "individual rationality" and "incentive compatibility".

CHAPTER 3 MECHANISM DESIGN FOR SCHEDULED FIRST-MILE RIDESHARING

3.1 Introduction

The proposed mechanism includes an optimal vehicle-passenger matching and vehicle routing plan and a customized pricing strategy. The matching and routing plan determines each passenger's personalized first-mile ridesharing service. The customized pricing strategy provides passengers with economic incentives to participate in ridesharing by offsetting the inconvenience caused by ridesharing. Our designed mechanism allows passengers to detail their personalized requirements on the following so-called "inconvenience factors", 1) extra in-vehicle travel time (for example, detour to pick up other passengers), 2) the number of co-riders sharing the vehicle, and 3) extra waiting time in the transit hub due to possible early arrival. Previous studies (Golledge et al. 1994, Ben-Akiva and Lerman 1985, Arentze 2013) recognized that travelers' choice of transportation mode is not only influenced by price but also by these "inconvenience" attributes. The methodology can be adapted to account for additional factors in future research. The proposed mechanism can promote passengers' participation by ensuring an important property, "individual rationality", which indicates that passengers' maximum willing-to-pay prices will never be exceeded by the actual paid prices. In addition, rational passengers may misreport their personalized requirements in order to maximize their utilities if the mechanism cannot prevent this. Thus, the designed mechanism needs to ensure another important property, namely "incentive compatibility", representing that truthfully reporting the requirement is each passenger's optimal strategy that maximizes the utility. This property can prevent passengers from misreporting their personalized requirements.

Moreover, the price is non-negative so that the service provider can gain revenue from passengers. Finally, a case study is proposed to interpret the mechanism and to demonstrate the effectiveness of the proposed mechanism.

This chapter is structured as follows. We identify knowledge gaps and research needs in Section 3.2. Then, we introduce our designed mechanism in Section 3.3. In Section 3.4, a case study is proposed to interpret the potential application of the proposed mechanism. Concluding remarks are made in Section 3.5.

3.2 Knowledge Gaps and Intended Contributions

To our knowledge, very little prior research addressed the incentive mechanism design for first-mile ridesharing with respect to public transit accessibility. First-mile ridesharing has four characteristics. 1) All passengers have the same destination (i.e., the transit hub); 2) Passengers may have a strict deadline for arriving at the transit hub; 3) Passengers can schedule the first-mile ridesharing service in advance if they know their transit schedules (particularly for commuters); 4) In addition to the number of shared riders and extra in-vehicle travel time, the first-mile ridesharing imposes passengers another potential inconvenience factor, extra waiting time at the transit hub due to early arrival, if passengers served by the same vehicle have different arrival deadlines.

Very limited prior research accounted for passengers' personalized requirements on inconvenience factors (e.g. extra in-vehicle travel time, number of shared riders, and additional waiting time) caused by ridesharing in optimizing the vehicle-passenger matching and vehicle routing plan as well as designing customized incentive price simultaneously. The interactive relationship among passengers' personalized requirements,

optimization of matching and routing plan, and incentive pricing scheme has not been well studied in the literature.

This chapter intends to make the following contributions.

- This chapter identifies some potential inconvenience factors of scheduled first-mile ridesharing service, including the number of shared riders, extra in-vehicle travel time due to detour, and extra waiting time at the transit hub due to early arrival.
- We present the first work to design an incentive mechanism based on passengers' personalized requirements on these inconvenience attributes by simultaneously optimizing the vehicle-passenger matching and vehicle routing plan and designing a corresponding customized pricing scheme. As Figure 3.1 shows, this designed mechanism accounts for the interactive relationship among passengers' personalized requirements, optimization of matching and routing plan, and incentive pricing scheme. Passengers' personalized requirements affect the values of the inconvenience factors in optimizing the matching and routing plan. Customized incentive pricing scheme, which is determined by the matching and routing plan, promotes passengers' participation by offsetting their inconvenience and truthful report of their personalized requirements.
- The incentive mechanism is proved to have the properties of "individual rationality" and "incentive compatibility". It indicates that the mechanism is able to promote rational passengers' participation willingness and also to prevent passengers from manipulating the algorithm.

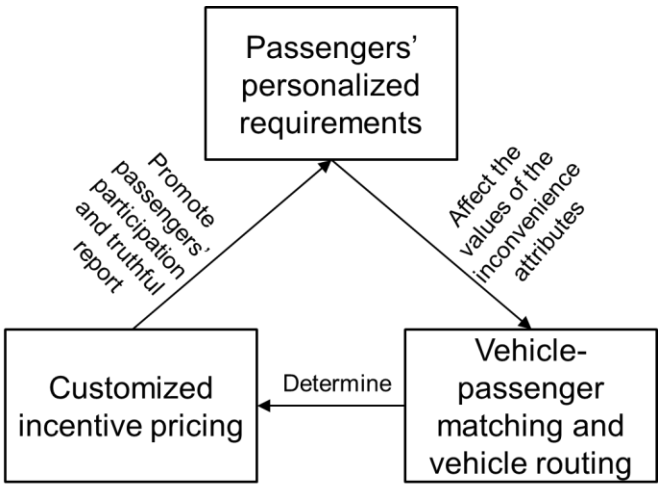

Figure 3.1 Inhenrent Mechansim

3.3 Mechanism Design Model

This section introduces a ridesharing incentive mechanism based on passengers' personalized requirements. Subsection 3.3.1 introduces the problem statement, 3.3.2 analyzes passengers' value and utility when they participate in the service, 3.3.3 clarifies the objective of the proposed mechanism using an optimization model, 3.3.4 introduces how the mechanism is obtained, and 3.3.5 gives the proofs of the propositions.

3.3.1 Problem Statement

Passengers can schedule the first-mile ridesharing service in advance. All passengers have the same destination (i.e. the transit hub) to catch their next transit mode (e.g. trains). The service provider, which can be the transit agency or a ridesharing service provider collaborating with the transit agency, has sufficient available vehicles that can provide the first-mile accessibility service. Individual passengers may have different preferred times of arrival. Some people may prefer to arrive much earlier than the

scheduled train departure time, while others enjoy arriving right on time to catch a train. Thus, our mechanism allows passengers to specify their preferred arrival deadlines at the transit hub. Passengers with close arrival deadlines are likely to share a ride. Vehicles must drive these passengers to the transit hub before the specified deadlines. For example, if Mike wants to take the train with the departure time of 9:00 am, and the train that John will take departs at 9:10 AM. Mike wants to arrive at the transit hub on time and thus he specifies 8:50 AM as his arrival deadline. John wants to arrive at the transit hub 25 minutes earlier for breakfast and his arrival deadline is 8:45 AM. If John and Mike share the ride, the vehicle must arrive at the transit hub before 8:45 AM.

We use Figure 3.2 to demonstrate the operation of the first-mile ridesharing service. The system consolidates passengers' requests with close arrival deadlines. When a passenger schedules the service, he/she is notified of an estimated time window for pickup and a range of trip fare. The time window can be estimated based on passengers' reported arrival deadlines and personalized requirements on extra in-vehicle travel time and extra waiting time at the transit hub. For example, suppose that a passenger's arrival deadline is DL_i, the shortest time for driving this passenger to the transit hub is t_{i0}. Then the latest pickup time is $DL_i - t_{i0}$. If this passenger's maximum tolerable extra in-vehicle travel time and extra waiting time at the transit hub are α_i^{IVT} and α_i^{WT}, respectively, then the earliest pickup time is $DL_i - t_{i0} - \alpha_i^{IVT} - \alpha_i^{WT}$. The range of the trip fare can be estimated by historical prices as Uber does. The interface can also show the real-time taxi price in the market. The final price will never exceed this taxi price. When the service is approaching (at time *ts* in Figure 3.2), the system optimizes the vehicle-passenger matching and vehicle routing plan, and calculates the customized prices. The request processing time point (*ts*) should be early

enough so that all passengers can be driven to the transit hub before their arrival deadlines. After the requests are processed, each passenger will be notified of the vehicle that will serve him, the exact pickup time, and the exact price, which are determined by our mechanism (the matching and routing plan and the pricing scheme). The drivers will be directed to pick up passengers in a specified order and drive them to the transit hub before the earliest arrival deadline.

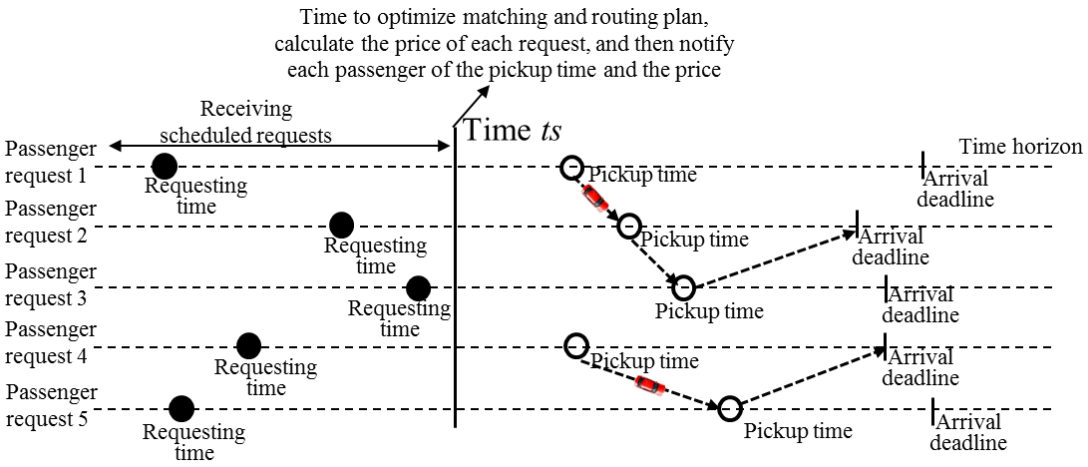

Figure 3.2 Operation of the First-Mile Ridesharing Service

In addition to the passengers' pickup locations and preferred arrival deadlines, passengers are allowed to report their personalized mobility requirements on different inconvenience factors. In this chapter, "*inconvenience factors*" include 1) the number of co-riders, 2) extra in-vehicle travel time beyond the direct shipment time due to detour, and 3) extra waiting time at the transit hub due to possible early arrival. Golledge et al. (1994), Ben-Akiva and Lerman (1985), and Arentze (2013) recognized that travelers' choice of transportation mode is influenced not only by price but also by these "inconvenience"

attributes. After the system receives the passengers' information, an optimal vehicle-passenger matching and vehicle routing plan is generated based on the personalized requirements. The price is then obtained based on the plan and passengers' reported personalized requirements. Passengers will finally receive a personalized service and customized price. The personalized service is tailored to satisfy passengers' requirements on the inconvenience attributes of the first-mile trip and the customized price is used to incentivize them to participate in the first-mile ridesharing service.

In this chapter, it is assumed that each passenger's objective is to maximize their own utility (defined as the difference between the maximum willing-to-pay price and the actual paid price). It is possible that passengers may misreport their requirements on inconvenience factors if lying is more beneficial for them. A desirable property of the pricing mechanism is that expressing the true requirements is the passenger's "best" strategy (i.e. the utility is maximized) regardless of what other passengers report. This property is called "*incentive compatibility*" in the literature (Myerson 1979). Passengers' behavioral rationality also implies that if the price is higher than their maximum willing-to-pay price, they are unlikely to participate in the ridesharing service. Thus, another indispensable property, "*individual rationality*", is that each passenger should always receive non-negative utility with respect to the price charged. This property aims to ultimately incentivize more travelers to participate in the ridesharing service. Moreover, the service provider must receive payment from each passenger (i.e. the price is non-negative). In summary, the proposed mechanism needs to have the three important properties, "incentive compatibility", "individual rationality" and "price non-negativity".

Based on the problem background, we will determine the mechanism, denoted as $M(X, \mathbf{p})$, consisting of a vehicle-passenger matching and vehicle routing plan X and all passengers' customized prices $\mathbf{p} = \{p_1, p_2, \ldots, p_n\}$.

The following assumptions are made, in line with the scope of the study.

1) We focus on a static case where passengers' information is known in advance. The ridesharing market has placed demand on pre-scheduled optimization. For example, Uber and Lyft have developed APPs that allow passengers to send pre-scheduled request for car usage. In this chapter, we only optimize the vehicle task execution plan for the passengers who send request before vehicles start to execute the task. In a dynamic scenario, passengers are likely to send requests after the static optimization process is finished, the system can re-optimize all decisions to accommodate spontaneous demands. However, the dynamic scenario for spontaneous passengers is beyond the scope of this study but will be considered in our future research.

2) The travel time between two locations is assumed to be deterministic. Future research will incorporate travel time reliability in the optimization analysis.

3) The fleet size is sufficient to serve all passengers who send requests in advance, and all passengers who send requests will receive the service. The number of passengers in each request does not exceed the seat capacity of a vehicle. Future research will consider fleet shortage given an extraordinarily large ridesharing demand.

4) We assume that passengers will not misreport other travel information such as the departure locations, the destination (the transit hub) and the arrival deadlines.

Before we detail the mathematical formulation of the mechanism design, we will

use a simple hypothetical example to explain the goal of the research. In this illustrative example, three passengers, named "John", "Peter" and "Alice", in three different locations, book the ridesharing service to get to the train station. The transportation cost and the travel time between each two locations as well as the pickup time span at each location are known in advance. For illustration convenience, the transportation cost (c_{ij}) between two locations is defined as the Euclidean distance (d_{ij}) with one dollar per mile. The travel time (t_{ij}) between two locations is three times the Euclidean distance $t_{ij} = 3d_{ij}$. Note that this illustrative example uses Euclidean distance only for simplification in order to demonstrate how the mechanism is obtained. Our mechanism design model does not assume that the travel distance between two locations should be Euclidean distance. After the vehicle reaches each passenger's location, the vehicle needs some time to pick up the passenger(s). We set the pickup time span as two minutes (pu_j =2) in this example. The coordinate of the transit hub location is set to be (0, 0). The arrival deadlines are determined by the selected train they will catch at the transit hub. We also introduce the taxi service (direct shipment without shared riders) for passengers' alternative first-mile travel mode. The price of the taxi service is \$5 for the first mile and increases \$1.5 per each additional mile. The available information based on the problem setting is listed in Table 3.1.

Table 3.1 Information for the Illustrative Example

Parameters	Passengers		
	John	Peter	Alice
Location coordinates	(2, 2)	(2.6, 2.3)	(3, 2.8)
$V^i_{\max} = 5 + 1.5 \times \max(d_{i0} - 1,\ 0)$ (taxi price, in	7.74	8.71	9.66

dollars)			
Time of direct shipment ($t_{i0} = 3 \times d_{i0}$)	8.485	10.414	12.311
Arrival deadlines	13:00 pm	13:10 pm	13:00 pm

Passengers can report their personalized requirements. In this example, we assume that they can report the maximum in-vehicle travel time, the maximum number of co-riders, and the maximum waiting time at the transit hub that they can tolerate. Suppose that their real requirements are given in Table 3.2.

Table 3.2 Passengers' Personalized Requirements

Tolerances	Passengers		
	John	Peter	Alice
Maximum in-vehicle travel time (minutes)	10	15	20
Maximum number of shared riders	3	3	2
Maximum waiting time at the transit hub (minutes)	10	15	8

The problem is how to determine the matching and routing plan and price for each passenger, accounting for passengers' personalized mobility requirements. The proposed mechanism should be able to incentivize passengers to participate in the ridesharing service instead of taking taxi service. Besides, the designed mechanism should force passenger to truthfully report their preferences instead of lying. The results of the mechanism for this

example will be displayed in Subsection 3.3.4.

3.3.2. Passengers' Value Function and Utility Function

The value function, which reflects passengers' maximum willing-to-pay prices, is used to model passengers' participating willingness considering their personalized requirements on inconvenience attributes. The utility is defined as the net value, which is the maximum willing-pay price minus the actual paid price. This chapter assumes that rational passengers' objective is to maximize their utilities. Before introducing the value and utility functions, we list the notations in Table 3.3.

Table 3.3 Notations in the Value Function and Utility Function

Notations	Descriptions
i	Index of passenger requests. There can be more than one passenger in each request. For denotation convenience, we let "passenger(s) i" represent the passenger(s) in request i.
NR_i	Number of co-riders with passenger(s) i.
IVT_i	Passenger(s) i's in-vehicle travel time.
WT_i	Passenger(s) i's extra waiting time at the transit hub, i.e. the time interval between the arrival time and the deadline DL_i (see Table 3.4).
α_i^{NR}, α_i^{IVT} and α_i^{WT}	Passenger(s) i's personalized requirements on the number of shared riders, extra in-vehicle travel time that exceeds the direct shipment time, and extra waiting time at the transit hub, respectively. The three parameters are obtained from passengers' reported information.
C_i^{ICN}	Passenger(s) i's inconvenience cost caused by ridesharing. The

	inconvenience cost is measured as each passenger's acceptable minimum reduced price with the specific degree of inconvenience factors.
X	A vehicle-passenger matching and vehicle routing plan.
$V_i(X)$	Passenger(s) i's value gained from the ridesharing service given a plan X. V_i can also be interpreted as the maximum price that this passenger is willing to pay.
$V_{\max}^i$	The value gained by passenger(s) i when transported from the origin to the transit hub directly without any inconvenience (i.e. $NR_i = 0$, $IVT_i = t_{i0}$, where t_{i0} is passenger(s) i's direct shipment time, and $WT_i = 0$).
$U_i(X, p_i)$	Passenger(s) i's utility given a vehicle-passenger matching and vehicle routing plan X and a price p_i.

In the context of this research, a passenger's value is defined as the maximum price that he/she is willing to pay, in line with the prior research (Zou et al. 2015, Zhao et al. 2015, Kamar and Horvitz 2009). This subsection proposes a generalized value function that establishes the relationship between a passenger's value and a given set of inconvenience attributes as well as this passenger's personalized requirements. The personalized requirements, represented by α_i^{NR}, α_i^{IVT} and α_i^{WT}, on the three inconvenience attributes (number of shared riders, extra in-vehicle travel time that exceeds the direct shipment time due to detour, and extra waiting time at the transit hub due to early arrival) can be any form, as long as the three parameters α_i^{NR}, α_i^{IVT} and α_i^{WT} can convey passengers' different tolerances for the inconvenience attributes.

Kamar and Horvitz (2009) proposed a passengers' value function based on

inconvenience cost. We incorporate the parameters α_i^{NR}, α_i^{IVT} and α_i^{WT} as passengers' personalized requirements into the value function.

$$V_i(X) = V_{\max}^i - C_i^{ICN}\left(NR_i(X), IVT_i(X), WT_i(X), \alpha_i^{NR}, \alpha_i^{IVT}, \alpha_i^{WT}\right) \quad (1)$$

We list three reasonable assumptions of the parameters in the value function, which are used in the proof of the properties of the proposed mechanism.

1) C_i^{ICN} is a monotone increasing function of NR_i, IVT_i, and WT_i. We assume that when people share the trip with more people, stay in the vehicle for longer time or wait at the transit hub for longer extra time, the passengers' inconvenience cost will never decrease.

2) We define $V_{\max}^i$ as the price charged by the taxi when this passenger takes this taxi directly to the transit hub without other shared riders. If a passenger participates in the ridesharing service but receives a direct shipment service without other shared riders, the service is treated as taxi service. The maximum willing-to-pay price is equal to the taxi price, because if the price is higher than the taxi price, the customer is unwilling to participate into the ridesharing service and will choose the taxi service. Thus, when $NR_i = 0$, $IVT_i = t_{i0}$, and $WT_i = 0$, the inconvenience cost equals zero. That is

$$C_i^{ICN}\left(NR_i = 0, IVT_i = t_{i0}, WT_i = 0, \alpha_i^{NR}, \alpha_i^{IVT}, \alpha_i^{WT}\right) = 0 \quad (2)$$

This assumption is easy to understand because when $NR_i = 0$, $IVT_i = t_{i0}$, and $WT_i = 0$, the service is the same as taxi service – direct shipment for passenger(s) *i*.

3) It is assumed that taxi always makes profit. That is the taxi price is always greater than the transportation cost:

$$V_{\max}^{i} > c_{i0} \tag{3}$$

Passenger's utility (the difference between the maximum willing-to-pay price and the actual price paid) is given in Formula (4), which is also defined in the literature (Zou et al. 2015, Zhao et al. 2015, Kamar and Horvitz 2009).

$$U_i\left(X, p_i\right) = V_i\left(X\right) - p_i \tag{4}$$

We use an illustrative example of the value function for better understanding. This value function will be used in the example in Subsection 3.3.4 to illustrate how the mechanism is obtained. In this example, if one passenger shares the ride with others, the maximum willing-to-pay price is set to be the taxi price multiplied by a discount rate (λ_i, here we set the discount rate as λ_i = 0.85) if the service satisfies the passenger's requirements. Note that the discount rate λ_i can be other values, which is also reported by passengers. If the passengers' requirements are not satisfied, the passenger is unwilling to pay anything. Based on this assumption, the value function is defined as:

$$V_i = \begin{cases} V_{\max}^{i}, \text{ direct shipment} \\ 0, \text{ ridesharing, requirements are not satisfied} \\ \lambda_i V_{\max}^{i}, \text{ ridesharing, requirements are satisfied} \end{cases}$$

The inconvenience cost is thus defined as:

$$C_i^{ICN} = \begin{cases} 0, \text{ direct shipment} \\ V_{\max}^i, \text{ ridesharing, requirements are not satisfied} \\ (1-\lambda_i)V_{\max}^i, \text{ ridesharing, requirements are satisfied} \end{cases}$$

Let us return to the example in Subsection 3.3.1, John's value function is as follows.

$$V_{\text{John}} = \begin{cases} 7.74, \ IVT_{\text{John}} = t_{i0}, \ NR_{\text{John}} = 0, \ WT_{\text{John}} = 0 \\ 0, \ IVT_{\text{John}} > 10, \ NR_{\text{John}} > 3 \text{ or } WT_{\text{John}} > 10 \\ \lambda_i \times 7.74, \text{ otherwise} \end{cases}$$

Note that the example above is just an illustrative example. The value function can take a generalized form that is adapted to any reasonable scenarios. Developing specific value functions and designing an interface that allows users to report their requirements are beyond the scope of this chapter but will be considered in future research.

3.3.3 Optimization of Vehicle-Passenger Matching and Routing

We consider the ridesharing service provider (the agency) and passengers (the users) as a system to optimize the vehicle-passenger matching and routing plan. The agency and the users are two indispensable components of a system, and both the agency cost and the user cost are often considered collaboratively in the literature (Kim et al. 2015, Hajibabai et al. 2014, Amirgholy and Gonzales 2016). The objective of the proposed mechanism is to minimize the agency's transportation cost (e.g. vehicle dispatch cost, energy consumption cost, driver labor cost, and emission) and the users' inconvenience cost caused by ridesharing associated with their personalized requirements. This formulates an

optimization problem to determine an optimal vehicle-passenger matching and vehicle routing plan.

Table 3.4 Additional Notations of Variables and Parameters in the Optimization Model

Sets	
P	Set of passenger requests, $P = \{1, 2, \dots, n\}$
V	Set of vehicles, $V = \{1, 2, \dots, m\}$
H	Set of the transit hub, $H = \{0\}$
Variables	
$x_{ijk} = \begin{cases} 1, & \text{if vehicle } k \text{ travels to location } j \text{ after picking up passenger(s) in location } i \text{ immediately} \\ 0, & \text{otherwise} \end{cases}$ $i \in P, j \in P \bigcup H, k \in V$	
$y_{ik} = \begin{cases} 1, & \text{if vehicle } k \text{ is dispatched to pick up passenger(s) in location } i \\ 0, & \text{otherwise} \end{cases}$ $i \in P, k \in V$	
$X = \{x_{ijk}, y_{ik} \mid i \in P, j \in P \bigcup H, k \in V\}$ can represent a vehicle-passenger matching and vehicle routing plan.	
$w_{ik} = \begin{cases} 1, & \text{if passenger(s) in location } i \text{ is the first to be picked up by vehicle } k \\ 0, & \text{otherwise} \end{cases}$ $i \in P, k \in V$	
NR_i	Number of co-riders with passenger(s) i.
IVT_i	Passenger(s) i's in-vehicle travel time.
WT_i	Passenger(s) i's extra waiting time at the transit hub

C_i^{ICN}	Passenger(s) i's inconvenience cost caused by ridesharing.
Parameters	
np_i	Number of passengers in request i.
DL_i	Passenger(s) i's preferred deadline before which he/she/they must arrive at the transit hub.
t_{ij}	The travel time from node i to node j, i and $j \in P \bigcup H$. The pickup time is included in t_{ij}. We assume a triangle inequality assumption $t_{ij} \leq t_{ig} + t_{gj}$ for any i, j and g, which will be used to guarantee non-negative prices (Subsection 3.3.5 Proposition 4). This is a reasonable assumption because the nonstop travel time is unlikely longer than the vehicle's travel time to detour to pick up another passenger plus an additional pickup time.
c_{ij}	The transportation cost from node i to node j, i and $j \in P \bigcup H$. We assume $c_{ij} \leq c_{ig} + c_{gj}$, for any i, j and g for the same purpose.
Q	The seat capacity of a vehicle, excluding the driver.

The problem can be formulated as the following Integer Programming (*IP*). For the notations, please refer to Table 3.3 and Table 3.4.

$$Z = \min \sum_{i \in P} C_i^{ICN}(NR_i, IVT_i, WT_i, \alpha_i^{NR}, \alpha_i^{IVT}, \alpha_i^{WT}) + TC(X) \tag{5}$$

where $TC(X)$ is the transportation cost of the vehicle-passenger matching and

vehicle routing plan: $TC(X) = \sum_{k \in V} \sum_{i \in P} \sum_{j \in P \cup H \setminus i} x_{ijk} c_{ij}$

Subject to

$$\sum_{k \in V} y_{ik} = 1, \text{ for all } i \in P \tag{6}$$

$$\sum_{i \in P} y_{ik} np_i \le Q, \text{ for all } k \in V \tag{7}$$

$$w_{jk} + \sum_{i \in P \setminus j} x_{ijk} = y_{jk}, \text{ for all } k \in V, j \in P \tag{8}$$

$$\sum_{j \in P \cup H \setminus i} x_{ijk} = y_{ik}, \text{ for all } k \in V, i \in P \tag{9}$$

$$\sum_{i \in P} w_{ik} \le 1, \text{ for all } k \in V \tag{10}$$

$$IVT_i = \sum_{k \in V} \sum_{j \in H \cup P \setminus i} x_{ijk} \left(IVT_j + t_{ij} \right), \text{ for all } i \in P \tag{11}$$

$$IVT_i \ge 0, \text{ for all } i \in P \tag{12}$$

$$WT_i = DL_i - \min_{j \in P} \left\{ M \left(1 - \sum_{k \in V} y_{jk} y_{ik} \right) + DL_j \right\}, \text{for all } i \in P \tag{13}$$

$$NR_i = \sum_{j \in P \setminus i} \sum_{k \in V} y_{ik} y_{jk} np_j, \text{ for all } i \in P \tag{14}$$

$$x_{ijk}, y_{ik}, w_{ik} \in \{0,1\}, \text{ for all } i, j \in P \cup H, k \in V \tag{15}$$

Formula (5) is the objective function that minimizes both the passengers' inconvenience cost and the agency's transportation cost. One passenger's inconvenience cost is a function of the number of co-riders, in-vehicle travel time, and extra waiting time at the transit hub. Formulas (6) ensures that all passengers will be picked up by one vehicle

and only be served once. Formula (7) represents the maximum capacity of each vehicle should not be exceeded. Formulas (8) and (9) ensure the balanced flow from and out of each passenger location. Formula (10) ensures that each vehicle can only be dispatched once at most. Formula (11) gets all passengers' in-vehicle travel times. Formula (12) is to ensure the non-negativity of all passengers' in-vehicle travel times. Formulas (13) and (14) get all passengers' extra waiting time at the transit hub and the number of shared riders, respectively. Formulas (15) signifies that x_{ijk}, y_{ijk}, and w_{ik} are binary variables.

We do not use constraints to formulate passengers' requirements because we already use the inconvenience cost function to represent the passengers' requirements. Thus, adding constraints to represent passengers' requirements is redundant and unnecessary. In the example in Subsection 3.3.2, we prove that adding such inconvenience cost function into the objective function can ensure that passenger(s) i's (for all $i \in P$) personalized requirements can be always satisfied.

Proof:

Suppose that X^* is the optimal solution of model IP and passenger(s) i's requirement is not satisfied given the optimal matching and routing plan X^*. Thus, passenger(s) i's inconvenience cost is $C_i^{ICN}(X^*) = V_{\max}^i$. Let $Z(X^*)$ represent the objective function value of model IP (Formula 5). If passenger(s) i does not participate in the first-mile ridesharing service, the optimal objective function value is assumed to be Z_{i-}. It is easy to understand that $Z_{i-} \leq Z(X^*) - C_i^{ICN}(X^*) = Z(X^*) - V_{\max}^i$, because extra transportation cost is needed for a vehicle to serve passenger(s) i. Now consider a solution X_i in which passenger(s) i is shipped to the transit hub directly without shared riders, and matching and routing plan is optimized for other passengers. Thus, $Z(X_i) = Z_{i-} + C_i^{ICN}(X_i) + c_{i0}$. Since passenger(s) i is

shipped to the transit hub directly without shared riders in X_i, passenger(s) i does not have inconvenience cost ($C_i^{JCN}(X_i) = 0$), and thus $Z(X_i) = Z_{i-} + c_{i0}$. $Z_{i-} = Z(X_i) - c_{i0} \leq Z(X^*) - V_{\max}^i$, then $Z(X^*) - Z(X_i) \geq V_{\max}^i - c_{i0}$. Based on Formula (3), $V_{\max}^i - c_{i0} > 0$. Thus $Z(X^*) > Z(X_i)$. Since X_i is a feasible solution of model IP, the optimality of solution X^* is violated. Thus, passengers' requirements can be always satisfied in the optimal solution X^* of model IP.

□

3.3.4 Customized Incentive Pricing Scheme

This subsection introduces the pricing scheme. This pricing framework is calculated by designing and solving a series of models, including one model IP_0 and n models IP_g (for all $g \in P$). Model IP_0 should be equivalent to the original model IP proposed in Subsection 3.3.3. Each model IP_g is used to calculate the price only and does not have practical meaning. Both models IP_0 and IP_g use passengers' reported information as input data. Both models IP_0 and IP_g have maximizing objective functions. Then the pricing scheme is given by

$$p_g = g(X^{IP_g*}) - (f(X^{IP_0*}) - V_g(X^{IP_0*})) \tag{16}$$

X^{IP_0*} is the optimal solution of model IP_0 with the maximizing objective function $f(.)$, which includes summation of all passengers' values.

$$f(X) = \sum_{i \in P} V_i(X) + h(X) \quad \text{(16-a)}$$

where $h(X)$ is used to make the model IP_0 equivalent to the original model IP proposed in Subsection 3.3.3.

X^{IP_g*} is the optimal solution of model IP_g, and $g(.)$ is the maximizing objective function of the model.

This pricing scheme makes the mechanism "individual rational" if the following condition is always satisfied

$$g(X^{IP_g*}) \leq f(X^{IP_0*}) \quad \text{(16-b)}$$

This is because passenger(s) g's utility is $U_g = V_g(X^{IP_0*}) - p_g = f(X^{IP_0*}) - g(X^{IP_g*}) \geq 0$, if the condition above is satisfied. A direct idea to satisfy this condition is to design the model IP_g that makes the objective function $g(X)$ identical with $f(X)$ and let the feasible regions of models IP_g (for all g) be included in the feasible region of model IP_0. That is

$$g(X) = f(X) \quad \text{(16-c)}$$

$$CS_{IP_g} \subseteq CS_{IP_0} \quad \text{(16-d)}$$

where the CS_{IP_g} and CS_{IP_0} are the feasible regions of models IP_g and IP_0, respectively.

If model IP_g is independent of passenger(s) g's report, then the mechanism is "incentive compatible".

If passenger(s) g misreports the requirement, then we assume that the optimal solution of model IP_0 changes from $X^{IP_0^*}$ to $Y^{IP_0^*}$, $g(X^{IP_g^*})$ remains constant because $g(X^{IP_g^*})$ is independent of passenger(s) g's report, and $f(X^{IP_0^*})$ changes to

$$f'(Y^{IP_0^*}) = \sum_{i \in P, i \neq g} V_i(Y^{IP_0^*}) + V_g'(Y^{IP_0^*}) + h(Y^{IP_0^*}) \quad \text{(16-e)}$$

Then, the price becomes

$$p_g' = g(X^{IP_g^*}) - \left(f'(Y^{IP_0^*}) - V_g'(Y^{IP_0^*}) \right) = g(X^{IP_g^*}) - \left(\sum_{i \in P, i \neq g} V_i(Y^{IP_0^*}) + h(Y^{IP_0^*}) \right) \quad \text{(16-f)}$$

Then passenger(s) g's utility becomes

$$U_g' = V_g(Y^{IP_0^*}) - p_g' = \left(\sum_{i \in P} V_i(Y^{IP_0^*}) + h(Y^{IP_0^*}) \right) - g(X^{IP_g^*}) = f(Y^{IP_0^*}) - g(X^{IP_g^*}) \quad \text{(16-g)}$$

$Y^{IP_0^*}$ may no longer be optimal for model IP_0, indicating that the objective function of model IP_0, $f(.)$, will suffer from a decrease caused by her misreporting. Thus, her utility $U_g = f(X^{IP_0^*}) - g(X^{IP_g^*})$ will decrease as well if she misreports her personalized requirement. Therefore, truthful reporting is passengers' optimal strategy.

This chapter utilizes this individual rational and incentive compatible pricing

scheme in Formula (16). The designed models IP_0 and IP_g (for all $g \in P$) are summarized in Table 3.5.

Table 3.5 Mathematical Models for Obtainment of the Mechanism

Model denotations	Objective functions	Constraints	Optimal solution	Optimal objective function value
IP_0	$f(X)$: Formula (17)	CS_{IP_0} Formulas (18)	$X^{IP_0*} = \left\{x_{ijk}^{IP_0*}, y_{ik}^{IP_0*}\right\}$	$Z_{IP_0}^*$
IP_g for all $g \in P$	$g(X)$: Formula (17)	CS_{IP_g} Formulas (18, 19)	$X^{IP_g*} = \left\{x_{ijk}^{IP_g*}, y_{ik}^{IP_g*}\right\}$	$Z_{IP_g}^*$

Model IP_0 :

Objective function:

$$\max Z_0(X) = \sum_{i \in P} V_i(X) - TC(X) \tag{17}$$

where $TC(X)$ is the transportation cost of the routing plan X.

$$TC(X) = \sum_{k \in V} \sum_{i \in P} \sum_{j \in P \cup H \setminus i} x_{ijk} c_{ij}$$

Constraints:

$$X \in CS_{IP_0} \tag{18}$$

The constraint set CS_{IP_0} consists of Formulas (6)-(15).

IP_0 is mathematically equivalent to the original optimization model (*IP*) in Subsection 3.3.3. First, IP_0 and *IP* have identical constraints. Second, the objective functions of the two models are equivalent implied by Formulas (1), (5) and (17). Thus, X^{IP_0*} is also the optimal solution of the original optimization model (*IP*) in Subsection 3.3.3. The optimal vehicle-passenger matching and routing plan can also be obtained by the model IP_0. The model IP_0 is proposed for direct calculation of prices (please see Formula (20) below).

Models IP_g (Along with IP_0, IP_g is to calculate each passenger's price if he/she/they participates in the first-mile ridesharing service):

Objective function: Formula (17).

Constraints (CS_{IP_g}): Formulas (18) and (19)

$$NR_g = 0 \tag{19}$$

These models do not have practical meaning but are used to calculate all prices. Each model optimizes all passengers' values minus the transportation cost in the system given that passenger(s) *g* is transported to the transit hub directly without any shared riders (see Figure 3.3).

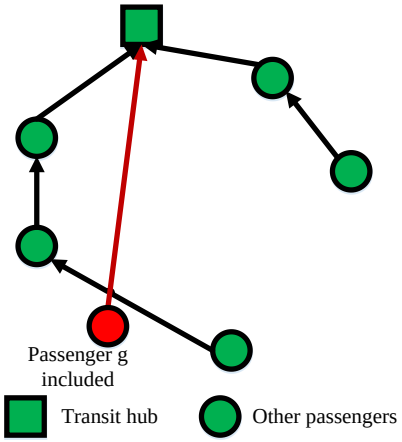

Figure 3.3 An Optimal Solution of IP_g

The mechanism is denoted as $M\left(X^{IP_0*}, \mathbf{p}\right)$. X^{IP_0*} is the optimal vehicle-passenger matching and vehicle routing plan. All passengers' prices are $\mathbf{p} = \{p_1, p_2, ..., p_n\}$, in which each price is calculated by

$$p_g = Z^*_{IP_g} - \left(Z^*_{IP_0} - V_g\left(X^{IP_0*}\right)\right) \tag{20}$$

Note that model IP_0 and IP_g have identical objective function (Formula 17), and that the feasible region of model IP_g is included in the feasible region of model IP_0 because model IP_g has an additional constraint (Formula 19) compared with model IP_0. Thus, the mechanism is "individual rational" based on Formulas (16-c) and (16-d). Moreover, the optimal solution of model IP_g is independent of passenger(s) g's report of the parameters of α_i^{NR}, α_i^{IVT} and α_i^{WT} because passenger(s) g's inconvenience cost is zero and the value is

a constant ($V_{\max}^{i}$) if the passenger(s) is transported to the transit hub directly without shared riders, no matter what values of α_i^{NR}, α_i^{IVT} and α_i^{WT} the passenger(s) reports. This can ensure "incentive compatibility" based on Formulas (16-e)–(16-g). The mechanism has another important property, "price non-negativity", that ensures that the service provider can receive revenue from passengers. The detailed proof of these three properties are given in Subsection 3.3.5.

Algorithm 1 shows how the mechanism is obtained.

Algorithm 1 obtaining the pricing mechanism

Input all parameters;

Solve the optimization model IP_0 and get the optimal solution $X^{IP_0^*}$, the optimal objective function value $Z_{IP_0}^*$, and each passenger's value $V_g\left(X^{IP_0^*}\right)$ in $X^{IP_0^*}$;

For g = 1:n

Solve the optimization model IP_g, and get the optimal objective function value $Z_{IP_g}^*$;

Calculate passenger(s) g's price $p_g = Z_{IP_g}^* - \left(Z_{IP_0}^* - V_g\left(X^{IP_0^*}\right)\right)$;

End for

Output the mechanism $M\left(X^{IP_0^*}, \mathbf{p}\right)$.

Let us return to the simple example proposed in Subsection 3.3.1 to show how the mechanism is obtained. The three passengers John, Peter and Alice are numbered as "1",

"2" and "3", and the transit hub is numbered as "0". We use the value function in the example proposed in Subsection 3.3.2. We firstly optimize the model IP_0 to get the optimal solution X^{IP_0*} of model IP_0, which is a vehicle-passenger matching and vehicle routing plan: "Alice-Peter-John-Transit hub" (3-2-1-0, Figure 3.4). The total transportation cost of this routing plan ($TC\left(X^{IP_0*}\right)$) is 4.140 dollars. The optimization results are summarized in Table 3.6.

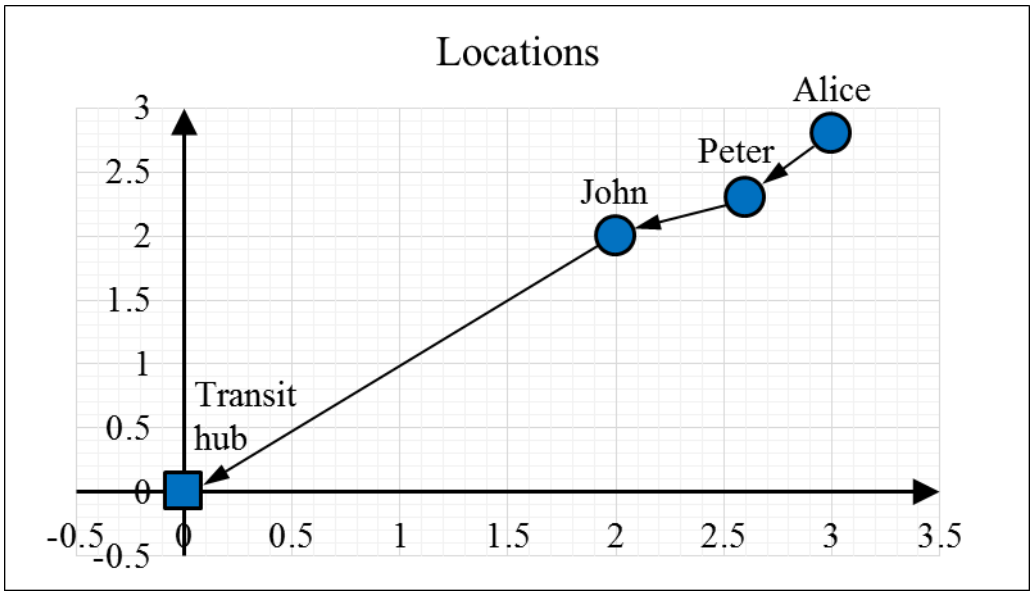

Figure 3.4 Optimal Routing Plan of the Example

Table 3.6 Optimization Results of IP_0

Optimization results	Passengers		
	John	Peter	Alice
Total travel time (minutes)	8.5	12.5	16.4

Extra waiting time at the transit hub (minutes)	0	10	0
Number of shared riders	2	2	2
Values $V_i\left(X^{IP_0*}\right)$ (dollars)	6.58	7.40	8.21

Notation: $V_i\left(X^{IP_0*}\right)$, passenger *i*'s value given the optimal plan X^{IP_0*}, i.e. the maximum willing-to-pay price.

Then we consider the three models IP_1, IP_2 and IP_3 (IP_g, g = 1, 2 and 3. John: 1, Peter: 2, Alice: 3). The optimization results are listed in Table 3.7.

Table 3.7 Optimization Results of IP_g

	Models (IP_g)								
	IP_1			IP_2			IP_3		
Optimal solution	X^{IP_1*} (3-2-0, 1-0)			X^{IP_2*} (3-1-0, 2-0)			X^{IP_3*} (2-1-0, 3-0)		
Total Transportation cost (TC (X^{IP_g*}))	6.94			7.58			7.60		
Passenger indexes (i)	1	2	3	1	2	3	1	2	3
Travel time (minutes)	8.49	10.41	14.34	8.49	10.41	14.33	8.49	12.50	12.31

Waiting time at transit hub (minutes)	0	10	0	0	0	0	0	10	0
Number of shared riders	0	1	1	1	0	1	1	1	0
$V_i\left(X^{IP_g*}\right)$ (dollars)	7.74	7.40	8.21	6.58	8.71	8.21	6.58	7.40	9.66

Notation: $V_i\left(X^{IP_g*}\right)$, passenger i's (i=1, 2, 3) value (i.e. the maximum willing-to-pay price) given the optimal solution (X^{IP_g*}) of the model IP_g. (3-2-0, 1-0), a vehicle-passenger matching and vehicle routing plan, two vehicles are used (Vehicle 1: 3-2-0, Vehicle 2: 1-0).

Take John as an example to show how his price is calculated. John's price is calculated by Formula (20):

$$p_1 = \left(V_1\left(X^{IP_1*}\right)+V_2\left(X^{IP_1*}\right)+V_3\left(X^{IP_1*}\right)-TC\left(X^{IP_1*}\right)\right)-\left(V_2\left(X^{IP_0*}\right)+V_3\left(X^{IP_0*}\right)-TC\left(X^{IP_0*}\right)\right)$$

$= (7.743 + 7.401 + 8.207 – 6.940) – (7.401 + 8.207 – 4.140) = 4.94$ (dollars).

Others' prices are calculated in the same method. The result of the mechanism is given in Table 3.8.

Table 3.8 The Result of Customized Pricing Mechanism

Optimal routing plan	Alice->Peter->John->the transit hub		
Passengers	John	Peter	Alice
Taxi price ($V^i_{\max}$, in dollars)	7.74	8.71	9.65
Maximum willing-to-pay price	6.58	7.40	8.21

($\lambda_i \times V_{\max}^i$, in dollars)			
Actual payment (dollars)	4.94	5.27	6.21
Utility (WTP price – actual payment, in dollars)	1.64	2.13	2.00

All of the three passengers have positive utilities, indicating that they are willing to participate in the ridesharing service.

We then take Alice as an example to show why truthfully reporting the requirements is the optimal strategy. She has three strategies, 1) taking a taxi to achieve direct shipment, 2) participating in the ridesharing service and truthfully reporting her requirement (α_i^{IVT}=20, α_i^{NR}=2, and α_i^{WT}=8, the maximum in-vehicle travel time, the maximum number of co-riders and the maximum extra waiting time at the transit hub that the passenger can tolerate are 20 minutes, 2, and 8 minutes, respectively); and 3) participating in the ridesharing service and misreporting her requirements (α_i^{IVT} =**15**, which is a misreported value, α_i^{NR}=2, α_i^{WT}=8). Table 3.9 shows the results of the three strategies. We can see that when Alice misreports her requirement (she lies and reports that she does not want to stay in the vehicle for more than 15 minutes but in fact she is able to tolerate this), the system changes the plan from "Alice-Peter-John-the transit hub" to "Alice-Peter-the transit hub" & "John-the transit hub" because of the stricter requirement. From the table, the price increases from 6.21 to 7.85, and her utility decreases from 2.00 to 0.36. This table also demonstrates that participating in the ridesharing service and telling the truth is the optimal strategy for this passenger (the bold number "2.00" is the maximum utility).

Table 3.9 Three Strategies and the Corresponding Results

Alice's service attributes	Strategies		
	Direct shipment (take taxi)	Ridesharing, telling the truth	Ridesharing, misreport
Optimal routing plan generated by the system	(3-0, 2-0, 1-0)	(3-2-1-0)	(3-2-0, 1-0)
Actual value (dollars)	9.66	8.21	8.21
Price (dollars)	9.66	6.21	7.85
Utility (dollars)	0	**2.00**	0.36

3.3.5 Theoretical Analysis

This subsection presents the properties of the proposed mechanism and gives brief proofs of these properties. There are three important properties, "individual rationality", "incentive compatibility" and "price non-negativity". Individual rationality is to guarantee all passengers are willing to participate in the service. More passengers will be incentivized to participate in the ridesharing service if the mechanism is individual rational. Incentive compatibility ensures that passengers are willing to truthfully report their personalized requirements. If the mechanism is not incentive compatible, passengers may manipulate the algorithm by misreporting their requirements and the overall cost of the system may not be minimized. Finally, the service provider must receive payment from each passenger and thus prices should be non-negative.

Proposition 1: Individual Rationality

As long as a passenger participates in the service system, the mechanism $M\left(X^{IP_0*}, \mathbf{p}\right)$ ensures that each passenger's utility ($U_g\left(X^{IP_0*}, p_g\right)$) received from the ridesharing service is always non-negative (aka. individual rationality)

$$U_g\left(X^{IP_0*}, p_g\right) = V_g\left(X^{IP_0*}\right) - p_g \geq 0, \text{ for any } g \in P \tag{21}$$

Proof:

$$\begin{aligned} U_g\left(X^{IP_0*}, p_g\right) &= V_g\left(X^{IP_0*}\right) - p_g \\ &= V_g\left(X^{IP_0*}\right) - Z^*_{IP_g} + \left(Z^*_{IP_0} - V_g\left(X^{IP_0*}\right)\right) \\ &= Z^*_{IP_0} - Z^*_{IP_g} \\ &= Z^*_{IP_0} - Z_0\left(X^{IP_g*}\right) \end{aligned}$$

The first part of the formula above is the optimal objective function value of IP_0. X^{IP_g*} is a feasible solution of IP_0, and thus the second part of the formula is not necessarily the optimal objective function value of IP_0. Thus,

$$U_g\left(X^{IP_0*}, p_g\right) = Z^*_{IP_0} - Z_0\left(X^{IP_g*}\right) \geq 0$$

Proposition 2: Incentive Compatibility

Telling the truth is always the optimal reporting strategy for each passenger who participates in the service under the mechanism $M\left(X^{IP_0*}, \mathbf{p}\right)$ regardless of other passengers' reporting strategies (aka. incentive compatibility, Nisan et al. 2007).

Proof:

We assume that passenger(s) g misreports the requirements on the number of shared riders, extra in-vehicle travel time, and extra waiting time (α_i^{NR}, α_i^{IVT} and α_i^{WT}), respectively.

We define $V_i'(X) = V_{\max}^i - C^{ICN}\left(NR_i(X), IVT(X)_i, WT_i(X), \beta_i^{NR}, \beta_i^{IVT}, \beta_i^{WT}\right)$, where β_i^{NR}, β_i^{IVT} and β_i^{WT} are passenger(s) i's misreported values of α_i^{NR}, α_i^{IVT} and α_i^{WT}, respectively.

The optimization problem IP_0 becomes IP_0':

$$Z_{IP_0'}^* = \max Z_0'(X) = \sum_{i \in P, i \neq g} V_i(X) + V_g'(X) - TC(X), \text{ s.t. } X \in CS_{IP_0}$$

Note that model IP_0' uses all passengers' reported personalized requirements as input data, in which passenger(s) g's personalized requirement is misreported. Other passengers' values ($V_i(X)$, for all $i \neq g$) are calculated based on their reported personalized requirements no matter if these passengers' reports are truthful or not. The only difference of IP_0 from IP_0' is that model IP_0 uses passenger(s) g's truthful report as an input data. We assume that $X^{IP_0'*}$ is the optimal solution of IP_0'. Optimization model IP_g does not change, because problem IP_g is independent of passenger(s) g's report. More precisely, passenger(s) g's value always equals $V_{\max}^i$ (implied from Formulas 1 and 2) because the passenger(s) is directly transported to the transit hub without shared riders in IP_g.

Then, the price charged for passenger(s) g is:

$$p'_g = Z^*_{IP_g} - \left(Z^*_{IP_0'} - V_g' \left(X^{IP_0'^*} \right) \right)$$

The utility that passenger(s) g can receive is:

$$\begin{aligned}
&U_g \left(X^{IP_0'^*}, p'_g \right) = V_g \left(X^{IP_0'^*} \right) - p'_g \\
&= V_g \left(X^{IP_0'^*} \right) - \left(Z^*_{IP_g} - \left(Z^*_{IP_0'} - V_g' \left(X^{IP_0'^*} \right) \right) \right) \\
&= V_g \left(X^{IP_0'^*} \right) - \left(Z^*_{IP_g} - \left(\sum_{i \in P, i \neq g} V_i \left(X^{IP_0'^*} \right) + V_g' \left(X^{IP_0'^*} \right) - TC \left(X^{IP_0'^*} \right) - V_g' \left(X^{IP_0'^*} \right) \right) \right) \\
&= \sum_{i \in P} V_i \left(X^{IP_0'^*} \right) - TC \left(X^{IP_0'^*} \right) - Z^*_{IP_g} \\
&= Z_0 \left(X^{IP_0'^*} \right) - Z^*_{IP_g}
\end{aligned}$$

$X^{IP_0'^*}$ is not necessarily the optimal solution of IP_0, thus

$$Z_0 \left(X^{IP_0'^*} \right) \leq Z_0 \left(X^{IP_0^*} \right)$$

Thus, we have

$$U_g \left(X^{IP_0'^*}, p'_g \right) = Z_0 \left(X^{IP_0'^*} \right) - Z^*_{IP_g} \leq Z_0 \left(X^{IP_0^*} \right) - Z^*_{IP_g} = U_g \left(X^{IP_0^*}, p_g \right)$$

where $U_g \left(X^{IP_0^*}, p_g \right)$ is the passenger(s) g's utility and $X^{IP_0^*}$ is the optimal solution of model IP_0 when he reports the true values of α_i^{NR}, α_i^{IVT} and α_i^{WT}. $X^{IP_0'^*}$ and

$X^{IP_0^*}$ are respectively the optimal solutions of models IP_0' and IP_0 regardless of other passengers' reporting strategies. This indicates that telling the truth is always the best strategy for each passenger regardless of other passengers' reporting strategies.

□

Then, we introduce the definition of "transition solution" and analyze its property (Proposition 3). The definition of "transition solution" will be used to demonstrate that the mechanism has the property of "price non-negativity" (Subsection 3.3.5 Proposition 4).

Definition 1 $Y_g = TRS_g(X)$ is the g^{th} transition solution from a feasible solution X of the model IP_0 to the corresponding feasible solution Y_g of the model IP_g if the transition process is given by Algorithm 2.

Algorithm 2 Obtain the transition solutions $Y_g = TRS_g(X)$

Input a solution $X = \{x_{ijk}, y_{ik}\}$;

Let $Y_g = X$;

If $NR_g > 0$

Find k that $y_{gk} = 1$, and let $y_{gk} = 0$;

Let another vehicle k' without tasks to pick up passenger(s) g, $y_{gk'} = 1$ and $x_{g0k'} = 1$;

Find j that $x_{gjk} = 1$, and let $x_{gjk} = 0$;

Find i that $x_{igk} = 1$, and let $x_{igk} = 0$;

Let $x_{ijk} = 1$;

End if

Output Y_g.

Figure 3.5 shows an example of transition solution generation. Passenger(s) g goes to the transit hub directly without any other shared passengers, and the broken links are re-connected.

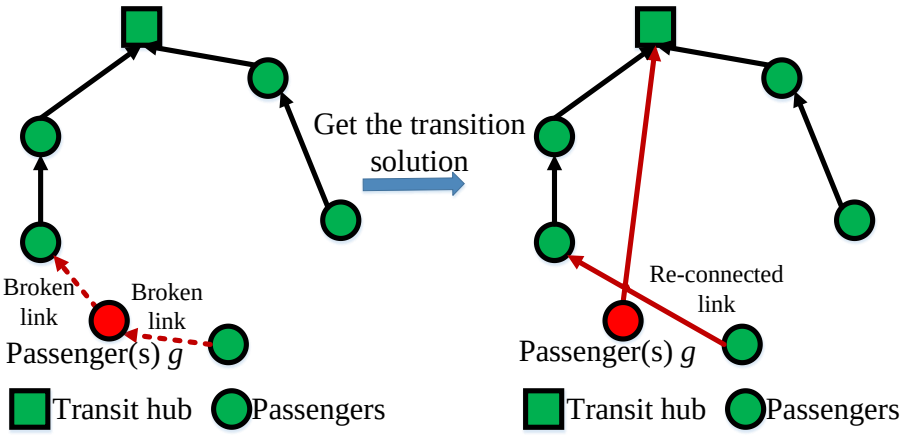

Figure 3.5 Example of the Transition Solution Obtainment

Proposition 3 For any passenger(s) i, $V_i\left(Y_g\right) \geq V_i\left(X\right)$ for any solution X, where $Y_g = TRS_g\left(X\right)$ for any $g \in P$. This proposition will be used in the proof of the "price non-negativity" proposition (Subsection 3.3.5 Proposition 4)

Proof:

If $i = g$, $V_i\left(Y_g\right) = V_{\max}^i$, thus $V_i\left(Y_g\right) \geq V_i\left(X\right)$.

If passengers in requests i and g are served by the same vehicle, we have

$IVT_i\left(Y_g\right) \le IVT_i\left(X\right)$, $NR_i\left(Y_g\right) \le NR_i\left(X\right)$, and $WT_i\left(Y_g\right) \le WT_i\left(X\right)$. Since the passengers' value function is a monotone decreasing function of NR_i, IVT_i and WT_i, we have $V_i\left(Y_g\right) \ge V_i\left(X\right)$.

If passenger(s) *i* and *g* are served by different vehicles, $V_i\left(Y_g\right) = V_i\left(X\right)$, because passenger(s) *i*'s matching and routing plan is the same in Y_g as in *X*.

Thus, for any passenger(s) *i*, we have $V_i\left(Y_g\right) \ge V_i\left(X\right)$ for any transition solution *g*.

□

Proposition 4: Price Non-Negativity

If two preconditions are satisfied: 1) the transportation cost and travel time between two locations comply with the triangle inequality $c_{ij} \le c_{ig} + c_{gj}$ and $t_{ij} \le t_{ig} + t_{gj}$ for any *i*, *j* and *g*, and 2) $V_{\max}^{i} > c_{i0}$ (Formula 3), the service provider can always receive revenue from each passenger under the mechanism $M\left(X^{IP_0*}, \mathbf{p}\right)$ (aka. price non-negativity).

$$p_g = Z_{IP_g}^{*} - \left(Z_{IP_0}^{*} - V_g\left(X^{IP_0*}\right)\right) \ge 0 \tag{22}$$

Let $Y_g = TRS_g\left(X^{IP_0*}\right) = \left\{x_{ijk}^{g}, y_{ik}^{g} \middle| i \in P, j \in P \cup H, k \in V\right\}$ (see Definition 1). Since Y_g is a feasible solution of IP_g and X^{IP_g*} is the optimal solution of IP_g, we have $Z_0\left(X^{IP_g*}\right) \ge Z_0\left(Y_g\right)$. Thus,

$$p_g = Z_0\left(X^{IP_g*}\right) - \left(Z^*_{IP_0} - V_g\left(X^{IP_0*}\right)\right) \geq Z_0\left(Y_g\right) - \left(Z^*_{IP_0} - V_g\left(X^{IP_0*}\right)\right)$$

Since in solution Y_g passenger(s) g is transported to transit hub without shared riders, $V_g\left(Y_g\right) = V^g_{\max}$. Thus

$$Z_0\left(Y_g\right) = \sum_{i\in P\setminus g} V_i\left(Y_g\right) - \sum_{k\in V}\sum_{i\in P\setminus g}\sum_{j\in P\cup H\setminus i,g} x^g_{ijk}c_{ij} + \left(V^g_{\max} - c_{g0}\right)$$

From Formula (3), we have

$$Z_0\left(Y_g\right) > \sum_{i\in P\setminus g} V_i\left(Y_g\right) - \sum_{k\in V}\sum_{i\in P\setminus g}\sum_{j\in P\cup H\setminus i,g} x^g_{ijk}c_{ij}\ .$$

From Proposition 3, we have

$$\sum_{i\in P\setminus g} V_i\left(Y_g\right) \geq \sum_{i\in P\setminus g} V_i\left(X^{IP_0*}\right)$$

Thus

$$Z_0\left(Y_g\right) > \sum_{i\in P\setminus g} V_i\left(X^{IP_0*}\right) - \sum_{k\in V}\sum_{i\in P\setminus g}\sum_{j\in P\cup H\setminus i,g} x^g_{ijk}c_{ij}$$

$\sum_{k\in V}\sum_{i\in P\setminus g}\sum_{j\in P\cup H\setminus i,g} x_{ijk}^{g} c_{ij}$ is the transportation cost excluding the transportation cost that is related to passenger(s) g in solution Y_g. It is easily proved smaller than or equal to the total transportation cost in solution $X^{IP_0^*}$ ($\sum_{k\in V}\sum_{i\in P}\sum_{j\in P\cup H\setminus i} x_{ijk}^{IP_0^*} c_{ij}$) because of the triangle equality. Thus

$$Z_0\left(Y_g\right) > \sum_{i\in P, i\neq g} V_i\left(X^{IP_0^*}\right) - \sum_{k\in V}\sum_{i\in P}\sum_{j\in P\cup H\setminus i} x_{ijk}^{IP_0^*} c_{ij} = Z_{IP_0}^{*} - V_g\left(X^{IP_0^*}\right)$$

Thus

$$p_g > Z_0\left(Y_g\right) - \left(Z_{IP_0}^{*} - V_g\left(X^{IP_0^*}\right)\right) \geq 0$$

□

3.4 Case Study

3.4.1 Data Setting

This section presents a case study to visualize the results of the designed mechanism and its theoretical properties. In the following case, we select ten locations near the New Brunswick Train Station (New Jersey, in the United States) on the Google Maps. The addresses of the ten locations are listed in Table 3.10 and are identified in Figure 3.6 on the map. The travel times between two locations are estimated by Google Maps at 12:30 pm on July 13 2017. The travel distance between two locations is obtained based on the actual routes using the information from Google Maps. For clarification convenience, the

transportation cost is set to be proportional to the travel distance. The taxi price ($V_{\max}^{i}$) is \$5 for the first mile and \$1.5 for each additional mile, $V_{\max}^{i} = 5 + 1.5 \times \max(d_{i0} - 1,\ 0)$. Each location has one passenger sending the request for the service. We assume that each passenger catches one of the three trains in New Brunswick Station. Passengers' train schedule information is listed in Table 3.11. In our case study, for simplicity and illustrative convenience, all the passengers' preferred arrival deadlines are set to be ten minutes before their train departure times. Our model can also handle the problems when their preferred arrival deadlines are different. A fleet of cars with seat capacity of "4" will be dispatched to pick up all the passengers and transport them to the transit hub before the specified deadlines.

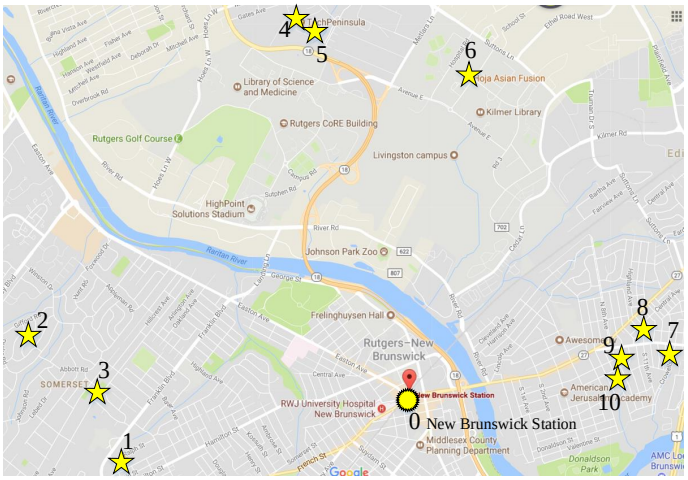

Figure 3.6 Selected Locations near New Brunswick Station

Table 3.10 Addresses of the Ten Selected Locations

Passengers	Addresses	Passengers	Addresses

1	458 Ralph St, Somerset, NJ	6	Rockafeller Road, Piscataway Township, NJ
2	16 King Rd, Somerset, NJ	7	227 Hilton St, Highland Park, NJ
3	58 Arden St, Somerset, NJ	8	121 S 11th Ave, Highland Park, NJ
4	235 Hampshire Court, Piscataway Township, NJ	9	109 S 8th Ave, Highland Park, NJ
5	375 Lancaster Ct, Piscataway Township, NJ	10	219 S 7th Ave, Highland Park, NJ

Table 3.11 Trains in New Brunswick Station Selected by the Ten Passengers

Passengers indexes (i)	Train numbers	Train departure times	Passengers indexes (i)	Train numbers	Train departure times
1	Q3846	1:20 pm	6	Q3846	1:20 pm
2	Q3846	1:20 pm	7	Q3843	1:35 pm
3	Q3848	1:36 pm	8	Q3843	1:35 pm
4	Q3848	1:36 pm	9	Q3843	1:35 pm
5	Q3843	1:35 pm	10	Q3848	1:36 pm

The case study uses two types of value functions and passengers' report methods in order to show that the generalized mechanism can be adapted into difference scenarios. In

the first scenario, passengers can report the maximum extra in-vehicle travel time, maximum number of shared riders and maximum extra waiting time at the transit hub (see Table 3.12) as the example in Section 3.3. Passengers' value function is as that of the example in Subsection 3.3.2:

$$V_i = \begin{cases} V_{\max}^i, & \text{direct shipment} \\ 0, & \text{ridesharing, requirements are not satisfied} \\ 0.85V_{\max}^i, & \text{ridesharing, requirements are satisfied} \end{cases}$$

Passengers' reporting methods and the value function are only used for illustration, and the method can be adapted to any specific form.

Table 3.12 Passengers' Personalized Requirements in the First Scenario

Personalized requirements	Passenger indexes									
	1	2	3	4	5	6	7	8	9	10
α_i^{NR}	3	3	3	4	4	3	4	4	4	4
α_i^{IVT} (minutes)	10	15	15	10	6	8	7	15	10	10
α_i^{WT} (minutes)	20	20	5	10	10	20	10	5	10	15

α_i^{NR}: the maximum number of shared riders that the passenger i can tolerate.

α_i^{IVT}: the maximum extra in-vehicle travel time that the passenger i can tolerate.

α_i^{WT}: the maximum extra waiting time at the transit hub that the passenger i can tolerate.

In the first scenario, passengers can directly report their personized requirements. The interactive system is straightforward for users to manipulate. However, the system has one limitation: as long as one passenger's requirements are satisfied, the value (maximum

willing-to-pay price) is assumed to be a constant, $0.85V_{\max}^{i}$, even though the service has different degrees of inconvenience attributes. In the example of Section 3.3, John's maximum willing-to-pay price is assumed to be always 6.58 with the in-vehicle travel time increasing from 8.5 minutes to 10 minutes.

In other scenarios, the maximum willing-to-pay price may decrease as the inconvenience degree increases. Thus, we adapt the mechanism into the second scenario, in which passengers' maximum willing-to-pay prices decrease as the inconvenience degree increases. In the second scenario, passengers can report the reduction rate of maximum willing-to-pay price in terms of the three inconvenience attributes. For example, if a passenger reports $\alpha_i^{NR}=0.5$, it indicates that each time when the number of co-riders increases by one, the maximum willing-to-pay price decreases by 0.5 dollar. Similarly, $\alpha_i^{IVT}=0.5$ means that each time when the extra in-vehicle travel time increases by 5 minutes, the maximum willing-to-pay price decreases by 0.5 dollar; $\alpha_i^{WT}=0.5$ means that each time when the extra waiting time at the transit hub increases by 5 minutes, the maximum willing-to-pay price decreases by 0.5 dollar. Thus, the three parameters α_i^{NR}, α_i^{IVT} and α_i^{WT} represent the strictness of the requirements. The values of α_i^{NR}, α_i^{IVT} and α_i^{WT} are given in Table 3.13.

Table 3.13 Passengers' Personalized Requirements in the Second Scenario

Personalized requirements	Passenger indexes									
	1	2	3	4	5	6	7	8	9	10
α_i^{NR}	0.12	0.29	0.41	0.35	0.18	0	0.10	1.00	0.19	0.20
α_i^{IVT}	0.30	0.40	0.51	0.44	0.82	1.66	0.62	1.89	0.32	1.20

α_i^{WT}	0.10	0.10	1.52	1.79	0.83	0.03	0.76	0.88	1.25	2.00

α_i^{NR} (dollars per co-rider): reduction rate of maximum willing-to-pay price in terms of the number of co-riders.

α_i^{IVT} (dollars every 5 minutes): reduction rate of maximum willing-to-pay price in terms of the extra in-vehicle travel time.

α_i^{WT} (dollars every 5 minutes): reduction rate of maximum willing-to-pay price in terms of the extra waiting time at the transit hub.

The hypothetical value function is naturally presented by Formula (23).

$$V_i = V_{\max}^i - \alpha_i^{NR} NR_i - \frac{\alpha_i^{IVT}\left(IVT_i - t_{i0}\right)}{5} - \frac{\alpha_i^{WT} WT_i}{5} \tag{23}$$

This value function achieves a more reasonable mechanism in which the maximum willing-to-pay price decreases as the inconvenience degrees increase. Note that we use this hypothetical function just to show that our mechanism can be adapted into generalized scenarios. This form of the value function in the second scenario is less straightforward than that in the first scenario, and the reporting method may be more complex for passengers.

3.4.2 The Meachanism Results

We solve the model IP_0 to get the optimal matching and routing plans for the first and second scenarios, (2-3-1-0, 8-7-9-10-0, 4-5-6-0) and (2-3-1-0, 4-5-6-0, 9-10-0, 7-8-0), shown in Figure 3.7 (a) and (b), respectively. Passengers' values gained from the service,

the actual prices charged by the service provider, and the utilities are presented in Table 3.14 (a) and Table 3.14 (b) for the two scenarios, respectively. The prices are all positive in both of the scenarios, indicating that the service provider receives revenue from the participants. Moreover, as long as participants share the trip with other riders, they pay less than the taxi price. All passengers' utilities are non-negative in both of the two scenarios. This indicates that all passengers are willing to participate in the ridesharing service under the proposed mechanism. Furthermore, we take the 7th passenger as an example to show the property of "incentive compatibility". Figure 3.7 (a) and (b) are straightforward demonstrations of "incentive compatibility" in the two scenarios, respectively. If the passenger truthfully reports the requirements on the inconvenience attributes, he will receive no smaller utility than that if he misreports the requirements. In Figure 3.8 (a), we assume that the maximum extra in-vehicle travel time that Passenger 7 can tolerate is 7 minutes. If the passenger truthfully reports the "7 minutes" (the red dash line), he receives the maximum utility ($0.47) from the service. If he misreports this value (the black dash line), his utility is no larger than $0.47. Similarly, in Figure 3.8 (b), truthfully reporting the reduction rate ($0.6 every five minutes) of the maximum willing-to-pay price in terms of the extra in-vehicle travel time is the optimal strategy for Passenger 7. Note that Figure 3.8 only presents one inconvenience attribute – extra in-vehicle travel time – as an example, and we can draw the same conclusion for the other inconvenience attributes. Finally, several previous studies (Zhao et al. 2014, Biswas et al. 2017) considered whether the payment collected from participants can cover the transportation cost. From the results of the mechanism, the profit (the summation of all prices minus the transportation cost, $\sum_{i=1}^{n} p_i - TC\left(X^{IP_0*}\right)$) is $40.74 in the first scenario and $46.08 in the second scenario, both

of which are positive. This property will be tested by a group of numerical examples with various numbers of passengers in Chapter 4.

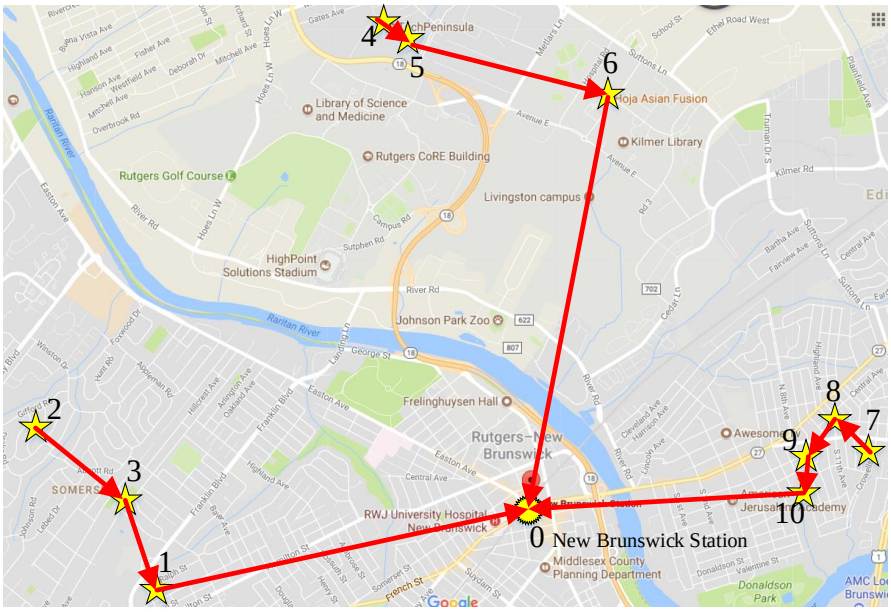

(a)

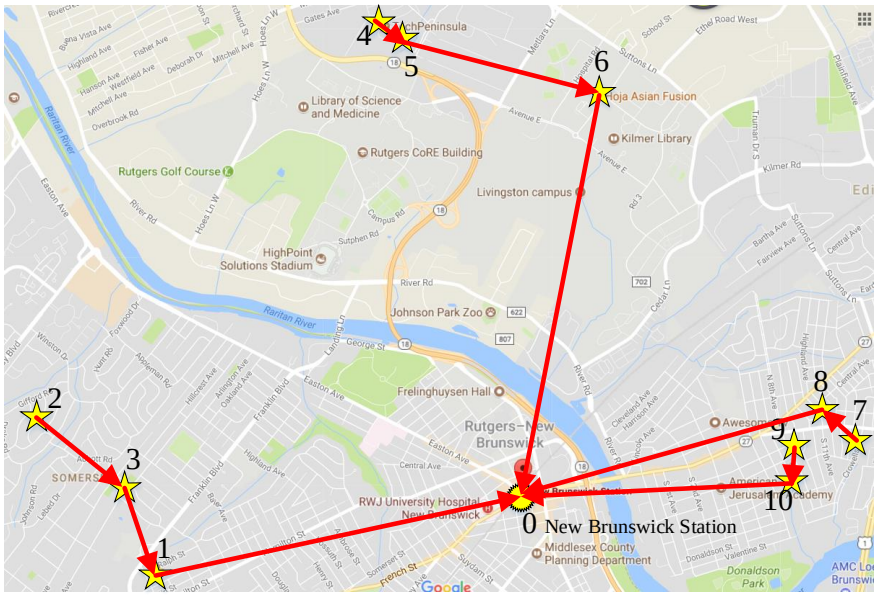

(b)

Figure 3.7 (a) Optimal Vehicle-Passenger Matching and Vehicle Routing Plan in the First Scenario (b) Optimal Vehicle-Passenger Matching and Vehicle Routing Plan in the Second Scenario

Table 3.14 (a) Results of the Mechanism in the First Scenario (b) Results of the Mechanism in the Second Scenario

(a)

Results	Passenger indexes (i)									
	1	2	3	4	5	6	7	8	9	10
$V_{\max}^{i}$ (in dollars)	7.25	8.60	8.15	10.55	10.70	8.30	6.20	6.05	5.75	5.90
V_i (in dollars)	6.16	7.31	6.93	8.97	9.10	7.06	5.27	5.14	4.89	5.02
p_i (in dollars)	4.95	6.01	5.63	6.05	6.20	5.40	4.80	4.55	4.35	4.50
U_i (in dollars)	1.21	1.30	1.30	2.92	2.90	1.66	0.47	0.59	0.54	0.52

(b)

Results	Passenger indexes (i)									
	1	2	3	4	5	6	7	8	9	10
V_i (in dollars)	6.69	6.98	6.82	9.15	9.52	8.20	5.85	5.05	5.25	5.70
p_i (in dollars)	6.56	6.53	6.14	6.40	6.81	6.96	5.70	4.96	5.02	5.49
U_i (in dollars)	0.13	0.45	0.68	2.75	2.71	1.24	0.15	0.09	0.23	0.21

$V_{\max}^{i}$: the taxi price. V_i: passenger i's value, i.e. the maximum willing-to-pay price. p_i: passenger i's real price. U_i: passenger i's utility, $U_i = V_i - p_i$.

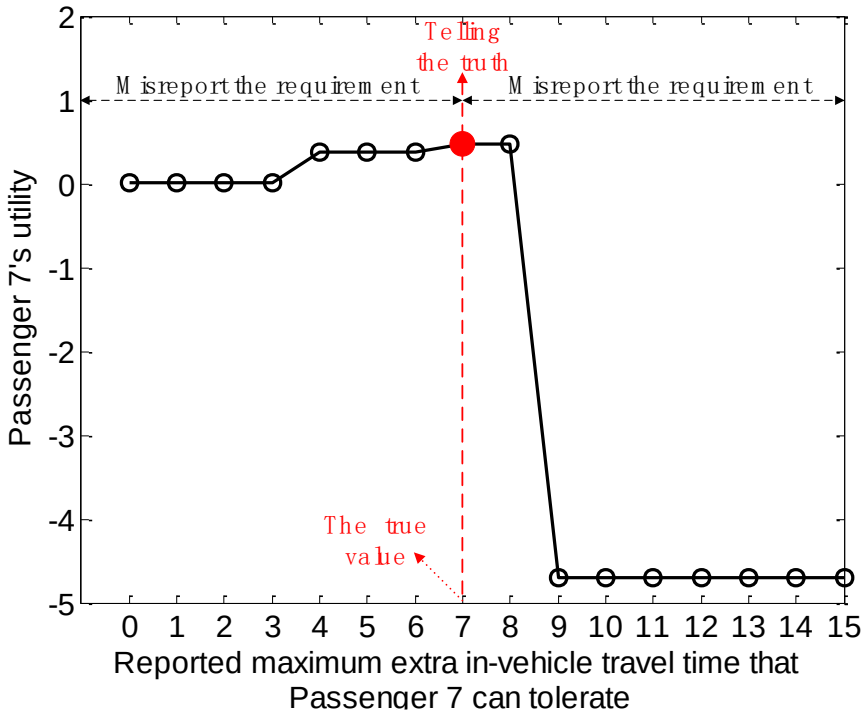
Telling the truth
Misreport the requirement
Misreport the requirement
The true value
Passenger 7's utility
Reported maximum extra in-vehicle travel time that Passenger 7 can tolerate

(a)

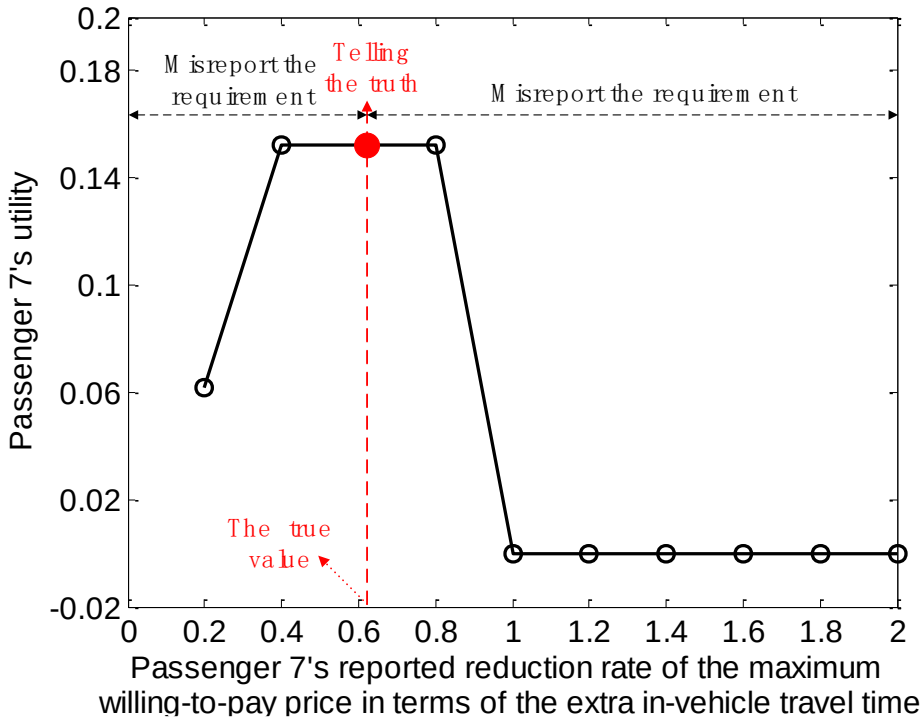
Misreport the requirement
Telling the truth
Misreport the requirement
The true value
Passenger 7's utility
Passenger 7's reported reduction rate of the maximum willing-to-pay price in terms of the extra in-vehicle travel time

(b)

Figure 3.8 (a) "Incentive Compatibility" in the First Scenario (b) "Incentive Compatibility" in the Second Scenario

3.4.3 Sensitivity Analysis

Sensitivity analysis aims to investigate the dynamic process of vehicle-passenger matching and vehicle routing plan and the prices as passengers change their requirements. We increase the strictness of one passenger's requirement on one of the three inconvenience attributes by fixing his requirements on the other two inconvenience attributes and all the other passengers' requirements. Figure 3.9 (a), (b) and (c) present how prices change due to decreasing the maximum degree of the three inconvenience attributes that the passengers can tolerate in the first scenario. Figure 3.10 (a), (b) and (c) show the changing process of the prices in the second scenario caused by increasing the reduction rate of maximum willing-to-pay price in terms of the increased degrees of three inconvenience attributes, respectively.

Different passengers have different price lines, because they have different travel information (e.g. departure location, arrival deadline, travel distance and time, etc.) and thus they have different utility functions. In Figure 3.9, when the maximum degree of the three inconvenience attributes that the passengers can tolerate decreases, each passenger's price either remains constant or increases. The price remains constant because passengers' changed tolerance does not impact the optimal solution of the optimization model IP_0 and the optimal vehicle-passenger matching and vehicle routing plan does not change. If the optimal matching and routing plan changes due to tightening the tolerance for the inconvenience attributes, the passengers' receives better-quality services and the price

increases. Take Passenger 6 in Figure 3.9 (a) as an example, when the maximum number of co-riders she can tolerate decreases from 3 to 2, the optimal vehicle-passenger matching and vehicle routing plan (Vehicle 1: 2-3-1-0; **Vehicle 2**: 4-5-**6**-0; Vehicle 3: 7-8-9-10-0) does not change and the price remains constant. When the maximum number of co-riders tolerated decreases from 2 to 1, the optimal vehicle-passenger matching and vehicle routing plan changes to "Vehicle 1: 2-3-1-0; Vehicle 2: 5-4-0; **Vehicle 3: 6-**0; Vehicle 4: 7-8-9-10-0" and the price increases due to the better-quality service. Similar conclusions are drawn from Figure 3.9 (b) and (c). Likewise, in Figure 3.10 (a), when Passenger 6 increases the reduction rate of maximum willing-to-pay price in terms of number of co-riders from \$0.4 per co-rider to \$0.6 per co-rider, the optimal vehicle-passenger matching and vehicle routing plan (Vehicle 1: 2-3-1-0; **Vehicle 2**: 4-5-**6**-0; Vehicle 3: 7-8-0; Vehicle 4: 9-10-0) and the price remain constant. When the reduction rate of the maximum willing-to-pay price in terms of number of co-riders is increased from \$0.6 per co-rider to \$0.8 per co-rider, the optimal vehicle-passenger matching and vehicle routing plan changes to "Vehicle 1: 2-3-1-0; Vehicle 2: 5-4-0; **Vehicle 3**: **6**-0; Vehicle 4: 7-8-0; Vehicle 5: 9-10-0" and the price increases accordingly. The sensitivity analysis implies that passengers can receive higher-quality service with higher price by placing stricter requirements on the corresponding inconvenience factors based on their preferences.

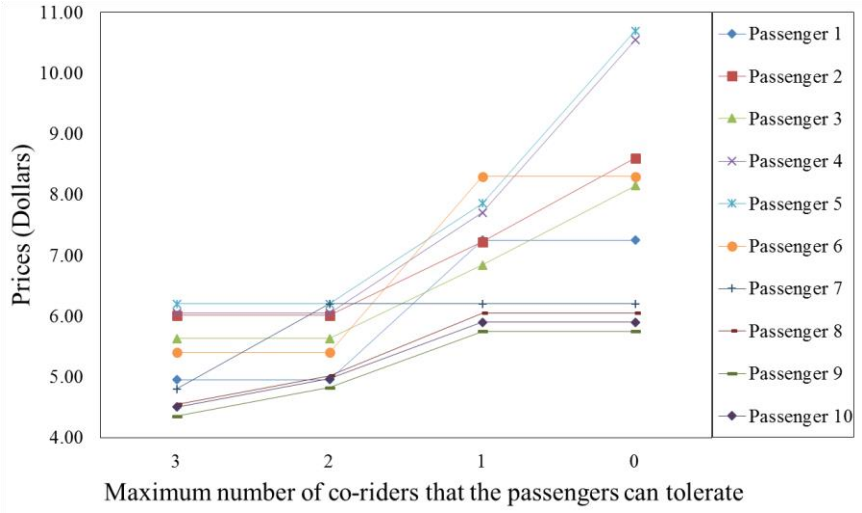
11.00
10.00
9.00
8.00
7.00
6.00
5.00
4.00
Prices (Dollars)
3
2
1
0
Maximum number of co-riders that the passengers can tolerate
Passenger 1
Passenger 2
Passenger 3
Passenger 4
Passenger 5
Passenger 6
Passenger 7
Passenger 8
Passenger 9
Passenger 10

(a)

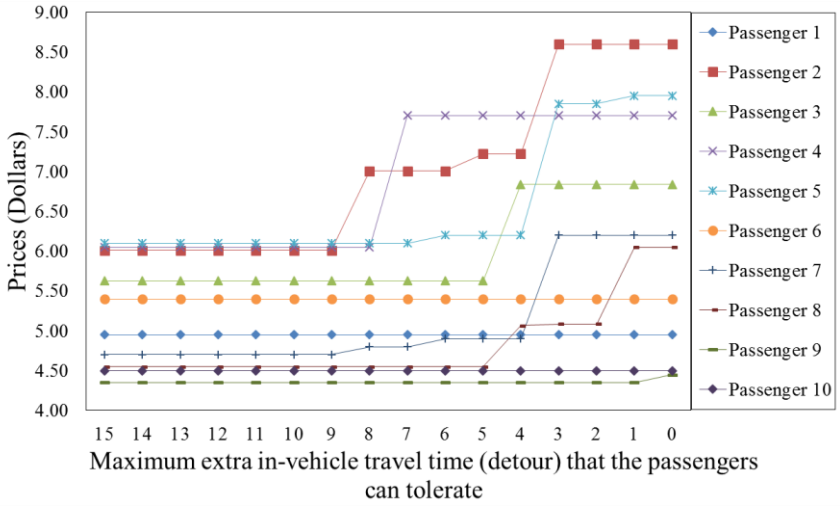
9.00
8.50
8.00
7.50
7.00
6.50
6.00
5.50
5.00
4.50
4.00
Prices (Dollars)
15 14 13 12 11 10 9 8 7 6 5 4 3 2 1 0
Maximum extra in-vehicle travel time (detour) that the passengers can tolerate
Passenger 1
Passenger 2
Passenger 3
Passenger 4
Passenger 5
Passenger 6
Passenger 7
Passenger 8
Passenger 9
Passenger 10

(b)

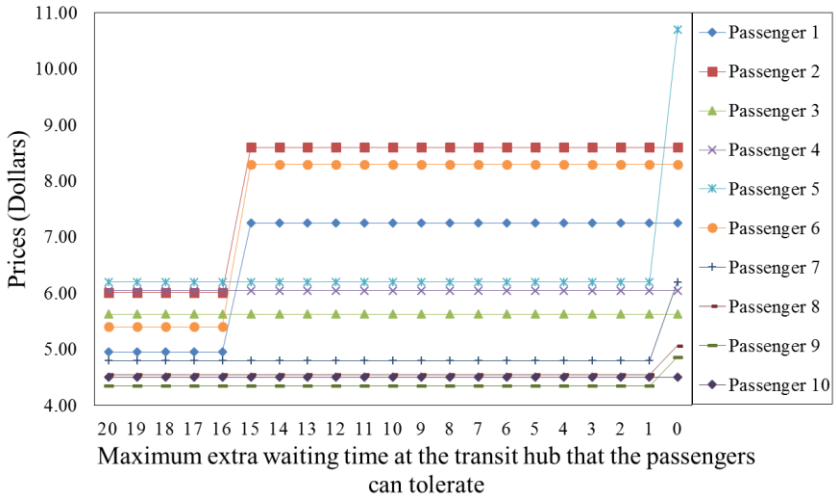

(c)

Figure 3.9 (a) Price Changing Caused by Tightening the Tolerance for the Number of Co-Riders in the First Scenario (b) Price Changing Caused by Tightening the Tolerance for Extra In-Vehicle Travel Time in the First Scenario (c) Price Changing Caused by Tightening the Tolerance for Extra Waiting Time in the First Scenario

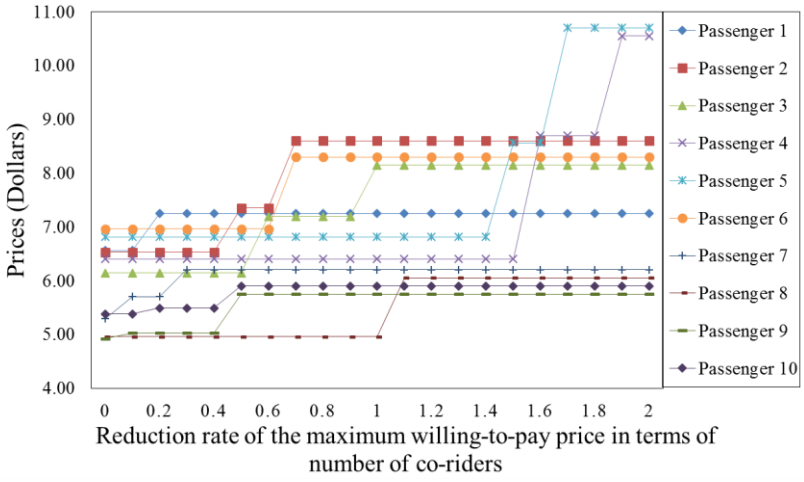

(a)

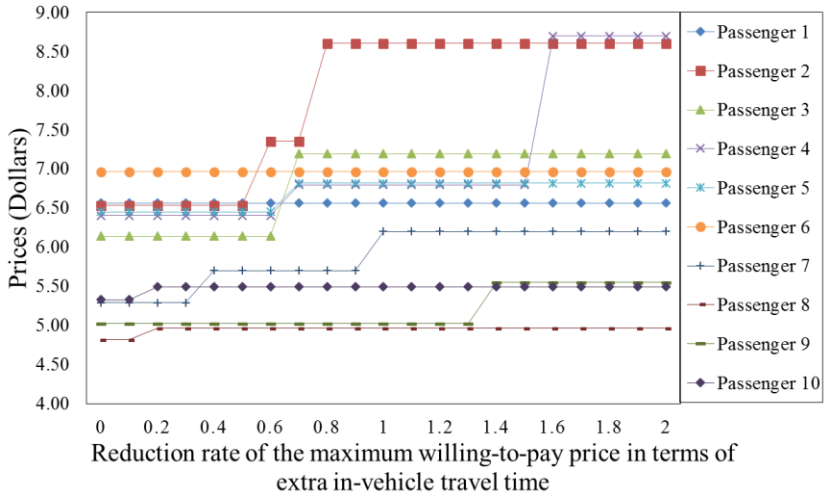

(b)

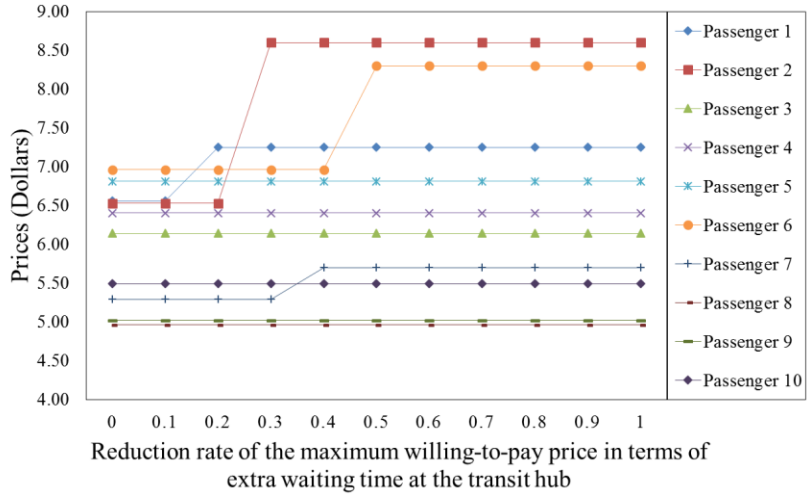

Figure 3.10 (a) Price Changing Caused by Tightening the Tolerance for the Number of Co-Riders in the Second Scenario (b) Price Changing Caused by Tightening the Tolerance for Extra In-Vehicle Travel Time in the Second Scenario (c) Price Changing Caused by Tightening for Extra Waiting Time in the Second Scenario

3.4.4 Summary

This section proposed a case study in two scenarios. The first scenario is more straightforward. Passengers can directly report their lowest tolerance for the three inconvenience attributes. However, the first scenario has a limitation for the value function: it assumes that as long as one passenger's requirements are satisfied, the maximum willing-to-pay price is constant. In the second scenario, the strictness of passengers' requirements is reflected in the reduction rate of the maximum willing-to-pay price in terms of the three inconvenience attributes. The value function shows that passengers' maximum willing-to-pay price decreases as the degree of any inconvenience attribute increases. We adopt these two scenarios to demonstrate the generality of the proposed mechanism that is flexible to be adapted into different scenarios. This case study straightforwardly shows the three properties, "individual rationality", "incentive compatibility" and "price non-negativity" of the mechanism in the two different scenarios. Moreover, the prices collected from participants can cover the transportation cost in this case. Chapter 4 will show the service provider's profit in more cases with various numbers of participants. The sensitivity analysis demonstrates that if passengers place stricter requirements on the inconvenience attributes, they may receive higher-quality service with a higher price.

In this case study, we only use one example in two specific scenarios to interpret the results of the mechanism. The scale of the problem is small because only ten passengers are involved. Thus, this example lacks generality and is incapable to test effectiveness of the potential algorithms in obtaining the mechanism for generalized large-scale problems. Chapter 4 will develop an efficient algorithm and test the performance of this algorithm using numerical examples with different scales.

3.5 Conclusions

This chapter considered passengers' personalized requirements when passengers use a first-mile ridesharing service. We design a mechanism to incentivize passengers to participate in the ridesharing service based on their personalized requirements. This mechanism simultaneously optimizes the vehicle-passenger matching and vehicle routing plan and determines each participant's incentive price. Passengers will receive a personalized service and a customized price based on their reported personalized requirements on the inconvenience attributes (e.g. number of co-riders, extra in-vehicle travel time, extra waiting time at the transit hub). We proved that the proposed mechanism is individual rational, incentive compatible, and price non-negative. A case study is given to demonstrate the generality of the mechanism to different scenarios.

CHAPTER 4 SOLUTION ALGORITHM FOR LARGE-SCALE PROBLEMS

4.1 Introduction

In order to incentivize more travelers to participate in the first-mile ridesharing service, the last chapter proposed an incentive mechanism based on passengers' personalized requirements on inconvenience attributes, including number of shared co-riders, extra in-vehicle travel time due to detour, and extra waiting time at the transit hub due to early arrival. It is proved that the mechanism has the properties of "individual rationality" and "incentive compatibility", respectively indicating that passengers' actual paid prices will never exceed their maximum willing-to-pay prices and truthfully reporting the personalized requirements is passengers' optimal strategy, if the mechanism is obtained by exact algorithms. The mechanism needs to solve one optimization problem to obtain the optimal vehicle-passenger matching and vehicle routing plan, as well as to solve n (the number of requests sent from passengers) different optimization models for calculating n prices for all passenger requests. All optimization models in the mechanism are extensions of vehicle routing problem and thus are NP hard (Lenstra and Kan 1981), which cannot be solved exactly within polynomial time. Thus, obtaining the desired mechanism has to address highly challenging computational complexity. Previous studies on truth-inducing mechanisms (Kamar and Horvitz 2009, Cheng et al. 2014, Zhao et al. 2014, Zhao et al. 2015, Asghari et al. 2016, Asghari and Shahabi 2017, Shen et al. 2016, Nguyen 2013, Zhang et al. 2016, Kleiner et al. 2011, Lloret-Batlle et al. 2017, Masoud et al. 2017b, Masoud and Lloret-Batlle 2016, Ma et al. 2018) for ridesharing organization have not developed effective solution algorithms that can handle large-scale, complex, NP-hard,

mechanism design models (particularly Vickrey-Clarke-Groves (VCG, Vickrey 1961, Clarke 1971, Groves 1973) prices). Thus, this chapter aims at addressing the challenging computational issue of mechanism obtainment.

When the scale of the problem is large, approximation or heuristic algorithms are more applicable to obtain the mechanism. However, VCG-based mechanisms obtained by regular approximation or heuristic algorithms may no longer be able to sustain the game theoretic properties, "individual rationality" and "incentive compatibility" (Nisan and Ronen 2007), and our mechanism is no exception. Several researchers developed some special approximation or heuristic algorithms to maintain "individual rationality" and/or "incentive compatibility" in obtaining their mechanisms. For example, Lehmann et al. (2002) proposed an approximately efficient mechanism for combinatorial auctions using a greedy algorithm; Mu'Alem and Nisan (2008), Parkes and Ungar (2001), and Dobzinski et al. (2010) developed approximation mechanisms that are incentive compatible for combinatorial auctions; Nisan and Ronen (2007) proposed a second chance mechanism to circumvent the problem, upon which participants can do no better than be truthful. Nevertheless, all of the methods are designed specifically for combinatorial auctions. These algorithms have never been adapted to solve generalized mechanism design models.

Based on the discussion of the knowledge gap, this chapter contributes to addressing these challenges by developing a computationally efficient heuristic algorithm called Solution Pooling Approach (SPA). The application of SPA is not limited to the mechanism design problem for first-mile ridesharing, but also can be spread to solve general mechanism design problems. Firstly, this chapter introduces the basic idea of SPA to solve generalized mechanism design problems, and analyzes specific circumstances

under which SPA is able to sustain the game-theoretic properties, including "individual rationality" and "incentive compatibility". The limitation of SPA is identified: if SPA needs to sustain "incentive compatibility", it may sacrifice solution quality more significantly than traditional heuristic algorithms compared with exact algorithms. Then, this chapter designs a specific SPA to obtain the personalized-requirement-based mechanism for the scheduled first-mile ridesharing service. We prove that the mechanism obtained by SPA is still "individual rational" and "incentive compatible". Moreover, SPA can reduce the computational time by simultaneously handling all models in this specific mechanism and does not need to solve all NP-hard problems one by one to obtain the mechanism. Numerical examples shows that the SPA is more efficient than the conventional heuristic algorithms (e.g. Hybrid Simulated Annealing–Tabu Search Algorithm and Hybrid Genetic Algorithm) with a tiny sacrifice of solution quality.

This chapter is structured as follows. Section 4.2 briefly introduces the basic idea of SPA to solve generalized mechanism design problems. Section 4.3 applies the SPA algorithm to solve the mechanism design problem for first-mile ridesharing based on passengers' personalized requirements. In Section 4.4, numerical examples are provided to verify the effectiveness of SPA. Concluding remarks are made in Section 4.5.

4.2 Basic Idea of SPA to Solve Generalized Mechanism Design Problems

4.2.1 Generalized Mechanism Design Problems

The market maker wants to design a mechanism to incentivize participants' collaboration to achieve a desirable objective (e.g. minimizing cost and maximizing the social welfare). Participants are allowed to report their personalized information to the system. Let $\theta = \{\theta_1, \theta_2, \dots, \theta_n\}$ denote all participants' reported information. Based on

participants' reported information, the mechanism needs to determine a plan ($X = O(\theta)$) and an incentive function (I_i). The plan (e.g. resource allocating plan, vehicle routing plan, matching plan, etc.) aims to achieve the desirable objective usually by solving an optimization model. We denote this optimization model as *IP*. Then the market maker will design an incentive function, which is denoted as $p_i = I_i(X, \theta)$, for individuals' participation based on the plan and participant's reported information. Incentive function has various forms, such as discounts, bonus points, credits, free service, etc. This chapter typically uses customized pricing as an incentive form.

4.2.2 A Generalized Individual Rational and Incentive Compatible Mechanism

In order to achieve the market maker's objective, the mechanism should 1) ensure that the participants are willing to collaborate with each other and 2) prevent them manipulating the mechanism by misreporting their personalized information on purpose. These two considerations necessitate the properties of "individual rationality" and "incentive compatibility". "Individual rationality" indicates that the actual paid price will never exceed participants' maximum willing-to-pay price. "Incentive compatibility" requires that participants' utility (defined as the difference between the maximum willing-to-pay price and the actual paid price) can be maximized if they truthfully report their personalized information. This section proposes a generalized individual rational and incentive compatible mechanism. The optimal plan is obtained by solving the model *IP*. The pricing framework is calculated by designing and solving a series of models, including one model IP_0 and n models IP_g (corresponding to participant g). Model IP_0 should be equivalent to the original optimization model *IP* and thus the optimal solutions of models *IP* and IP_0 are identical. Models IP_g are used to calculate the prices only and do not have

practical meaning. Both models IP_0 and IP_g use participants' reported information (θ) as input data and both have maximizing objective functions. Then the pricing scheme is given by

$$p_g = g(X^{IP_g^*}) - (f(X^{IP_0^*}) - V_g(X^{IP_0^*})) \quad (1)$$

p_g is participant g's price. $X^{IP_g^*}$ is the optimal solution of model IP_g, and $g(.)$ is the maximizing objective function of the model. $X^{IP_0^*}$ is the optimal solution of model IP_0 with the maximizing objective function $f(.)$. $V_g(X)$ is participant g's value, which is defined as participant g's maximum willing-to-pay price in this chapter, given the plan X. The objective function $f(.)$ includes summation of all participants' values.

$$f(X) = \sum_{i \in P} V_i(X) + h(X) \quad (2)$$

where $h(X)$ is used to make the model IP_0 equivalent to the original model IP.

This pricing scheme makes the mechanism "individual rational" if the following condition is always satisfied

$$g(X^{IP_g^*}) \leq f(X^{IP_0^*}) \quad (3)$$

This is because participant g's utility is $U_g = V_g(X^{IP_0^*}) - p_g = f(X^{IP_0^*}) - g(X^{IP_g^*}) \geq 0$, if the condition above is satisfied. A direct idea to satisfy this condition is to design the

model IP_g that makes the objective function $g(X)$ identical with $f(X)$ and let the feasible regions of models IP_g (for all g) be included in the feasible region of model IP_0. That is

$$g(X) = f(X) \tag{4}$$

$$CS_{IP_g} \subseteq CS_{IP_0} \tag{5}$$

where the CS_{IP_g} and CS_{IP_0} are the feasible regions of models IP_g and IP_0, respectively.

If model IP_g is independent of participant g's report, then the mechanism is "incentive compatible".

If participant g misreports the personalized information, then we assume that the optimal solution of model IP_0 changes from $X^{IP_0^*}$ to $Y^{IP_0^*}$, $g(X^{IP_g^*})$ remains constant because $g(X^{IP_g^*})$ is independent of participant g's report, and $f(X^{IP_0^*})$ changes to

$$f'(Y^{IP_0^*}) = \sum_{i \in P, i \neq g} V_i(Y^{IP_0^*}) + V_g'(Y^{IP_0^*}) + h(Y^{IP_0^*})$$

Then, the price becomes

$$p_g' = g(X^{IP_g^*}) - \left(f'(Y^{IP_0^*}) - V_g'(Y^{IP_0^*}) \right) = g(X^{IP_g^*}) - \left(\sum_{i \in P, i \neq g} V_i(Y^{IP_0^*}) + h(Y^{IP_0^*}) \right)$$

Then participant g's utility becomes

$$U'_g = V_g(Y^{IP_0*}) - p'_g = \left(\sum_{i \in P} V_i(Y^{IP_0*}) + h(Y^{IP_0*})\right) - g(X^{IP_g*}) = f(Y^{IP_0*}) - g(X^{IP_g*})$$

Y^{IP_0*} may no longer be optimal for model IP_0, indicating that the objective function of model IP_0, $f(.)$, will suffer from a decrease caused by her misreporting. Thus, her utility $U_g = f(X^{IP_0*}) - g(X^{IP_g*})$ may decrease as well if she misreports her personalized requirement. Therefore, truthful reporting is participants' optimal strategy:

$$U'_g = f(Y^{IP_0*}) - g(X^{IP_g*}) \leq f(X^{IP_0*}) - g(X^{IP_g*}) = U_g \tag{6}$$

The famous Vickrey-Clarke-Groves (Vickrey 1961, Clarke 1971, Groves 1973) mechanism, which is widely applied in various research fields (Friedman and Parkes 2003, Kamar and Horvitz 2009, Samadi et al. 2012, etc.), belongs to this category and thus has the properties of "individual rationality" and "incentive compatibility".

4.2.3 SPA to the Individual Rational and Incentive Compatible Mechanism

If the optimization models in the mechanism are NP hard, they are difficult to be solved exactly within reasonable amount of time when the problem scale is large. Many researchers (Wang et al. 2016, Lin et al. 2016, Gupta et al. 2017, Chao et al. 2017, etc.) sought heuristic or approximation algorithms to find a high-quality solution to their optimization problems instead of an exact one. However, applying traditional heuristic or approximation algorithms may lose the properties of "individual rationality" and "incentive compatibility". Let us return to the generalized mechanism in Subsection 4.2.2. The

mechanism is individual rational if the condition $g(X^{IP_g^*}) \leq f(X^{IP_0^*})$ (Formula 3) is always satisfied. However, if the solution $X^{IP_0^*}$ is obtained by a heuristic or approximation algorithm, the optimality of $X^{IP_0^*}$ cannot necessarily be guaranteed, and thus it is possible that $f(X^{IP_0^*}) < g(X^{IP_g^*})$ and $U_g < 0$. The property "individual rationality" is thus possibly violated. Similarly, the mechanism obtained by heuristic or approximation algorithms may not be incentive compatible as well. Suppose that $X^{IP_0^*}$ is the optimal solution of model IP_0 if participant g truthfully reports his personalized information and the solution becomes $Y^{IP_0^*}$ (not necessarily optimal) if participant g misreports the information. If heuristic or approximation algorithms are used to solve the model, it is possible that $f(Y^{IP_0^*}) > f(X^{IP_0^*})$, because the optimality of $X^{IP_0^*}$ cannot be guaranteed. Thus, implied from Formula (6), participants' utilities may not be maximized even though they tell the truth. Similar conclusions have already been drawn by other researchers (Mu'Alem and Nisan 2008, Parkes 2001, Dobzinski et al. 2010, Nisan and Ronen 2007).

Therefore, this chapter proposes a special heuristic algorithm, namely Solution Pooling Approach (SPA), to obtain the mechanism, sustaining the properties of "individual rationality" and "incentive compatibility" under specific circumstances. The SPA is inspired from the work of Bent and Hentenryck (2004)'s multiple plan approach and Gendreau et al. (1999)'s tabu search algorithm organized around multiple solutions and an adaptive memory. The basic idea of SPA can be described as follows. Firstly, the algorithm generates high-quality solutions of models IP_0 and IP_g (for all participants g) as solution pools. Then, the solutions of corresponding models with highest qualities are selected from the solution pools. Let $Xpool^{IP_0}$ and $Xpool^{IP_g}$ denote the solution pools of model IP_0

and IP_g, respectively. Let X^{IP_0*} and X^{IP_g*} denote the optimal solutions in the pools $Xpool^{IP_0}$ and $Xpool^{IP_g}$, respectively. Then, X^{IP_0*} is adopted as the matching and routing plan, and the pricing scheme still adopts Formula (1).

When generating solution pools, if the condition $g(X^{IP_g*}) \le f(X^{IP_0*})$ (Formula 3) is still satisfied, the mechanism is "individual rational". If we use Formulas (4) and (5) to satisfy Formula (3), SPA can easily guarantee "individual rationality" by the following approach. Since the feasible regions of models IP_g (for all g) are included in the feasible region of model IP_0, feasible solutions of model IP_g are feasible to model IP_0 as well. Solutions in pools $Xpool^{IP_g}$ can be integrated into the solution pool $Xpool^{IP_0}$. After the algorithm generates all of the solution pools $Xpool^{IP_g}$, all solutions in each pool $Xpool^{IP_g}$ are combined into the solution pool $Xpool^{IP_0}$ (i.e. $Xpool^{IP_g} \subset Xpool^{IP_0}$, for any g). Then, the optimal solution (X^{IP_0*}) is selected from $Xpool^{IP_0}$, and each X^{IP_g*} is selected from $Xpool^{IP_g}$. Since we have $X^{IP_g*} \in Xpool^{IP_g} \subset Xpool^{IP_0}$ and X^{IP_0*} is the optimal solution in $Xpool^{IP_0}$ with maximized objective $f(.)$, $f(X^{IP_g*}) \le f(X^{IP_0*})$. Based on Formula (4), $g(X^{IP_g*}) = f(X^{IP_g*}) \le f(X^{IP_0*})$, and then "individual rationality" can be guaranteed.

The property "incentive compatibility" is naturally guaranteed as long as the generation of solution pools of model IP_g (for any participant g) is independent of participant g's report and the solution pool of model IP_0 is pre-generated before participants' personalized information is revealed. Both X^{IP_0*} and Y^{IP_0*} in Formula (6) are selected from the pre-generated pool $Xpool^{IP_0}$. Since X^{IP_0*} is the optimal solution in $Xpool^{IP_0}$ while Y^{IP_0*} is not necessarily the optimal in $Xpool^{IP_0}$, $f(Y^{IP_0*}) \le f(X^{IP_0*})$ in Formula (6)

can always be satisfied. Thus, the mechanism obtained by SPA is incentive compatible.

SPA is an efficient heuristic algorithm that can sustain the properties of "individual rationality" and "incentive compatibility" under specific circumstances analyzed above, but it still has limitations. SPA needs to pre-generate the solution pools for models IP_0 and IP_g before participants report their personalized information to sustain "incentive compatibility", leading to possible more significant sacrifice of solution quality than traditional heuristic algorithms. SPA has to significantly increase the number of solutions in the pool in order to improve the solution quality, but this will consume more computer memory. In Section 4.4, our numerical examples are designed to test how much SPA will sacrifice the solution quality in obtaining the mechanism for first-mile ridesharing service.

4.3 Application of SPA to Solve the Mechanism Design Problem for First-Mile Ridesharing

This section designs a detailed solution pooling approach to solve the mechanism design problem for the scheduled first-mile ridesharing service proposed in our last chapter.

4.3.1 Mechanism Design Problem for First-Mile Ridesharing Based on Personalized Requirements

This subsection reviews the personalized-requirement-based mechanism design problem for a first-mile ridesharing service. Passengers near the transit hub book the first-mile ridesharing service in advance. The service provider dispatches a fleet of vehicles to execute the pickup and drop-off tasks. Each request specifies a deadline before which passenger(s) must arrive at the transit hub. In addition to the passengers' pickup locations and the arrival deadlines, passengers are allowed to report their personalized requirements

on three inconvenience factors, the number of co-riders, extra in-vehicle travel time, and extra waiting time at the transit hub. Before vehicles are dispatched, the system will determine an optimal vehicle-passenger matching and vehicle routing plan X^* and all passengers' customized prices $\mathbf{p} = \{p_1, p_2, \dots, p_n\}$, which form the mechanism $M(X^*, \mathbf{p})$. The optimal matching and routing plan X^* is obtained by solving an optimization model (denoted as *IP*) with the objective of minimizing passengers' inconvenience cost and the service provider's transportation cost. The model *IP* is the formulated by in Chapter 3. The pricing scheme is obtained by solving a series of optimization models, including one model IP_0 and n models IP_g for all $g \in P$, which are summarized in Table 4.1. For the notations and formulas, please refer to Chapter 3.

Table 4.1 Mathematical Models for Obtainment of the Mechanism

Model denotations	Objective functions	Constraints	Optimal solution	Optimal objective function value
IP_0	$f(X)$: Formula (A-2) Max $Z_0(X)$	CS_{IP_0} Formulas (A-3) – (A-12)	X^{IP_0*}	$Z^*_{IP_0}$
IP_g for all $g \in P$	$g(X)$: Formula (A-2) Max $Z_0(X)$	CS_{IP_g} Formulas (A-3) – (A-13)	X^{IP_g*}	$Z^*_{IP_g}$

Note that model IP_0 is equivalent to model *IP*, and thus the optimal solutions of

models IP_0 and IP are identical ($X^{IP_0*} = X^*$). The mechanism is denoted as $M\left(X^{IP_0*}, \mathbf{p}\right)$, where X^{IP_0*} represents the optimal vehicle-passenger matching and routing plan, and passengers' prices $\mathbf{p} = \{p_1, p_2, ..., p_n\}$ are calculated by

$$p_g = Z^*_{IP_g} - \left(Z^*_{IP_0} - V_g\left(X^{IP_0*}\right)\right) \tag{7}$$

Note that models IP_0 and IP_g have identical objective function, and that the feasible region of model IP_g is included in the feasible region of model IP_0 because model IP_g has an additional constraint (Formula A-13) compared with model IP_0. Thus, the mechanism is "individual rational" based on Formulas (4) and (5). Moreover, the optimal solution is independent on passenger(s) g's report of the parameters of α_i^{NR}, α_i^{IVT} and α_i^{WT} because passenger(s) g's inconvenience cost is zero and the value is a constant ($V^i_{\max}$) if the passenger(s) is transported to the transit hub directly without shared riders, no matter what values of α_i^{NR}, α_i^{IVT} and α_i^{WT} the passenger(s) reports. Thus, the mechanism is "incentive compatible". For detailed proof of these two properties, please refer to our last chapter.

4.3.2 Identified Challenges to Obtain the Mechanism

The optimization models in the mechanism, including IP_0 and IP_g ($g \in P$), are extensions of the classical vehicle routing problem and thus are NP hard (Lenstra and Kan 1981). When the scale of the problem is large, exact algorithms are difficult to obtain the optimal solution within reasonable amount of time. Heuristic algorithms are more applicable for large-scale problems. When passengers send n requests, the mechanism $M\left(X^{IP_0*}, \mathbf{p}\right)$ includes n+1 NP hard optimization models, including one optimization

model IP_0 used to determine the optimal vehicle-passenger matching and vehicle routing plan X^{IP_0*} and n optimization models IP_g (g=1, 2, … , n) that are used to calculate all prices. Regular heuristic algorithms (e.g. Simulated Annealing and Genetic Algorithm) are still time-consuming in solving these models one by one. Moreover, as analyzed in Subsection 4.2.3, if traditional heuristic algorithms are used to obtain the mechanism $M\left(X^{IP_0*}, \mathbf{p}\right)$, the properties of "individual rationality" and "incentive compatibility" are not necessarily guaranteed.

To overcome these challenges, we propose a novel heuristic algorithm called **Solution Pooling Approach (SPA)** to obtain the mechanism $M\left(X^{IP_0*}, \mathbf{p}\right)$. As we will show later, the method may not obtain exact results but can ensure the validity of game-theoretic properties, "individual rationality" and "incentive compatibility". This method can simultaneously handle all models in $M\left(X^{IP_0*}, \mathbf{p}\right)$ and does not need to solve all NP-hard problems one by one to obtain the mechanism because the n+1 models have very similar form. Thus, it is much more time-efficient than regular heuristic algorithms.

4.3.3 Solution Pooling Approach to Mechanism Design

The main idea of the SPA is to select the highest-quality solutions that are all feasible to the corresponding models from pre-generated solution pools to obtain a vehicle-passenger matching and vehicle routing plan and to calculate all passengers' prices. We denote the solution pools of IP_0 and IP_g as $Xpool^{IP_0}$ and $Xpool^{IP_g}$, respectively. The generation of $Xpool^{IP_0}$ and $Xpool^{IP_g}$ can be described as follows. First, SPA generates an initial solution pool in which all solutions are feasible to the optimization model IP_0 (see Algorithm 1). We denote it as *Xpool*. Then solution pools of models IP_g (g = 1, 2, … , n)

are obtained based on *Xpool*. We design a transition solution generation algorithm (see Algorithm 2) to generate solution pools $Xpool^{IP_g}$ of models IP_g. All solutions in $Xpool^{IP_g}$ for all $g = 1, 2, \ldots, n$ are combined into the initial pool *Xpool* and a new solution pool $Xpool^{IP_0}$ of model IP_0 is generated. Finally, the optimal solutions are selected from corresponding solution pools $Xpool^{IP_0}$ and $Xpool^{IP_g}$. The matching and routing plan adopts the optimal solution selected from the pool $Xpool^{IP_0}$. All passengers' prices are calculated based on Formula (7).

The initial solution pool *Xpool* should be pre-generated and passengers' reported personalized requirements (α_i^{NR}, α_i^{IVT} and α_i^{WT}, see notations in Table 3.3 in Chapter 3) on the three inconvenience attributes do not influence the generation of the solution pool so that the mechanism obtained by SPA is still incentive compatible (please refer to the proof of the incentive compatibility proposition of the SPA in Subsection 4.3.4). Thus, we propose two strategies to improve the quality of the selected solution from the obtained solution pool of IP_0: 1) generate a large enough number of solutions in the solution pool *Xpool* and select the best solutions from the pool; 2) randomly and periodically simulate virtual personalized requirements parameters (α_i^{NR}, α_i^{IVT} and α_i^{WT}) that are used to direct to generate the solutions in a wide range and the quality of the optimal solution can be guaranteed. A meta-heuristic algorithm, tabu search (TS) plays the role of solution generator. TS is able to avoid repeated the generation of identical solutions using a memory function (Gendreau et al. 1994). Algorithm 1 gives the pseudocode of the solution pool generation algorithm.

Algorithm 1 Generation of solution pool *Xpool*

Input the total number of iterations (*NI*), number of iterations in each period (*NIP*) for updating values α_i^{NR}, α_i^{IVT} and α_i^{WT}, number of candidate solutions (*CN*), number of solutions (*NS*) assigned into the solution pool for each iteration, and all other parameters of the problem;

Initialize a feasible solution X_0 to the model IP_0 as the current solution $X_{current}$, the virtual values of α_i^{NR}, α_i^{IVT} and α_i^{WT}, $it = 0$ (current number of iterations), $pit = 0$ (current number of iterations in one period), and the empty solution pool *Xpool*;

Do while $it < NI$

If $pit > NIP$

$pit = 0$;

Use the uniform distribution to re-generate the values of α_i^{NR}, α_i^{IVT} and α_i^{WT};

End if

Generate *CN* candidate solutions $\{X_1, X_2, \ldots, X_{CN}\}$ of $X_{current}$'s neighbors;

Calculate $\{\Delta Z_0(X_1), \Delta Z_0(X_2), \ldots, \Delta Z_0(X_{CN})\}$ ($\Delta Z_0(X_i) = Z_0(X_i) - Z_0(X_{current})$) and record the subscript *opt*, where $\Delta Z_0(X_{opt}) = \max\{\Delta Z_0(X_1), \Delta Z_0(X_2), \ldots, \Delta Z_0(X_{CN})\}$;

Randomly select *NS* solutions from *CN* candidate solutions $\{X_1, X_2, \ldots, X_{CN}\}$ and put them into the solution pool *Xpool*;

Do while X_{opt} is in tabu list

Select the suboptimal solution as X_{opt} from $\{X_1, X_2, \ldots, X_{CN}\}$;

End do

$X_{current} = X_{opt}$;

Update the tabu list;

it = *it* + 1;

pit = *pit* + 1;

End do

Output *Xpool*.

Then we introduce the definition of the "transition solution", which is also defined in our last chapter. "Transition solution" will be used to obtain solution pools $Xpool^{IP_g}$ of model IP_g for all $g = 1, 2, \ldots, n$ in the SPA algorithm. Let $Y_g = TRS_g(X)$ be the g^{th} transition solution from a feasible solution X of the model IP_0. The transition process is generated as follows. Let passenger(s) g go to the transit hub directly without any other shared riders, and let the broken routes be re-connect. In Y_g, since passenger(s) g is transported to the transit hub directly without shared riders, Formula (A-13) is satisfied and Y_g is a feasible solution of model IP_g.

Figure 4.1 shows an example of transition solution generation. Algorithm 2 shows how to get the transition solution.

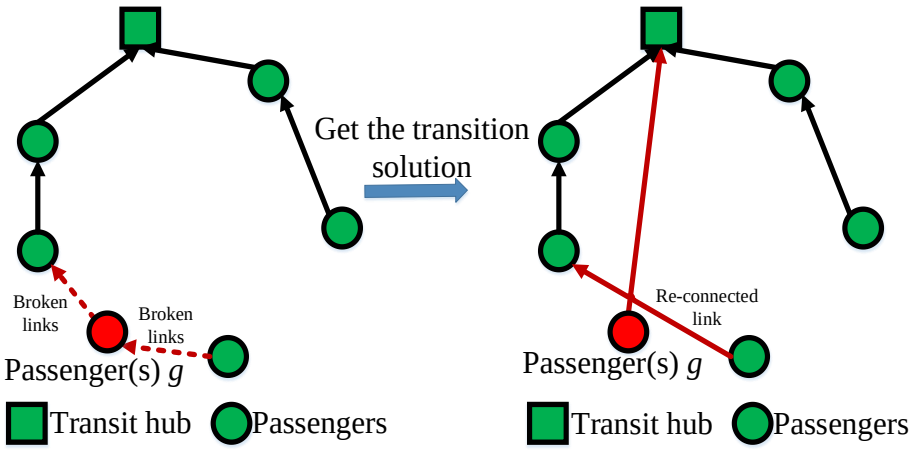

Figure 4.1 Example of the Transition Solution

Algorithm 2 Obtain the transition solutions $Y_g = TRS_g(X)$
Input a solution $X = \{x_{ijk}, y_{ik}\}$; Let $Y_g = X$; **If** $NR_g > 0$ Find k that $y_{gk} = 1$, and let $y_{gk} = 0$; Let another vehicle k' without tasks to pick up passenger(s) g, $y_{gk'} = 1$ and $x_{g0k'} = 1$; Find j that $x_{gjk} = 1$, and let $x_{gjk} = 0$; Find i that $x_{igk} = 1$, and let $x_{igk} = 0$; Let $x_{ijk} = 1$; **End if** Output Y_g.

Finally we use Algorithm 3 to get the mechanism, including the optimal matching and routing plan and all passengers' prices. Figure 4.2 is the flow chart of SPA.

Algorithm 3 SPA to the mechanism
Input the solution pool *Xpool* obtained by Algorithm 1 and all parameters of the problem; **For** $g = 1{:}n$

Use Algorithm 2 to get the transition solutions of all the solutions in *Xpool* as the solution pool of IP_g, $Xpool^{IP_g}$:

$$Xpool^{IP_g} = \left\{ Y_i^{IP_g} \middle| Y_i^{IP_g} = TRS_g\left(X_i\right), \text{ for all } X_i \in Xpool \right\};$$

End for

Let $Xpool^{IP_0} = \left\{ Xpool, Xpool^{IP_g} (\text{for all } g \in P) \right\}$;

Select the solution $X^{IP_0^*}$ from $Xpool^{IP_0}$ that $X^{IP_0^*} = \arg\max Z_0\left(X\right)$ $X \in Xpool^{IP_0}$;

Let $Z_{IP_0}^* = Z_0\left(X^{IP_0^*}\right)$;

For $g = 1{:}n$

Select the solution $X^{IP_g^*}$ from $Xpool^{IP_g}$ that $X^{IP_g^*} = \arg\max Z_0\left(X\right)$

$X \in Xpool^{IP_g}$;

Let $Z_{IP_g}^* = Z_0\left(X^{IP_g^*}\right)$;

Calculate the prices:

$$p_g = Z_{IP_g}^* - \left(Z_{IP_0}^* - V_g\left(X^{IP_0^*}\right)\right);$$

End for

Output the optimal solution of IP_0 ($X^{IP_0^*}$) and all passengers' prices

$\mathbf{p} = \{p_1, p_2, ..., p_n\}$.

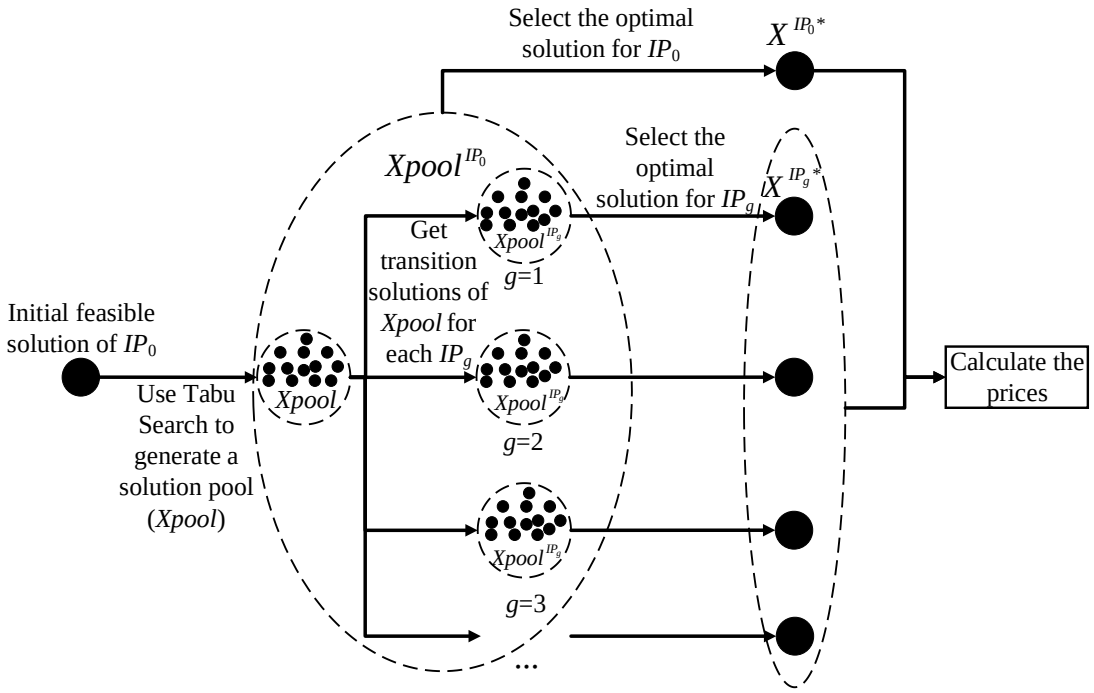

Figure 4.2 Flow Chart of SPA in Obtaining the Mechanism

4.3.4 Theoretical Analysis of SPA

The propositions of this mechanism including "individual rationality" and "incentive compatibility" are still valid if SPA is used to obtain the mechanism $M\left(X^{IP_0*}, \mathbf{p}\right)$. Before giving the proof of the propositions, we re-formulate the problems based on SPA.

In Algorithm 3, X^{IP_0*} is the optimal solution selected from the solution pool $Xpool^{IP_0}$, and thus X^{IP_0*} is also the optimal solution of the optimization model below (Formulas 8 and 9). We denote this model as $IPpool_0$.

$$Z^*_{IP_0} = \max Z_0(X) \tag{8}$$

Subject to,

$$X \in Xpool^{IP_0} \tag{9}$$

Similarly, $X^{IP_g^*}$ is the optimal solution of the optimization model below, which is used for calculation of passenger(s) g's customized price. We denote this model as $IPpool_g$ (Formulas 10 and 11)

$$Z^*_{IP_g} = \max Z_0(X) \tag{10}$$

Subject to,

$$X \in Xpool^{IP_g} \tag{11}$$

Proposition 1: Individual Rationality

If $X^{IP_0^*}$ and $X^{IP_g^*}$ are the optimal solutions of $IPpool_0$ and $IPpool_g$, respectively, the mechanism $M\left(X^{IP_0^*}, \mathbf{p}\right)$ is individual rational, i.e. the utility

$$U_g\left(X^{IP_0^*}, p_g\right) = V_g\left(X^{IP_0^*}\right) - p_g \geq 0, \text{ for any } g \in P \tag{12}$$

Proof:

$X^{IP_0^*}$ is the optimal solution of the model $IPpool_0$, and thus $Z_0\left(X^{IP_0^*}\right) \geq Z_0(X)$

for any $X \in Xpool^{IP_0}$. Since $X^{IP_g*} \in Xpool^{IP_g} \subseteq Xpool^{IP_0}$, X^{IP_g*} is a feasible solution of $IPpool_0$. Thus $Z_0\left(X^{IP_0*}\right) \geq Z_0\left(X^{IP_g*}\right)$.

$$
\begin{aligned}
&U_g\left(X^{IP_0*}, p_g\right) = V_g\left(X^{IP_0*}\right) - p_g \\
&= V_g\left(X^{IP_0*}\right) - Z_0\left(X^{IP_g*}\right) + \left(Z_0\left(X^{IP_0*}\right) - V_g\left(X^{IP_0*}\right)\right) \\
&= Z\left(X^{IP_0*}\right) - Z_0\left(X^{IP_g*}\right) \geq 0
\end{aligned}
$$

This implies that the participants can always receive non-negative utility from the first-mile ridesharing service

□

Proposition 2

The mechanism $M\left(X^{IP_0*}, \mathbf{p}\right)$ is incentive compatible if the optimal matching and routing plan X^{IP_0*} and the prices $\mathbf{p}$ are obtained by SPA.

Proof:

Suppose that passenger(s) g misreports the requirements on the number of shared riders, extra in-vehicle travel time and extra waiting time (α_i^{NR}, α_i^{IVT} and α_i^{WT}), respectively.

We define $V_i'(X) = V_{\max}^i - C^{ICN}\left(NR_i(X), IVT(X)_i, WT_i(X), \beta_i^{NR}, \beta_i^{IVT}, \beta_i^{WT}\right)$ regardless of other passenger's reporting strategy, where β_i^{NR}, β_i^{IVT} and β_i^{WT} are passenger(s) i's misreported values of α_i^{NR}, α_i^{IVT} and α_i^{WT}, respectively.

Since $Xpool^{IP_0}$ and $Xpool^{IP_g}$ are all generated independently on all passengers'

report of their personalized requirements, the solution pools $Xpool^{IP_0}$ and $Xpool^{IP_g}$ remain constant no matter how passengers report their requirements. Thus, the constraints of $IPpool_0$ and $IPpool_g$ remain constant regardless of passengers' reporting strategy. If passenger(s) g misreports the requirements, the optimization model $IPpool_0$ becomes $IPpool_0'$:

$$Z^*_{IP_0'} = \max Z_0'(X) = \sum_{i \in P, i \neq g} V_i(X) + V_g'(X) - TC(X), \text{ s.t. } X \in Xpool^{IP_0}$$

Other passengers' values are calculated based on their actual report of personalized requirements regardless of the truthfulness. The optimal solution (denoted by $X^{IP_0'^*}$) of $IPpool_0'$ is still feasible for $IPpool_0$. We have $Z_0\left(X^{IP_0^*}\right) \geq Z_0\left(X^{IP_0'^*}\right)$ because $X^{IP_0^*}$ is the optimal solution of $IPpool_0$ while $X^{IP_0'^*}$ is a feasible solution of $IPpool_0$. Moreover, the model $IPpool_g$ never changes no matter what passenger(s) g reports. This is because 1) the constraints of $IPpool_g$ remains constant no matter how passengers report their requirements and 2) the objective function value is independent of passenger(s) g's report. Thus the passenger(s) g's price is

$$p_g' = Z^*_{IP_g} - \left(Z^*_{IP_0'} - V_g'\left(X^{IP_0'^*}\right)\right)$$

The utility that passenger(s) g can receive is:

$$
\begin{aligned}
&U_g\left(X^{IP_0'^*}, p_g'\right) = V_g\left(X^{IP_0'^*}\right) - p_g' \\
&= V_g\left(X^{IP_0'^*}\right) - \left(Z^*_{IP_g} - \left(Z^*_{IP_0'} - V_g'\left(X^{IP_0'^*}\right)\right)\right) \\
&= V_g\left(X^{IP_0'^*}\right) - \left(Z^*_{IP_g} - \left(\sum_{i\in P, i\neq g} V_i\left(X^{IP_0'^*}\right) + V_g'\left(X^{IP_0'^*}\right) - TC\left(X^{IP_0'^*}\right) - V_g'\left(X^{IP_0'^*}\right)\right)\right) \\
&= \sum_{i\in P} V_i\left(X^{IP_0'^*}\right) - TC\left(X^{IP_0'^*}\right) - Z^*_{IP_g} \\
&= Z_0\left(X^{IP_0'^*}\right) - Z^*_{IP_g} \\
&\leq Z_0\left(X^{IP_0^*}\right) - Z^*_{IP_g} \\
&= U_g\left(X^{IP_0^*}, p_g\right)
\end{aligned}
$$

which indicates that the passenger receives largest utility when telling the truth regardless of other passengers' reporting strategy. Therefore the mechanism is incentive compatible.

□

Note that it is very difficult to develop approximate or heuristic algorithms to simultaneously guarantee "price non-negativity" as well as "individual rationality" and "incentive compatibility". The SPA algorithm is proved to be individual rational and incentive compatible but may not guarantee the property of "price non-negativity". However, the numerical experimental results in Section 4.4 show that SPA never obtains negative prices.

4.4 Numerical Experiment

4.4.1 Design of Numerical Examples

In Chapter 3, we developed a case study to interpret the results of the mechanism. However, it does not have generality because it only contains two specific scenarios, in which passengers have two different reporting methods and two types of value functions. Moreover, the scale of the problem in the case study is small: only ten passenger requests are involved. Thus it is not possible to test the effectiveness of the proposed algorithm in obtaining the large-scale generalized mechanism. In this chapter, we develop thirteen numerical examples to test the proposed algorithm in obtaining the mechanism $M\left(X^{IP_0*}, \mathbf{p}\right)$. In order to show the trend of experimental results with the scale of problems increasing, the number of passenger requests involved in the system increases from 4 to 52 by the interval of 4. Both horizontal and vertical coordinates (x_i, y_i) of all passenger locations in numerical examples are generated uniformly from the interval [6, 12]. All coordinates of the transit hubs are set to be (9, 9), approximately located in the center of all passengers. For convenience but without losing generality, the transportation cost between two locations is proportional to the Euclidean distance: $c_{ij} = 2d_{ij}$, where d_{ij} is the distance between two locations. We determine that $V^i_{\max} = 3 + 3d_{i0}$. The traveling time between two locations is not necessarily proportional to the distance. Thus, we use a different method to generate the travel time between two locations. Virtual coordinates (xv_i, yv_i) of locations are generated, which satisfy: $xv_i = x_i + \varepsilon$ and $yv_i = y_i + \varepsilon$. ε is normally distributed with the mean of "0" and variance of "0.1". ε is randomly generated by the computer. The travel time between i and j is set to be

$t_{ij} = 3\sqrt{\left(xv_i - xv_j\right)^2 + \left(yv_i - yv_j\right)^2}$.

Passengers' personalized requirements (α_i^{NR}, α_i^{IVT}, and α_i^{WT}, in any form) on the three inconvenience attributes can be processed into an interval [0, 1], representing the strictness of the requirements. Since the passengers' personalized requirements are processed, we cannot use the value functions proposed in Chapter 3 because the values of α_i^{NR}, α_i^{IVT}, and α_i^{WT} are no longer compatible with the value functions in Chapter 3. Thus, we propose another illustrative value function (Formula 13), which is compatible with the processed values of α_i^{NR}, α_i^{IVT}, and α_i^{WT}, and will be used in numerical examples to test the algorithm.

$$V_i = V_{\max}^i - \left(\frac{\alpha_i^{NR} NR_i}{Q - np_i} + \frac{\alpha_i^{IVT}\left(IVT_i - t_{i0}\right)}{t_{i0}} + \frac{\alpha_i^{WT} WT_i}{MD} \right)\left(\frac{V_{\max}^i - c_{i0}}{2} \right) \tag{13}$$

MD is the maximum difference among passengers' arrival deadlines. Here $MD = \max_{i,j \in P}\left(DL_i - DL_j\right) = 15$, indicating that we only optimize the matching and routing plan connecting to train schedules in which differences in passengers' arrival deadlines do not exceed 15 minutes. We set the default values of α_i^{NR}, α_i^{IVT}, and α_i^{WT} to 0.1. In other words, if the passengers do not report their requirements, the system will adopt the default values. We set half of the values α_i^{NR}, α_i^{IVT}, and α_i^{WT} to 0.1 as the default values, indicating that half of passengers do not open the interface to place stricter personalized requirements for the ridesharing service. The other half of the values α_i^{NR}, α_i^{IVT}, and α_i^{WT} are randomly generated from the uniform distribution interval [0, 1]. Formula (13) builds on the

assumption that passengers are willing to pay a price at least equal to the minimum transportation cost (c_{i0}) if they are transported to the transit hub within the minimum travel time t_{i0} ($V_i \geq c_{i0}$, if $IVT_i = t_{i0}$). This is a reasonable assumption because if passengers drive themselves to the transit hub, they have to bear the direct shipment cost (c_{i0}). Note that we use this hypothetical function just to test the algorithm and the accuracy of this value function has not been verified through practical survey. We will use another value function, in which passengers' attitude towards the price is stricter, in the sensitivity analysis to demonstrate the robustness of the proposed algorithm in obtaining the mechanism under different conditions.

4.4.2 Testing Method and Criteria

This subsection compares the solution pooling approach (SPA) with an exact algorithm, commercial solvers, and selected state-of-the-art heuristic algorithms. We use the enumeration algorithm (EA) as a representative of the exact algorithm to solve small-scale problems (numerical examples with 4 and 8 passenger requests). Effective exact algorithms (e.g. branch and bound) are not developed in this chapter because they are difficult to adapt to generalized models with different objective functions. We use seven commercial solvers, ANTIGONE, ALPHAECP, BARON, COUENNE, LINDOGLOBAL, SBB, and SCIP (https://neos-server.org/neos/solvers/index.html), which are all able to solve mixed integer non-linear programming (MINLP) models (Bussieck and Vigerske 2010) to obtain the mechanism results. For all the solvers, the maximum computing time in solving one MINLP model is set to 3600 seconds. Among the seven solvers, ANTIGONE has the highest performance both in terms of solution quality and computing speed. The possible reason is that ANTIGONE implements a spatial branch-and-bound

algorithm that utilizes MIPs for bounding. The MIP relaxation is generated from a reformulation of the MINLP. It employs a large collection of convexification and bound tightening techniques (Bussieck and Vigerske 2010). For conciseness, we select ANTIGONE to compare with the proposed SPA algorithm, but we attach the results of all seven solvers in Appendix A. Finally, it is difficult to test all state-of-the-art heuristic algorithms in the literature, but we select two representative heuristic algorithms for comparison with our proposed SPA. We select Hybrid Simulated Annealing - Tabu Search algorithm (HSATS) as a representative of local-search-based heuristic algorithms and select Hybrid Genetic and Local Search algorithm (HGLS) as a representative of swarm evolutionary heuristic algorithms. Both HSATS (Lin et al. 2016) and HGLS (Wang 2014) are effective for solving the classic Traveling Salesman Problem (TSP). We modify the mutation structures (e.g. neighborhood structure and crossover structure) to adapt the algorithms to the first-mile ridesharing matching and routing problem. The algorithm comparison is based on the following criteria:

1) **Objective function values**. We compare the performances of EA, ANTIGONE, HSATS, HGLS, and SPA in terms of the objective function values of IP_0 for all numerical examples.

2) **Computing time**. Computing time is used to measure the efficiency of an algorithm. This chapter will compare the computing time of ANTIGONE, HSATS, HGLS, and SPA in solving the optimization model IP_0 and calculating the prices.

3) **Mechanism properties**. We will show the reliabilities of these algorithms to sustain two properties “individual rationality” and “price non-negativity”. The property “incentive compatibility” is difficult to test and thus is not included in the comparison.

4) **Service provider profitability**. The experiment results will show if the price collected from passengers can cover the transportation cost.

4.4.3 Running Conditions

The algorithms, EA, HSATS, HGLS, and SPA, are programmed in Matlab R2014a. The commercial solvers are implemented on the website of NEOS Solvers (https://neos-server.org/neos/solvers/index.html). All algorithms are implemented on a Dell computer with processor Intel(R) Core(TM) i7-4790 CPU @ 3.60GHz and 8 GB RAM.

4.4.4 Experiment Results

We first compare five solution approaches, EA, ANTIGONE, HSATS, HGLS, and SPA, in terms of objective function values in solving model IP_0. Table 4.2 presents the comparison results. The numerical examples are denoted by "N_x", where "x" is number of passenger requests.

EA is able to solve only two small-scale problems (N_4 and N_8). When the number of passenger requests reaches "12", the computer registers a shortage of memory.

The solver ANTIGONE can return a solution, not necessarily optimal, within one hour (3600 seconds) for numerical examples with the numbers of passengers ranging from 4 to 28. The solution qualities obtained by ANTIGONE are very close to the heuristic algorithms, HGLS, HSATS, and SPA, in solving the numerical examples with passengers fewer than or equal to 24. When the number of passengers reaches "28", the quality of the solution obtained by ANTIGONE is much lower than those obtained by the heuristic algorithms: the objective function value obtained by ANTIGONE is 159.28, much lower than 186.47 of HGLS, HSATS, and SPA. When the number of passengers is larger than 28, ANTIGONE is unable to return a solution.

All of the three heuristic algorithms HSATS, HGLS, and SPA are able to find solutions for all numerical examples. They obtain the exact optimal solutions of numerical examples N_4 and N_8 as EA does. With the scale of the problem increasing, the solution qualities of HSATS and HGLS are slightly higher than those of SPA in general. However, the differences between SPA and HSATS and between SPA and HGLS are negligible. The maximum difference between SPA and HSATS/HGLS is only 1.55% (N_36).

Table 4.2 Objective Function Values Obtained by EA, ANTIGONE, HSATS, HGLS, and SPA

Numerical examples	EA	ANTIGONE	HSATS	HGLS	SPA		
					Objective function values	Difference from HSATS (%)	Difference from HGLS (%)
N_4	24.56	24.56	24.56	24.56	24.56	0.00	0.00
N_8	58.00	58.00	58.00	58.00	58.00	0.00	0.00
N_12		81.52	81.52	81.52	81.52	0.00	0.00
N_16		119.98	119.98	119.98	119.45	0.44	0.44
N_20		139.89	139.89	139.89	139.86	0.02	0.02
N_24		152.58	152.58	152.71	152.58	0.00	0.09
N_28		159.28	186.47	186.47	186.47	0.00	0.00
N_32			200.08	200.08	200.03	0.02	0.02
N_36			259.67	259.67	255.71	1.55	1.55
N_40			289.98	289.98	289.54	0.15	0.15
N_44			302.17	302.17	301.28	0.30	0.30

N_48	349.51	349.54	346.98	0.73	0.74
N_52	380.77	379.63	377.70	0.81	0.51

Note: the table only presents the data when the computer memory is sufficient and the computing time is less than or equal to one hour (3600 seconds).

Table 4.3 shows the computing time for obtaining an optimal matching and routing plan and calculating prices, as well as the total computing time spent by ANTIGONE, HSATS, HGLS, and SPA. The commercial solver ANTIGONE is much more time-consuming than the three heuristic algorithms HSATS, HGLS, and SPA in getting the mechanism results for numerical examples with more than 12 passengers. HSATS needs more than 3000 seconds (50 minutes) to obtain the mechanism for the largest-scale numerical example (N_52), and HGLS is unable to obtain the mechanism for the largest-scale numerical example within one hour. In contrast, SPA is able to obtain the mechanism for all numerical examples within 3 minutes. This is because both HSATS and HGLS need to solve n similar optimization models one by one to calculate the prices given that the number of passenger requests is n, while SPA is able to solve these similar models simultaneously. Moreover, it can be inferred from Figure 4.3 that the computing complexity of SPA is lower than those of HSATS and HGLS. With the scale of problems continuously increasing, the computing times of HSATS and HGLS increase faster than that of SPA.

Table 4.3 Computing Time (in Seconds) of ANTIGONE, HSATS, HGLS, and SPA

Numerical	ANTIGONE			HSATS			HGLS			SPA		
examples	TO	TP	TT	TO	TP	TT	TO	TP	TT	TO	TP	TT
N_4	0.09	0.34	0.43	0.11	0.42	0.53	0.09	0.34	0.43	0.14	0.00	0.14

N_8	1.95	5.46	7.41	1.23	8.94	10.17	0.73	5.87	6.60	1.47	0.35	1.82
N_12	2278.09	>3600	>3600	3.70	42.47	46.17	2.61	31.34	33.95	4.79	1.24	6.03
N_16	3600.00	>3600	>3600	12.27	193.15	205.42	11.61	177.59	189.20	14.89	5.03	19.92
N_20	3600.00	>3600	>3600	16.86	298.28	315.14	20.57	380.14	400.71	19.93	7.15	27.08
N_24	3600.00	>3600	>3600	19.98	474.04	494.02	38.68	910.37	949.05	24.38	9.44	33.82
N_28	3600.00	>3600	>3600	26.82	694.69	721.51	66.40	1724.21	1790.61	35.32	12.22	47.54
N_32				32.02	877.13	909.15	86.35	2665.13	2751.48	39.30	18.82	58.12
N_36				32.33	1227.69	1260.02	101.23	3553.58	3654.81	46.83	25.43	72.26
N_40				39.94	1646.68	1686.62	118.06	>3600	>3600	56.70	31.78	88.48
N_44				45.18	2032.65	2077.83	141.86	>3600	>3600	66.88	37.94	104.82
N_48				53.85	2652.70	2706.55	173.49	>3600	>3600	71.00	43.98	114.98
N_52				59.37	3063.98	3123.35	189.85	>3600	>3600	89.96	59.70	149.66

Annotation: TO, computing time in obtaining the optimal routing plan; TP, computing time in calculating the prices; TT, the total computing time.

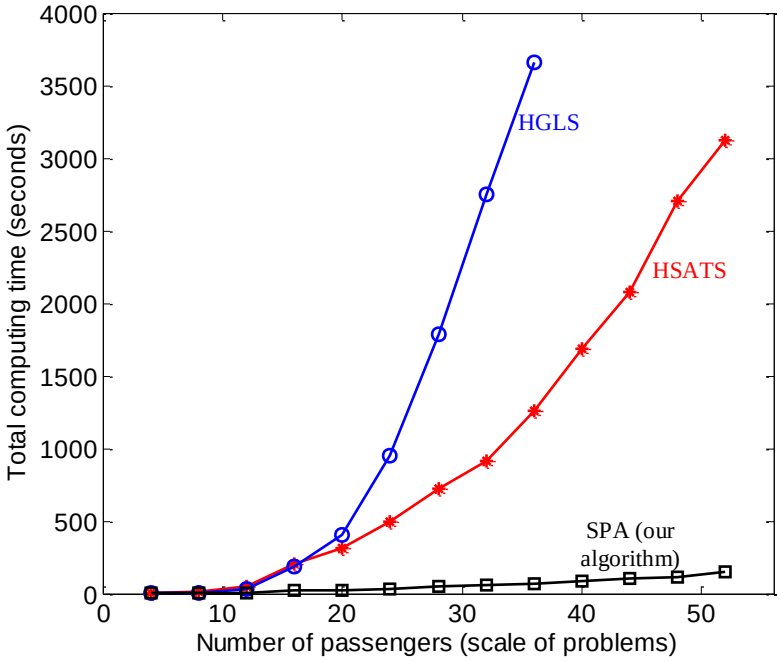

Figure 4.3 Computing Time of HSATS, HGLS, and SPA for Different Numerical

Examples

The mechanism obtained by the exact algorithm was proven, in Chapter 3, to have three properties: "individual rationality", "incentive compatibility", and "price non-negativity". We compare the ability of the four algorithms (EA, HSATS, HGLS, and SPA) in maintaining these properties. ANTIGONE is not presented here because it is very time-consuming. Table 4.4 presents the percentages of individual rational and non-negative prices in the total number of prices using four algorithms for all numerical examples. If the properties "individual rationality" and "price non-negativity" are strictly proved, the table cell shows "proved". Otherwise, only a percentage is shown in the table. Table 4.4 shows that the mechanism obtained by both HSATS and HGLS are possibly not "individual rational". In numerical examples N_24 and N_48, at least one passenger's utility is negative in the mechanism obtained by HSATS (the bold numbers are less than 100%). In the numerical example N_32, at least one passenger's utility is negative in the mechanism obtained by HGLS. Negative utilities indicate that these passengers are unwilling to pay the prices. Chapter 3 and this chapter respectively proved that the mechanisms obtained by EA and SPA are always individual rational, and thus all passengers' utilities are non-negative. Although we cannot strictly prove that the mechanisms obtained by HSATS, HGLS, and SPA have the property of "price non-negativity", the prices obtained via the three algorithms are all non-negative in these numerical examples. The property "incentive compatibility" is not tested because it is impossible to enumerate all combinations of passengers' reported requirements, but the mechanism obtained by SPA has been proved to be incentive compatible (Proposition 2), while the mechanism obtained by other heuristics

(e.g. HSATS and HGLS) is not incentive compatible based on the discussion in Subsection 4.2.3.

Table 4.4 Comparison Results of the Properties of "Individual Rationality" and "Price Non-Negativity"

Numerical examples	Percentage of "individual rational" prices				Percentage of non-negative prices			
	EA	HSATS	HGLS	SPA	EA	HSATS	HGLS	SPA
N_4	Proved (100)	100	100	Proved (100)	Proved (100)	100	100	100
N_8	Proved (100)	100	100	Proved (100)	Proved (100)	100	100	100
N_12	Proved	100	100	Proved (100)	Proved	100	100	100
N_16	Proved	100	100	Proved (100)	Proved	100	100	100
N_20	Proved	100	100	Proved (100)	Proved	100	100	100
N_24	Proved	**91.7**	100	Proved (100)	Proved	100	100	100
N_28	Proved	100	100	Proved (100)	Proved	100	100	100
N_32	Proved	100	**96.9**	Proved (100)	Proved	100	100	100
N_36	Proved	100	100	Proved (100)	Proved	100	100	100
N_40	Proved	100		Proved (100)	Proved		100	100
N_44	Proved	100		Proved (100)	Proved		100	100
N_48	Proved	**97.9**		Proved (100)	Proved		100	100
N_52	Proved	100		Proved (100)	Proved		100	100

Note: the table only presents the data when the computer memory is sufficient and the computing time is less than one hour (3600 seconds).

Table 4.5 shows that the profits (total price collected minus total transportation cost) are positive for all numerical examples in the mechanisms obtained by EA, HSATS, HGLS,

and SPA. The mechanisms obtained by EA, HSATS, HGLS, and SPA are all profitable for the service provider in all of the numerical examples.

Table 4.5 Profit Made by the Ridesharing Service Provider

Numerical examples	Profit made by the service provider (total price minus total transportation cost)			
	EA	HSATS	HGLS	SPA
N_4	19.9	19.9	19.9	19.2
N_8	35.2	35.2	35.2	35.2
N_12		59.4	59.4	59.4
N_16		79.8	79.8	80.8
N_20		94.4	94.4	94.2
N_24		113.5	112.7	106.9
N_28		136.7	136.4	134.1
N_32		145.0	147.8	144.4
N_36		169.1	158.3	160.3
N_40		194.7		191.2
N_44		207.4		186.0
N_48		239.1		227.0
N_52		236.1		234.7

Note: the table only presents the results when the computer memory is sufficient and the computing time is less than one hour (3600 seconds).

4.4.5 Sensitivity Analysis

Sensitivity analysis focuses on two aspects: 1) change of passengers' value functions and 2) change of the strictness of passengers' requirements on inconvenience factors. The first aspect aims at testing the effectiveness of the mechanism under different conditions, in which passengers have stricter attitudes towards the price. The second aspect is to study the changing process of the matching and routing plan and the price when a passenger in one location places stricter requirement on the inconvenience factors.

1) Change of the value function

Passengers' attitudes towards the price are reflected by the value function. We use a different hypothetical value function (Formula 14) instead of Formula (13) to represent passengers' stricter attitudes towards the price. Formula (14) assumes that passengers' lowest maximum willing-to-pay price is zero if they are transported to the transit hub directly, i.e. $V_i \geq 0$, if $IVT_i = t_{i0}$.

$$V_i = V_{\max}^i - \left(\frac{\alpha_i^{NR} NR_i}{(Q - np_i)} + \frac{\alpha_i^{IVT} \left(IVT_i - t_{i0} \right)}{t_{i0}} + \frac{\alpha_i^{WT} WT_i}{MD} \right) \frac{V_{\max}^i}{2} \tag{14}$$

We will test the mechanism using the same algorithms. The experiment results are listed in Table 4.6, Table 4.7, Table 4.8, and Table 4.9. The numerical examples are denoted as "N2_x", where x represents the number of requests sent by passengers. Yet again, ANTIGONE is not presented in Table 4.6, Table 4.7, Table 4.8, and Table 4.9 due to its unreasonably long computing time.

Table 4.6 Objective Function Values of IP_0 Obtained by EA, HSATS, HGLS, and

SPA (Value function: Formula 14)

Numerical examples	EA	HSATS	HGLS	SPA		
				Objective function values	Difference from HSATS (%)	Difference from HGLS (%)
N2_4	26.17	26.17	26.17	26.17	0.00	0.00
N2_8	48.00	48.00	48.00	48.00	0.00	0.00
N2_12		71.21	71.21	71.21	0.00	0.00
N2_16		98.56	98.56	98.56	0.00	0.00
N2_20		130.83	130.83	130.75	0.06	0.06
N2_24		169.09	169.09	168.44	0.39	0.39
N2_28		181.21	181.21	176.32	2.77	2.77
N2_32		199.44	199.38	197.86	0.80	0.77
N2_36		248.52	248.52	245.43	1.26	1.26
N2_40		253.24	252.88	246.61	2.69	2.54
N2_44		260.08	260.08	256.26	1.49	1.49
N2_48		314.25	314.54	311.52	0.88	0.97
N2_52		336.39	335.58	333.83	0.77	0.52

Table 4.7 Computing Time of HSATS, HGLS, and SPA (Value Function: Formula 14)

Numerical examples	HSATS			HGLS			SPA		
	TO (s)	TP (s)	TT (s)	TO (s)	TP (s)	TT (s)	TO (s)	TP (s)	TT (s)
N2_4	0.10	0.42	0.52	0.09	0.33	0.42	0.13	0.01	0.14
N2_8	1.14	7.98	9.12	0.72	5.65	6.37	1.44	0.31	1.75
N2_12	3.65	40.59	44.24	2.43	29.55	31.98	4.79	1.26	6.05

N2_16	10.34	159.98	170.32	11.47	172.75	184.22	13.96	3.50	17.46
N2_20	14.00	271.03	285.03	19.46	360.47	379.93	17.89	6.96	24.85
N2_24	17.94	441.51	459.45	37.44	901.17	938.61	22.84	9.64	32.48
N2_28	23.92	628.69	652.61	66.91	1729.90	1796.81	29.70	14.24	43.94
N2_32	27.93	907.01	934.94	85.38	2612.03	2697.41	34.11	16.96	51.07
N2_36	35.77	1266.50	1302.27	94.75	3635.89	3730.64	42.20	23.88	66.08
N2_40	40.68	1411.74	1452.42	109.55	>3600	>3600	51.65	25.36	77.01
N2_44	46.43	2090.88	2137.31	131.43	>3600	>3600	55.80	36.93	92.73
N2_48	53.84	2274.47	2328.31	157.79	>3600	>3600	71.03	47.81	118.84
N2_52	58.74	2620.70	2679.44	182.50	>3600	>3600	89.79	53.69	143.48

Table 4.8 Comparison Results of the Property of "Individual Rationality" and "Price Non-Negativity" (Value Function: Formula 14)

Numerical examples	Percentage of "individual rational" prices				Percentage of non-negative prices			
	EA	HSATS	HGLS	SPA	EA	HSATS	HGLS	SPA
N2_4	Proved (100)	100.0	100.0	Proved (100)	Proved (100)	100.0	100.0	100.0
N2_8	Proved (100)	100.0	100.0	Proved (100)	Proved (100)	100.0	100.0	100.0
N2_12	Proved	100.0	100.0	Proved (100)	Proved	100.0	100.0	100.0
N2_16	Proved	100.0	100.0	Proved (100)	Proved	100.0	100.0	100.0
N2_20	Proved	100.0	100.0	Proved (100)	Proved	100.0	100.0	100.0
N2_24	Proved	100.0	100.0	Proved (100)	Proved	100.0	100.0	100.0
N2_28	Proved	100.0	100.0	Proved (100)	Proved	100.0	100.0	100.0
N2_32	Proved	100.0	**84.4**	Proved (100)	Proved	100.0	100.0	100.0
N2_36	Proved	100.0	100.0	Proved (100)	Proved	100.0	100.0	100.0
N2_40	Proved	100.0		Proved (100)	Proved	100.0		100.0
N2_44	Proved	100.0		Proved (100)	Proved	100.0		100.0

N2_48	Proved	**95.8**	Proved (100)	Proved	100.0	100.0
N2_52	Proved	100.0	Proved (100)	Proved	100.0	100.0

Note: the table only presents the data when the computer memory is sufficient and the computing time is less than one hour (3600 seconds).

Table 4.9 Profit Made by the Ridesharing Service Provider (Value Function: Formula 14)

Numerical examples	Profit made by the service provider (total price minus total transportation cost)			
	EA	HSATS	HGLS	SPA
N2_4	22.30	22.30	22.30	22.30
N2_8	41.20	41.20	41.20	41.20
N2_12		59.50	59.50	59.40
N2_16		72.60	72.60	67.10
N2_20		96.00	96.00	92.80
N2_24		117.90	118.10	113.20
N2_28		141.40	141.40	115.80
N2_32		153.60	155.00	141.90
N2_36		173.90	172.70	143.10
N2_40		192.00		149.20
N2_44		200.80		186.50
N2_48		247.90		209.50
N2_52		242.40		147.60

Note: the table only presents the data when the computer memory is sufficient and the computing time is less than one hour (3600 seconds).

Table 4.6 and Table 4.7 present the comparison results in terms of the objective function value and computing time. SPA can still obtain satisfactory vehicle-passenger matching and routing plans within a reasonable time when passengers' value functions change. The results show that when the scale of the problem is small, HSATS, HGLS, and SPA are able to obtain the exact optimal solution. With the scale of the problem increasing, the solution qualities of HSATS and HGLS are slightly higher than those of SPA, but the differences between SPA and HSATS and between SPA and HGLS are still negligible. The largest difference between SPA and HSATS/HGLS in terms of the objective function value is only 2.77%. The total computing time of SPA is less than 3 minutes, significantly less than those of HSATS and HGLS. In Table 4.8, HSATS and HGLS may generate mechanisms that are not individual rational (numerical examples N2_48 and N2_32 with bold numbers). All of the prices obtained by HSATS, HGLS, and SPA are still non-negative even though passengers' attitudes towards prices becomes stricter. Table 4.9 shows the profits of all numerical examples based on the mechanism obtained by HSATS, HGLS, and SPA. All profits are positive, indicating that even though the passengers have stricter attitudes towards the price, the mechanism is still profitable for the service provider. The experimental results demonstrate the robustness of SPA even if passengers' attitude towards the prices changes.

2) Change of passengers' tolerance towards inconvenience factors

This sensitivity analysis studies the impact of changing passenger's requirements

on prices and routing plans. We state that the changing process of the mechanism $M\left(X^{IP_0^*}, \mathbf{p}\right)$ is *reasonable* if the passenger receives no worse service and the price does not decrease when the requirement becomes stricter. Figure 4.4 shows an example of a *reasonable* changing process of one passenger's (this passenger is highlighted by the red circle in the figure) mechanism $M\left(X^{IP_0^*}, p_i\right)$. There are three stages of the changing process in Figure 4.4. The price and the matching and routing plan do not change within each stage. As the passenger's requirements continue to grow stricter, the stage will transition to the next stage, and the passenger will receive higher-quality service and the price increases. The reasonable changing process is important because it avoids the following counter-situation: a passenger places a stricter requirement on an inconvenience attribute, but has to tolerate an increased degree of the corresponding inconvenience attribute and pay less money.

In the sensitivity analysis, the values of α_i^{NR}, α_i^{IVT}, and α_i^{WT} are all increased from 0.1 to 1 by 0.1 each time for each passenger. We solve the mechanism $M\left(X^{IP_0^*}, \mathbf{p}\right)$ each time α_i^{NR}, α_i^{IVT}, and α_i^{WT} increase. We record the number of passenger requests whose mechanism changing processes are *reasonable* and calculate the percentage of this number in the total number of passenger requests for each numerical example.

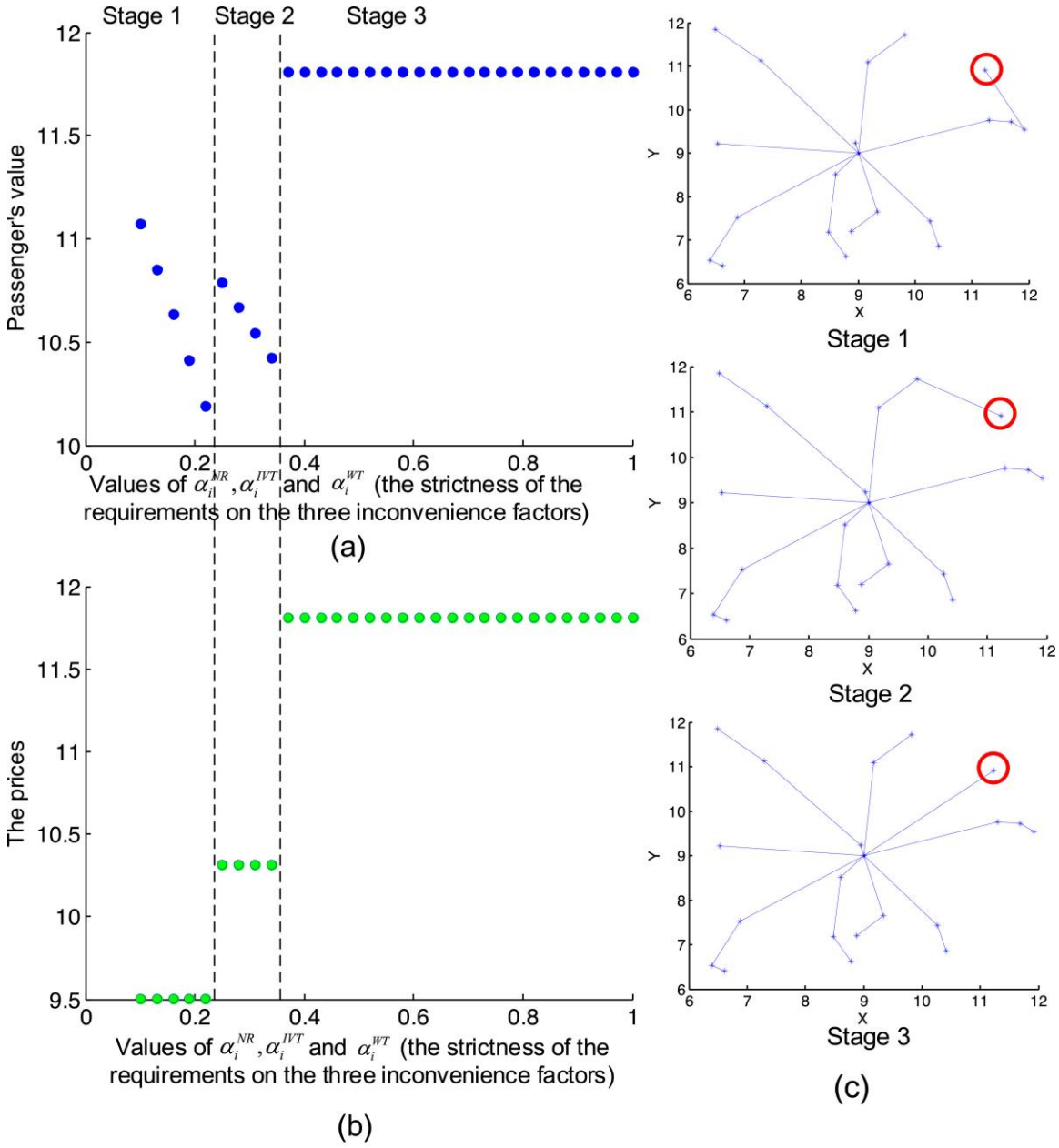

(a) Changing process of the passenger's value
(b) Changing process of the price
(c) Changing process of the routing plan

Figure 4.4 An Example of Reasonable Changing Process of One Passenger's Mechanism

Table 4.10 shows the percentages of the number of passenger requests, whose changing process of the mechanism is *reasonable*, in the total number of passenger requests. When the scale of the problems is small, all algorithms can ensure 100% *reasonable* changing processes. However, as the scale of problems increases, these percentages of regular heuristic algorithms, including HSATS and HGLS, decrease sharply (see Figure 4.5). Thus, when the scale of the problem is large, even though passengers' requirements become stricter, the routing plan is likely to become less convenient for such passengers and the price will decrease, which counteracts the mechanism design objective. For example, if a passenger places stricter requirement on the extra in-vehicle travel time, the system is likely to let her stay in the vehicle for a longer time and the price is likely to decrease by using HSATS or HGLS. In contrast, from the testing result, it seems that SPA can always ensure a *reasonable* changing process of the mechanism for all passengers (100%) in all of the numerical examples.

Table 4.10 Percentages of Reasonable Changing Processes

Numerical examples	Percentages of reasonable changing processes			
	EA	HSATS	HGLS	SPA
N_4	100	100.0	100.0	100.0
N_8	100	100.0	100.0	100.0
N_12		100.0	100.0	100.0
N_16		100.0	100.0	100.0
N_20		100.0	90.0	100.0
N_24		16.7	25.0	100.0

N_28		14.3	14.3	100.0
N_32		18.8	18.8	100.0
N_36		0.0	0.0	100.0
N_40		12.5		100.0
N_44		6.8		100.0
N_48		6.3		100.0
N_52		0.0		100.0
N2_4	100	100.0	100.0	100.0
N2_8	100	100.0	100.0	100.0
N2_12		100.0	100.0	100.0
N2_16		100.0	100.0	100.0
N2_20		95.0	100.0	100.0
N2_24		66.7	54.2	100.0
N2_28		96.4	89.3	100.0
N2_32		15.6	25.0	100.0
N2_36		19.4	16.7	100.0
N2_40		30.0		100.0
N2_44		27.3		100.0
N2_48		0.0		100.0
N2_52		3.8		100.0

Note: the table only presents the data when the computer memory is sufficient and the computing time is less than one hour (3600 seconds).

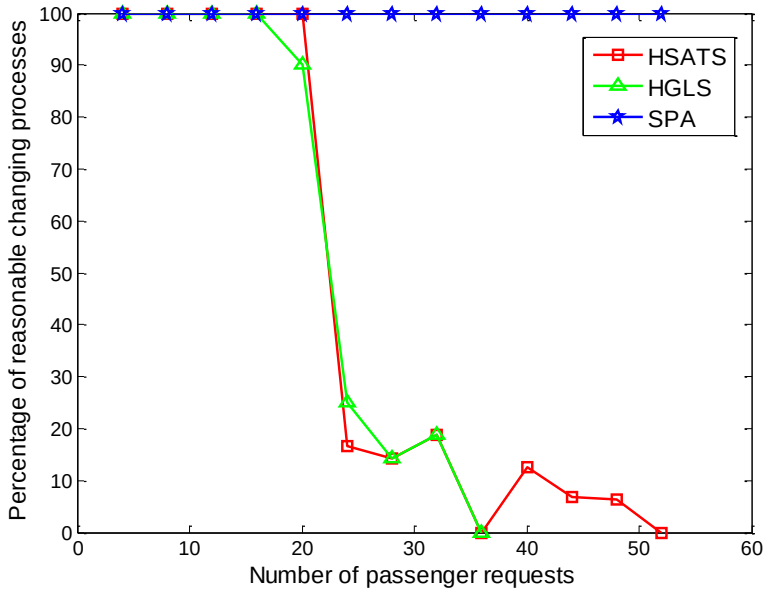

(a) Value function: Formula (13)

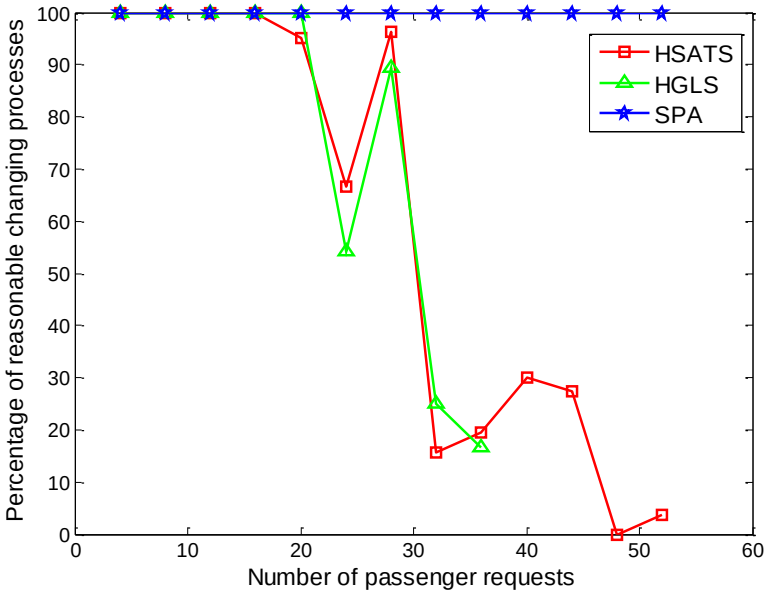

(b) Value function: Formula (14)

Figure 4.5 Percentages of Number of Reasonable Changing Processes for Different Numerical Examples

4.5 Conclusions

This chapter proposed a novel heuristic algorithm, Solution Pooling Approach (SPA), to obtain the mechanism proposed in our last chapter. The SPA is able to ensure two important properties, "individual rationality" and "incentive compatibility". The experimental results on the numerical example show that SPA can significantly decrease the computational complexity with a tiny sacrifice of solution quality, compared with traditional heuristic methods, such as Hybrid Simulated Annealing–Tabu Search Algorithm and Hybrid Genetic Algorithm. From the sensitivity analysis, we can conclude that SPA is robust to efficiently obtain the mechanism without sacrificing too much accuracy and to maintain some other nice properties, including price non-negativity and service provider profitability based on the numerical examples. The sensitivity analysis also implies that passengers can receive a higher-quality service by placing stricter requirements on corresponding inconvenience factors based on their mobility preferences, and correspondingly, they are charged a higher price when participating in ridesharing. SPA can be adapted to solve generalized mechanism design problems. We analyze the specific circumstances under which SPA can sustain the game-theoretic properties, including "individual rationality" and "incentive compatibility", and identifies its limitation in solving generalized mechanism design problems. Our future work will apply the solution pooling approach to solve other mechanism design problems and test its effectiveness.

Appendix A

This appendix presents the performance of seven commercial solvers, ANTIGONE (Algorithms for coNTinuous/Integer Global Optimization), ALPHAECP (α-Extended

Cutting Plane), BARON (Branch-And-Reduce Optimization Navigator), COUENNE (Convex Over and Under ENvelopes for Nonlinear Estimation), LINDOGLOBAL, SBB (Simple Branch-and-Bound) and SCIP (Solving Constraint Integer Programs), in terms of the objective function values and the computing time in solving the non-convex mix integer non-linear programming model IP_0. Among these seven solvers, ANTIGONE, COUENNE, LINDOGLOBAL, and SCIP can guarantee the global optimal solutions for non-convex MINLP models if the solvers are terminated normally, while ALPHAECP, BARON, and SBB cannot ensure the global optimality (Bussieck and Vigerske 2010). The results are shown in Table 4.11 and Table 4.12. The two tables do not show the result when the solvers are unable to return a solution.

Table 4.11 Objective Function Values of Model IP_0 Obtained by Seven Solvers

Numerical examples	Objective function values (dollars)						
	ANTI-GONE	ALPHA-ECP	BARON	COUENNE	LINDO-GLOBAL	SBB	SCIP
N_4	24.56	24.56	24.56	24.56	24.56	24.56	24.56
N_8	58.00	58.00	58.00	58.00	58.00	55.30	58.00
N_12	81.52	81.52	81.52	81.11	81.52	78.44	81.52
N_16	119.98	115.36	117.57				116.79
N_20	139.89	134.13	131.11				136.51
N_24	152.58	139.59	140.73				133.72
N_28	159.28						147.18

Table 4.12 Computing Times of Seven Solvers in Solving Model IP_0

Numerical examples	Computing time (seconds)						
	ANTI-GONE	ALPHA-ECP	BARON	COUENNE	LINDO-GLOBAL	SBB	SCIP
N_4	0.09	8.07	0.15	0.87	0.28	0.17	0.20
N_8	1.95	423.69	8.55	139.39	21.46	12.36	5.37
N_12	2278.09	3600.00	3600.00	3600.00	3600.00	441.02	3600.00
N_16	3600.00	3600.00	3600.00				3600.00
N_20	3600.00	3600.00	3600.00				3600.00
N_24	3600.00	3600.00	3600.00				3600.00
N_28	3600.00						3600.00

CHAPTER 5 MECHANISM DESIGN FOR ON-DEMAND FIRST-MILE RIDESHARING

5.1 Introduction

This chapter designs a mechanism for the on-demand first-mile ridesharing, a service that arranges real-time shared rides on a very short notice to bring passengers to the nearby transit hub (Amey et al. 2011). The mechanism provides an incentive pricing scheme along with an optimization solution to the vehicle-passenger matching and vehicle routing based on real-time information of passenger requests and available vehicles near the transit hub.

The on-demand first-mile ridesharing service has three additional considerations compared with the scheduled service.

1) On-demand first-mile ridesharing requires that the service should be quickly responsive so that vehicles can be dispatched promptly to drive passengers to the transit hub in time. It also requires prompt decision of vehicle-passenger matching and vehicle routing as well as pricing. This indicates that the algorithm should be efficient to quickly obtain the mechanism design results.

2) The system needs to capture real-time locations of available vehicles, which is the input information for the optimization of the vehicle-passenger matching and vehicle routing.

3) It is possible that in the on-demand scenario, not necessarily all passengers can be served to reach the transit hub before specified deadlines because of limited vehicle resources and/or limited time. Thus, an auction-based mechanism that allows passengers to bid for the service is preferred.

This chapter addresses passengers' mobility preferences in designing the mechanism because travelers' choice of transportation mode is significantly influenced by these mobility preferences (Golledge et al., 1994; Ben-Akiva and Lerman, 1985; Arentze, 2013; Biswas et al., 2017a; BBC news, 2016). First, the designed mechanism allows passengers to report personalized arrival deadlines since they need to catch the next transit mode at the transit hub in time. Second, in the on-demand scenario, available vehicles may not be sufficient to drive all passengers to the transit hub before the arrival deadlines. Some passengers may not be served. Thus, the mechanism is auction-based, in which passengers can bid for the service by reporting their maximum willing-to-pay prices. Third, we consider the problem if the incentive is able to offset different passengers' inconvenience cost induced by the detour due to ridesharing. The mechanism allows passengers to report their personalized detour tolerances (details will be in Section 3), which is the input in our algorithm to determine the matching and routing plan and passengers' corresponding customized prices.

Our proposed mechanism design mechanism is improved upon the classical Vickrey -Clarke-Groves (VCG) mechanism (Vickrey, 1961; Clarke, 1971; Groves, 1973). The VCG is a widely-used auction-based mechanism that maximizes the total social welfare with two important properties – "individual rationality" (passengers are willing to participate in the service) and "incentive compatibility" (truthful reporting is a passenger's best strategy) (Parkes et al., 2001). As a starting point, we apply the traditional VCG mechanism to solve our on-demand first-mile ridesharing problem. The rolling horizon planning, an efficient approach to handle dynamic ridesharing optimization problems (Agatz et al., 2010; Agatz et al., 2011), is developed to implement the mechanism. The

rolling horizon planning approach automatically determines time slices, within which newly arrived passenger requests are processed until the end of this time slice (Montemanni et al., 2005).

As the following analyses of this chapter will show that, the traditional VCG mechanism has its inherent limitations in this first-mile ridesharing application. We found that some prices derived from the VCG mechanism are unreasonably low and the cumulative prices may not be able to offset the service provider's transportation cost. This is probably because the general-purpose VCG mechanism simply charges passengers by the marginal benefit that they contribute to the service system, but lacks a baseline price control strategy, which is also important for financially sustainable ridesharing services.

To address the identified limitations of the VCG mechanism, this chapter proposes a novel mechanism named **Mobility-Preference-Based Mechanism with Baseline Price Control (MPMBPC)**. MPMBPC consists of two pricing layers – a baseline pricing layer and a mobility-preference-based pricing layer. The baseline pricing layer aims to avoid passengers' unreasonably low prices and prevent service provider's deficit based on an important property, named as "price controllability". This property ensures that served passengers' prices are no lower than the baseline prices. We suggest that the baseline price can be determined by the shortest travel distance from passenger location to the transit hub. The mobility-preference-based pricing layer promotes passengers' collaboration and prevents passengers from misreporting their mobility preferences by guaranteeing the properties of "individual rationality" and "incentive compatibility", respectively. Another important property, "detour-discounting reasonability" is theoretically proved to demonstrate that passengers can have their customized services depending on their

tolerance of possible detours. For instance, if a passenger is less tolerant of detour, she will have higher-quality service with less detour but pays a higher price.

In order to obtain the mechanism results, a series of mixed integer nonlinear programming models need to be solved to obtain an optimal matching and routing plan as well as to calculate prices of all passenger requests. This chapter develops two solution approaches for small-scale and large-scale problems, respectively. The first solution approach is to reformulate mixed integer nonlinear models as mixed integer linear programming and then use a commercial solver (CPLEX) to solve these models exactly. The second solution approach is developing an efficient heuristic algorithm, named "solution pooling approach (SPA)" that can quickly obtain the mechanism results for large-scale problems. It will be theoretically proved that SPA is able to sustain the properties of "individual rationality", "incentive compatibility", and "detour-discounting reasonability".

The following analyses will show that both the CPLEX solver and our proposed SPA algorithm can exactly obtain the mechanism results very quickly for small-scale numerical examples. The MPMBPC will be compared with the classical VCG mechanism, demonstrating its superiority in reasonability and practicability. Further, we design a series of large-scale numerical examples to test the performance of SPA. We find that the SPA is able to efficiently solve the mechanism design problem for all numerical examples with high solution quality. We select another efficient heuristic algorithm, Hybrid Simulated Annealing–Tabu Search Algorithm (HSATS, Lin et al., 2016), as a representative of the latest heuristic algorithms to compare with SPA. The comparison result demonstrates that SPA is much faster than HSATS. Also, SPA sustains the three proved properties, whereas HSATS cannot.

The remainder of the chapter is organized as follows. Section 5.2 summarizes contributions of the chapter. The mechanism design problem for the on-demand first-mile ridesharing is explained in Section 5.3. Section 5.4 introduces the application of the traditional VCG mechanism in the on-demand first-mile ridesharing and identifies its limitations. Section 5.5 proposes a novel mobility-preference-based mechanism with baseline price control. Section 5.6 introduces the solution approaches for solving large-scale ridesharing mechanism design problems. Section 5.7 designs numerical examples to interpret the results and test the proposed algorithms. Conclusions are drawn in Section 5.8.

5.2 Intended Contributions

In summary this chapter aims to bring the following contributions.

- To our best knowledge, this is the first research that accounts for passengers' *personalized mobility preferences* in designing an *auction-based mechanism* for *on-demand (dynamic) first-mile* ridesharing service. We identify the limitations in reasonability and practicability of using the traditional VCG mechanism – some passengers' prices may be unreasonably low and the service provider may have a deficit. Therefore, we design a novel mechanism, called mobility-preference-based mechanism with baseline price control (MPMBPC), to overcome the limitations of the traditional VCG mechanism. MPMBPC consists of a baseline pricing layer and a mobility-preference-based pricing layer. The baseline pricing layer can avoid passengers' unreasonably low prices and service provider's deficit via an important property, named as "*price controllability*". This property ensures served passengers' prices greater than or equal to the baseline prices. The mobility-preference-based pricing layer also simultaneously ensures "*individual rationality*" and

"*incentive compatibility*". Moreover, the MPMBPC mechanism has another important property, named as "*detour-discounting reasonability*". It means that if passengers are less tolerant of detour, they may have higher-quality service with less extra in-vehicle travel time but pay higher prices if they are served.

- To solve the proposed ridesharing mechanism design problem in a computationally efficient manner, we develop a new heuristic algorithm, called *solution pooling approach* (SPA) that can quickly obtain the mechanism results of large-scale problems, which cannot be solved by the solver CPLEX within a reasonable amount of time. It is theoretically proved that SPA is able to sustain the properties of "individual rationality", "incentive compatibility", and "detour-discounting reasonability".

5.3 Problem Description

Passengers near the transit hub continuously send on-demand requests for pick-up from their locations and drop-off at the transit hub. The service provider, which can either be the transit agency or a ridesharing service provider collaborating with the transit agency, has a fleet of vehicles to provide the first-mile accessibility service.

We use the rolling horizon planning approach (Agatz et al., 2010, 2011) to implement the mechanism for on-demand first-mile ridesharing as shown in Figure 5.1. After a passenger sends a request (e.g. typically via a smartphone application program), the system needs to respond to this request within a certain time (e.g. 1 or 2 minutes). This chapter defines this duration as a "time slice". When the response deadline is approaching, the system simultaneously consolidates and processes all of the requests sent within a time slice. At the end of a time slice, the system uses GPS to capture the locations of available

vehicles. There are two types of available vehicles. The first type of vehicle is empty and can be dispatched immediately at the end of the time slice. The second type of vehicle has not finished the current service at the end of the time slice but is about to finish soon. The time when and the locations where these vehicles will be available to provide the first-mile service can be estimated. Then, the system determines a vehicle-passenger matching and vehicle routing plan, as well as the price corresponding to each passenger request. In the example in Figure 5.1, Passenger 6 is the first to send a request. This passenger has a response deadline, before which the estimated pickup time and price must be sent to him. The time between Passenger 6's requesting time and the response deadline is defined as "time slice". Within the time slice, two other passengers (Passengers 4 and 5) send requests as well, whose response deadlines are later than Passenger 6's response deadline. When Passenger 6's response deadline is approaching, the system consolidates the three passengers' requests, optimizes the matching and routing plan, and calculates the prices. Then a new time slice begins when the next passenger (Passenger 3 in Figure 5.1) sends a request. The system conducts the same calculation cyclically to continuously process passengers' requests.

The length of time slice can be determined based on passengers' urgency. For example, when the current time is close to the train departure time, the mechanism can set a close response deadline for these urgent passengers after they send the requests since they cannot wait too long to be responded. Thus, the time slice will be short. On the contrary, the mechanism can set a relatively later response time for those passengers with late train departure times, because they have enough time to wait for pickup. The time slice is thus longer and the system can consolidate more passenger requests to ensure a higher vehicle

occupancy. The mechanism is always feasible regardless of the length of a time slice. However, unreasonable length of a time slice has the following impacts on the mechanism results. If the time slice is too long, some passengers may be impatient to wait or they may arrive at the destination late but they could have arrived in time if the time slice had been short and they had been responded soon. If the time slice is too short, the vehicle occupancy may be low because there is no enough time to consolidate more passenger requests.

After the mechanism results are obtained, passengers will be notified of the vehicles serving them, the estimated pickup times, the routing plans, and the prices. Drivers will be notified of the pickup task and will be strictly directed by the navigation system to pick up passengers in a specified sequence.

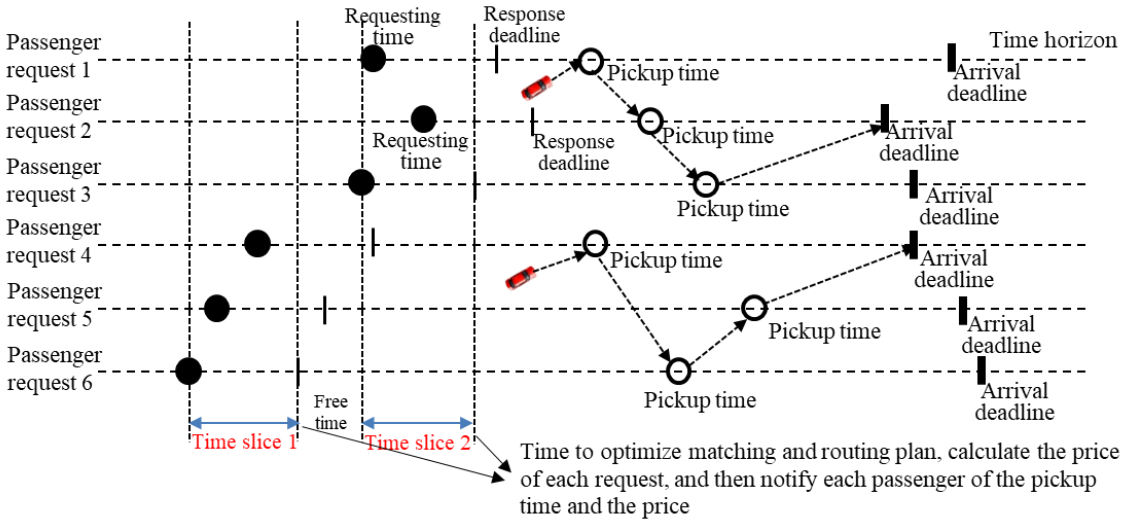

Figure 5.1 The Rolling Horizon Planning Approach for On-Demand First-Mile Ridesharing

There exist popular ridesourcing services in the market, such as Uber and Lyft

(Wang and Yang, 2019). We summarize some differences between these ridesourcing services and our studied first-mile ridesharing service.

Uber/Lyft service mainly targets generalized ridesharing service while our mechanism is more specific to the particular first-mile ridesharing service and aims to promote more passengers to use the public transit service. Compared with Uber/Lyft, our proposed mechanism is more human-centric, interactive, and personalized by satisfying passengers' mobility preferences (e.g. personalized arrival deadline, maximum willing-to-pay price, and detour tolerance), because travelers' choice of transportation mode is significantly influenced by these mobility preferences (Golledge et al., 1994; Ben-Akiva and Lerman, 1985; Arentze, 2013; Biswas et al., 2017a; BBC news, 2016).

1. In our designed mechanism, passengers can specify the arrival deadlines since they need to catch the next transit mode at the transit hub in time. This is inspired by the industrial trend: some news on the website (SMARTRAIL, 2018) stated that Uber would add public transportation to its app, providing multi-modal ridesharing-public transit mobility service in New York, Boston, Los Angeles, and other cities around the world. Users have the option to book and display transit tickets in the app, allowing for seamless transfers from ride-sharing to public transit service for convenient multi-modal journeys. This indicates that passengers can specify which train they will catch, and thus should be able to key in their arrival deadlines in the application program. In contrast, the current Uber/Lyft service does not have the function for passengers to key in the arrival deadlines. The interface only shows an estimated latest arrival time after a passenger keys in the destination. Some passengers, therefore, may be unable to arrive at the transit hub before their arrival deadlines if they take the current Uber or Lyft ridesourcing service, and thus

may miss the next transit mode.

2. In the first-mile ridesharing service, some passengers may be more eager to be served in time since they do not want to miss the next transit mode. These passengers may be willing to pay a higher price for the first-mile service because of the importance of the next transit mode. Therefore, the designed mechanism in this chapter is an "auction-based" mechanism, in which passengers are allowed to "bid" for the service by reporting their maximum willing-to-pay prices. The service can ensure that the actual paid prices will never be higher than their willing-to-pay prices if they are served. Basically, the higher maximum willing-to-pay price reported, the passenger has a higher priority to be served. In the literature, many researchers have realized the importance of passengers' personalized values (Nguyen, 2013; Lam, 2016; Asghari et al., 2016; Zhang et al., 2017, 2018; Zheng et al., 2019), and thus proposed auction-based mechanisms. In order to guide passengers to quantify their maximum willing-to-pay prices, we can set default prices for reference. If the passenger does not key in the maximum willing-to-pay price, the system will adopt the default reference price as his maximum willing-to-pay price. This reference price can be the ridesharing price in the market (e.g. Uberpool price). Passengers can estimate their maximum willing-to-pay prices compared with the reference prices. The interface can also indicate a message that the passenger will definitely be rejected if he reports a maximum willing-to-pay price lower than the baseline price. Given this information, passengers can have their own maximum willing-to-pay prices in mind and report to the system. In contrast, current Uber and Lyft service directly determines the prices based on passengers' destinations. Upon reviewing the information, passengers are able to choose to accept or reject the offer.

3. “Detour” is a commonly aware inconvenience factor in the ridesharing service (Biswas et al., 2017a; Pelzer et al., 2015; BBC news, 2016). Our designed mechanism allows passengers to report their detour tolerances in order to satisfy different passengers’ personalized requirements. In the designed mechanism, the price is also influenced by detour, which is defined as the “extra in-vehicle travel time” beyond the direct shipment time. Generally, the longer extra in-vehicle travel time that a passenger needs to tolerate, the lower price the passenger needs to pay. Accordingly, we use the following value function (Nguyen 2013) to formulate the passengers’ maximum willing-to-pay prices considering their detour tolerances.

$$VA_i(X) = \begin{cases} V_i^{\max} - \alpha_i \times EIVT_i(X), & \text{if passenger(s) } i \text{ is served} \\ 0, & \text{if passenger(s) } i \text{ is not served} \end{cases} \quad (1)$$

where $VA_i(X)$ is passenger(s) i’s value (i.e. maximum willing-to-pay price) given a matching and routing plan X, $V_i^{\max}$ is passenger(s) i’s maximum willing-to-pay price of direct shipment service without detour (i.e. non-detour value). Passenger(s) i’s detour disvalue (i.e. reduced maximum willing-to-pay price caused by detour) is determined by $\alpha_i \times EIVT_i$. Particularly, detour is measured by the extra in-vehicle travel time $EIVT_i$ beyond direct shipment time. α_i is passenger(s) i’s detour tolerance parameter, for example, detour discounting rate. The maximum willing-to-pay price decreases α_i dollars if the extra in-vehicle travel time increases per minute. For example, a passenger reports that the maximum willing-to-pay price of direct shipment service is \$10, and the acceptable detour discounting rate is \$0.5 per minute. If the routing plan X imposes him 4 minutes of extra

in-vehicle travel time, his maximum willing-to-pay price is $10 – 4 × $0.5 = $8. In order to guide passengers to quantify their acceptable detour discounting rate, we can set a reference as the default value as well. The default detour discounting rate can be set to a value that is acceptable for most people (e.g. $1 per extra five-minute in-vehicle travel time). This reference value can be obtained by a practical survey. If the passenger does not change it, the platform will adopt the default value. We can also design a drop-down list with some alternative options (e.g. $0.5, $1, $1.5, $2.0, etc. per 5 minutes) for passengers to choose. Passengers who are less tolerant of detour can choose a higher detour discounting rate and who are more tolerant of detour can choose a lower detour discounting rate. Note that we use this value function as an example for passengers to clarify their detour tolerances, and the value function can change to other forms. For example, passengers can simply report their maximum tolerable extra in-vehicle travel time along with their maximum willing-to-pay prices (Bian and Liu, 2019a). Such detour-based value functions can also prevent drivers from detouring deliberately and thus reduce passengers' complaints about drivers' deliberate detour, because detour cannot increase passengers' payments but increases drivers' transportation cost under this mechanism. Current Uber and Lyft service does not allow passengers to report their detour tolerances, and the price may increase with longer detour under normal circumstances, possibly leading to some drivers' deliberate detour and passengers' complaints (BBC news, 2016).

We should notice that passengers' mobility preference input is not mandatory but is an option designed for passengers to have a personalized service in the mechanism. The mobility preference input is an additional benefit rather than a burden for passengers. Passengers can opt to rather than be forced to key in their mobility preferences if they

indeed have specific requirements. They can opt not to key in these inputs and the system will adopt the default values.

Due to the additional achieved functions, the events' sequence of the studied first-mile ridesharing service is different from that of the Uber/Lyft service, unless the passenger does not key in the mobility preferences and the system adopts the default values. In lieu of considering ridesharing service as a simple "take or not" option, we consider mobility as a human-centric service in interaction with passengers' personalized preferences. In our studied first-mile ridesharing service, after a passenger keys in the mobility preferences, the request is sent to the system, and finally the passenger is notified of the matching and routing plan as well as the price information. In comparison, Uber/Lyft service directly shows the price and the latest arrival time after a passenger keys in the destination, and the passenger can choose to accept or reject the offer before the request is sent.

In summary, this chapter aims to solve the mechanism design problem, how to satisfy passengers' personalized mobility preferences, by developing an optimization approach for matching and routing and designing an incentive pricing scheme.

We make the following assumptions:

- The travel time between two locations is set to be deterministic. The existing navigation apps (e.g. Google Maps) can accurately predict the travel time based on the real-time traffic condition (Wang and Xu, 2011; Amirian et al., 2016). The travel time uncertainty of the on-demand first-mile ridesharing service may be less significant with these advanced navigation apps, and the deterministic treatment might be reasonable for this problem.

- We assume that the change of travel time caused by assignment of first-mile

ridesharing vehicles to different roads in the network is negligible. For the time being, first-mile mobility service accounts for only a small portion of the whole transportation network. We deem that the number of ridesharing vehicles may not be sufficient to be the main factor contributing to road congestion, and thus the travel time will not be significantly impacted as long as first-mile ridesharing vehicles are reasonably assigned to different roads.

- It is assumed that passengers are rational with the objective of maximizing their own utilities, which is defined as the maximum willing-to-pay prices minus the actual paid prices, when deciding the reporting strategies (truthful reporting versus misreporting).
- We assume that passengers will not misreport the departure location and the destination (the transit hub).

5.4 VCG Mechanism in the On-Demand First-Mile Ridesharing Service

As a starting point, we introduce the classical VCG mechanism, which is originally proposed by Vickrey (1961), Clarke (1971), and Groves (1973). VCG mechanism has been widely used in transportation (Xu et al., 2014; Lam, 2016; Zou et al., 2015) to promote individuals' participation and truthful report of their mobility preferences via two important properties, "individual rationality" and "incentive compatibility".

"Individual rationality" means that participants are all willing to participate in the service. This property also indicates that participants' actual payments are no greater than their maximum willing-to-pay prices. Another property "incentive compatibility" indicates that truthfully reporting their preferences is the optimal strategy regardless of other participants' reporting. The matching and routing optimization and pricing for on-demand first-mile ridesharing service are essentially a mechanism design problem. We firstly use

the VCG mechanism due to its important properties. The general VCG payment can be expressed as:

$$p_i = (TV_{-i})^* - TV^*_{-i} \tag{2}$$

p_i is agent i's payment. $(TV_{-i})^*$ is the optimal total social welfare when agent i does not participate. TV^*_{-i} is all except agent i's social welfare of the optimal allocation plan involving all agents' participation (i.e. $TV^*_{-i} = TV^* - VA_i$, where VA_i is agent i's value). The VCG mechanism is also named as Generalized Vickrey Auction (GVA) when there is a single seller or sell-side aggregation (Parkes et al., 2001). The GVA is budget balanced because the auctioneer (the transit agency) simply collects the total payment made by the buyers (passengers) and passes it on to the seller (the service provider) (Parkes et al., 2001).

The objective of VCG is to maximize the social welfare, which has various definitions (e.g. cumulative maximum willing-to-pay prices or summations of reduced costs, etc.) in various applications. In the on-demand first-mile ridesharing application, the social welfare includes passengers' values and the service provider's value. A passenger's value is defined as his/her maximum willing-to-pay price. The service provider's value can be defined as the transportation cost that needs to be covered (Ma et al., 2018). Thus, the objective can be represented by Formula (3).

$$TV^* = \max \sum_g VA_g(X) - TC(X) \tag{3}$$

where $VA_g(X)$ is passenger request g's value and $TC(X)$ is the total transportation

cost given the matching and routing plan X. Let $X^* = \arg\max \sum_g VA_g(X) - TC(X)$ denote the optimal matching and routing plan. Let $(TV_{-i})^* = \max \sum_{g \neq i} VA_g(X) - TC(X)$ and $X_{-i}^* = \arg\max \sum_{g \neq i} VA_g(X) - TC(X)$. We use Figure 5.2 to demonstrate how the VCG payment is calculated. Take Passenger 1 as an example. Passenger 1's price is $VA_2\left(X_{-1}^*\right) + VA_3\left(X_{-1}^*\right) - TC\left(X_{-1}^*\right) - \left(VA_2\left(X^*\right) + VA_3\left(X^*\right) - TC\left(X^*\right)\right) = 6 + 5 - 3.5 - (6 + 5 - 4) = \$0.5$.

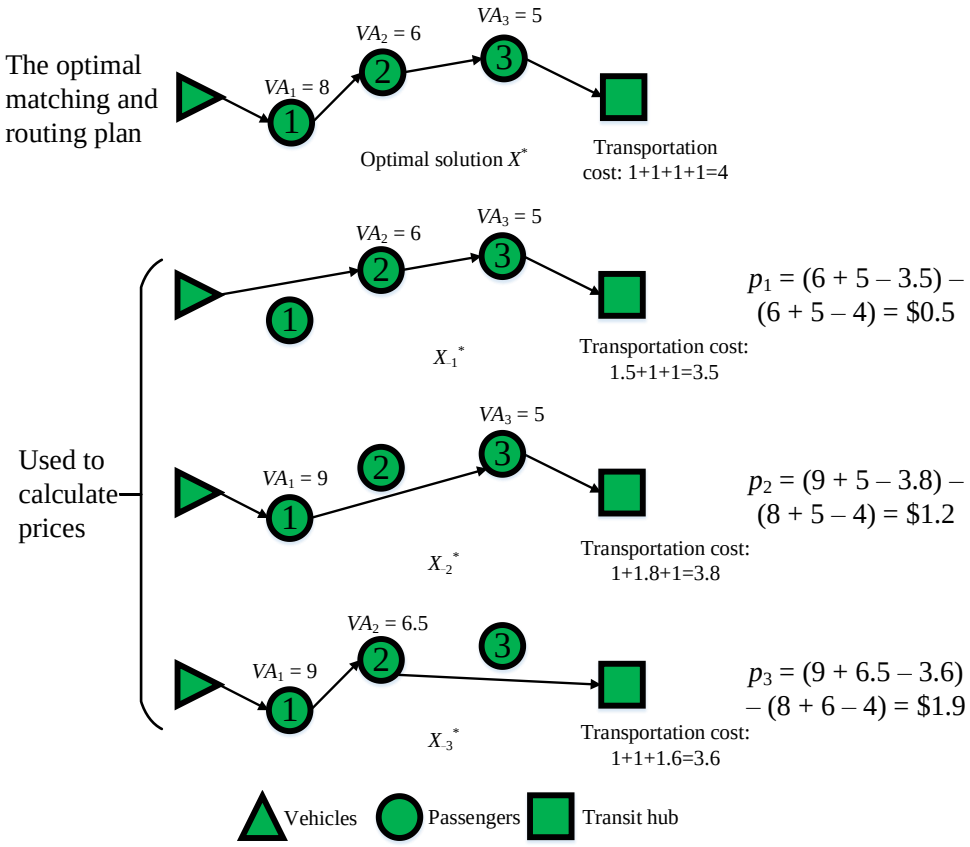

Figure 5.2 A Simple Example to Calculate VCG Prices

From Figure 5.2, we see the limitations of VCG mechanism in the application of

on-demand first-mile ridesharing service. The VCG prices collected from all passengers may not be able to cover the service provider's transportation cost. As the example in Figure 5.2 shows, the total price collected from three passengers is only \$0.5 + \$1.2 + \$1.9 = \$3.6, unable to cover the \$4 transportation cost.

Moreover, the VCG price can sometimes be unreasonably low. For example, in Figure 5.2, Passenger 1 is the farthest away from the transit hub, but his/her price is the cheapest, only \$0.5. In practice, almost no service providers are willing to charge such a low price that is even difficult to cover the fuel cost. The VCG mechanism has these limitations because it simply charges players by the marginal benefit that they contribute to the service system, but does not have a mechanism for price control to ensure service provider' financial sustainability. Based on the above discussions, Section 5 proposes a series of new strategies to overcome the limitations of the application of VCG mechanism in on-demand first-mile ridesharing service.

5.5 Proposed Mobility-Preference-Based Mechanism with Baseline Price Control (MPMBPC)

We propose a mechanism with two pricing layers, which are baseline pricing layer and mobility-preference-based pricing layer (Figure 5.3). The baseline price reflects the minimum price that the service provider wants to earn from a served passenger request. It can be flexibly determined based on passenger locations, relationship between supply and demand, and other factors. The mobility-preference-based pricing layer is determined by three inputs mutually: 1) the matching and routing plan, 2) passengers' mobility preferences (e.g. arrival deadline, maximum willing-to-pay price, and detour tolerance),

and 3) the baseline pricing layer. The detail will be introduced in Section 5.2.

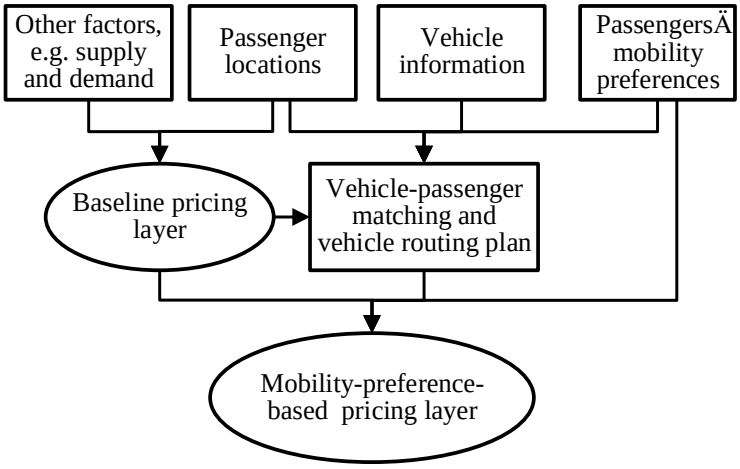

Figure 5.3 Schematic Framework of MPMBPC

5.5.1 Baseline Pricing Layer

In MPMBPC, baseline price control component places a minimum threshold for the actual price so that the price will never be unreasonably low: $p_i \geq PC_i$, where p_i is passenger(s) i's price, and PC_i is the controlled baseline price for passenger(s) i. We suggest that the baseline price rule can apply the widely-used taxi pricing scheme in the market (Taxi calculator, 2018), including a constant initial fee (cf) and the direct shipment distance (d_{i0}) multiplied by a distance rate (dr) (Formula 4).

$$PC_i = cf + dr \times d_{i0} \tag{4}$$

The initial fee and distance rate in the baseline price can be flexibly adjusted based on the service provider's requirement, the transit agency's policy, and the relationship

between supply and demand (e.g. Uber's surging price, Hall et al., 2015). We give the mechanism designers freedom to be able to flexibly set the baseline price. However, modeling these factors in determining the baseline price is beyond the scope of this chapter and is not considered in our mechanism.

5.5.2 Mobility-Preference-Based Pricing Layer

This section introduces the mobility-preference-based pricing layer. In Section 5.2.1, the matching and routing plan is optimized based on the vehicles' and passengers' information. Section 5.2.2 gives the pricing scheme.

5.2.1 The optimal vehicle-passenger matching and vehicle routing plan

In this mechanism, we build an optimization model, denoted as Md_0, for vehicle-passenger matching and vehicle routing, considering the baseline price control component, in each time slice. The optimization model is given by Formulas (5-15). For the notation, please refer to Table 5.1.

Table 5.1 Notation of the Optimization Model

Sets	
P	Set of n passenger requests, $P = \{1, 2, \dots, n\}$, sent in a time slice
V	Set of m available vehicles, $V = \{ n+1, n+2, \dots, n+m \}$, at the end of a time slice
H	Set of the transit hub, $H = \{0\}$
Variables	
$x_{ij}^k = \begin{cases} 1 & \text{if vehicle } k \text{ travels from passenger location } i \text{ to passenger location } j \\ 0 & \text{otherwise} \end{cases}$	

$i, j \in P; k \in V$	
$y_i^k = \begin{cases} 1 & \text{if vehicle } k \text{ picks up passenger(s) of request } i \\ 0 & \text{otherwise} \end{cases}$ $k \in V, i \in P$	
$z_i^k = \begin{cases} 1 & \text{if passenger(s) in request } i \text{ is the first to be served by vehicle } k \\ 0 & \text{otherwise} \end{cases}$ $k \in V, i \in P$	
$w_i^k = \begin{cases} 1 & \text{if vehicle } k \text{ travels to the transit hub immediately after serving passenger(s) in request } i \\ 0 & \text{otherwise} \end{cases}$ $k \in V, i \in P$	
$X = \{x_{ij}^k, y_i^k, z_i^k, w_i^k, \mid i, j \in P, k \in V\}$ is the collection of all of the decision variables, representing a vehicle-passenger matching and vehicle routing plan.	
IVT_i	Passenger(s) i's in-vehicle travel time.
VA_i	Passenger(s) i's value (i.e. maximum willing-to-pay price).
Parameters	
np_i	Number of passengers of request i. For denotation convenience, we let "passenger(s) i" represent the passenger(s) in request i.
AT_k	The time when vehicle k is available.
DL_i	Passenger(s) i's arrival deadline.
c_{ij}	The transportation cost from node i to node j, $i \in P \cup V$ and $j \in P \cup H$
t_{ij}	The travel time from node i to node j, $i \in P \cup V$ and $j \in P \cup H$. The pickup time for passenger(s) j is included in t_{ij}.
Q	The seat capacity of a vehicle, excluding the driver.
α_i	Passenger(s) i's detour discounting rate. The maximum willing-to-pay price

	decreases α_i dollars if the extra in-vehicle travel time increases per minute.
V_i^{max}	Passenger(s) i's non-detour value. Passenger(s) i's maximum willing-to-pay price is V_i^{max} if he is driven to the transit hub without any extra in-vehicle travel time.
PC_i	Passenger(s) i's baseline price.

Objective function:

$$\max f(X) = \sum_{i \in P} VA_i(X) - TC(X) + \sum_{i \in P} PC_i \left(1 - \sum_{k \in V} y_i^k\right) \tag{5}$$

where

$$TC(X) = \sum_{k \in V} \sum_{i \in P} \sum_{j \in P} x_{ij}^k c_{ij} + \sum_{k \in V} \sum_{i \in P} z_i^k c_{ki} + \sum_{k \in V} \sum_{i \in P} w_i^k c_{i0}$$

Subject to

$$z_j^k + \sum_{i \in P} x_{ij}^k = y_j^k \quad \text{for all } k \in V, j \in P \tag{6}$$

$$w_i^k + \sum_{j \in P} x_{ij}^k = y_i^k \quad \text{for all } k \in V, i \in P \tag{7}$$

$$\sum_{i \in P} z_i^k \le 1 \quad \text{for all } k \in V \tag{8}$$

$$\sum_{k \in V} y_i^k \leq 1 \quad \text{for all } i \in P \tag{9}$$

$$\sum_{i \in P} y_i^k np_i \leq Q \quad \text{for all } k \in V \tag{10}$$

$$\sum_{i \in P} \sum_{j \in P} x_{ij}^k t_{ij} + \sum_{i \in P} z_i^k t_{ki} + \sum_{i \in P} w_i^k t_{i0} \leq y_i^k \left(DL_i - AT_k \right) + \left(1 - y_i^k\right) M \quad \text{for all } i \in P, k \in V \tag{11}$$

$$IVT_i = \sum_{k \in V} \sum_{j \in P} x_{ij}^k \left(IVT_j + t_{ij} \right) + \sum_{k \in V} w_i^k t_{i0} \text{ for all } i \in P \tag{12}$$

$$IVT_i \geq 0 \text{ for all } i \in P \tag{13}$$

$$VA_i = \left(V_i^{\max} - \alpha_i \cdot \left(IVT_i - t_{i0} \right) \right) \sum_{k \in V} y_i^k \quad \text{for all } i \in P \tag{14}$$

$$x_{ij}^k, y_i^k, z_i^k, w_i^k \in \{0,1\} \quad \text{for all } i, j \in P, k \in V \tag{15}$$

The objective function integrates three parts, including passengers' cumulative values, the service provider's transportation cost, and the baseline price control component. The first two parts, passengers' values and the negative transportation cost, are defined as "social welfare" (Ma et al., 2018). The objective includes maximization of the total social welfare instead of profit maximization because of the following reason. In our research, we consider ridesharing as a means to bridge the first-mile gap to public transit. We design a mechanism to incentivize more passengers to take the ridesharing service. In the long run, this not only makes the ridesharing serve more people but also probably encourages more people to use "ridesharing plus public transportation" in lieu of driving alone to the destinations. We anticipate that a smooth, integrated multimodal connection will have significant societal benefits (e.g. reduced congestion, emission, and energy use). With this goal in mind, we will need to consider passengers' values (in order to incentivize more

passengers to take ridesharing). Additionally, we also consider transportation cost so that the ridesharing service can be financially sustainable (even if the profit is not the maximal). The objective of maximizing profit has been widely studied in other studies (Biswas et al., 2017a,b; Asghari et al., 2016). The maximum profit goal may not necessarily encourage people to have low-cost access to public transit nor achieve the societal goals as considered in this chapter. The third part of the objective function is the baseline price control component. Under normal circumstances, the service provider has a minimum baseline price threshold (PC_i, $i \in P$) to serve passenger(s) in one location. In order to ensure passenger(s) i's payment p_i greater than or equal to PC_i given this passenger(s) being served, his value must be greater than or equal to PC_i if the mechanism is individual rational (see Definition 1). That is if $p_i \geq PC_i$, the condition $VA_i \geq PC_i$ must be satisfied; otherwise, the mechanism is not individual rational.

Proposition 1 Adding the baseline price control component in the objective function can ensure that if any passenger(s) i's request is accepted, his value will never be smaller than PC_i; otherwise, this passenger request will be rejected (for the detailed proof, please see Appendix A).

The objective function (Formula 5) has another more straightforward interpretation after equivalent reformulation.

$$f(X) = \sum_{i \in P} VA_i(X) - TC(X) + \sum_{i \in P} PC_i \left(1 - \sum_{k \in V} y_i^k\right)$$

$$= \sum_{i \in P} VA_i(X) - TC(X) + \sum_{i \in P} PC_i - \sum_{i \in P} PC_i \sum_{k \in V} y_i^k$$

where $\sum_{i\in P} PC_i$ is a constant and can be removed from the objective function. Then Formula (5) is equivalent to

$$\max \sum_{i\in P} VA_i\left(X\right) - TC(X) - \sum_{i\in P} PC_i \sum_{k\in V} y_i^k$$

Based on Formula (14), $VA_i = \left(V_i^{\max} - \alpha_i\left(IVT_i - t_{i0}\right)\right)\sum_{k\in V} y_i^k$, when $\sum_{k\in V} y_i^k = 0$, $VA_i = 0$, and when $\sum_{k\in V} y_i^k = 1$, $VA_i = V_i^{\max} - \alpha_i(IVT_i - t_{i0})$. Thus, the objective function is equivalent to Formula (16) below.

$$\begin{aligned} &\max \sum_{i\in P} VA_i \sum_{k\in V} y_i^k - TC(X) - \sum_{i\in P} PC_i \sum_{k\in V} y_i^k \\ &\Leftrightarrow \max \sum_{i\in P} \left(VA_i - PC_i\right) \sum_{k\in V} y_i^k - TC(X) \end{aligned} \tag{16}$$

where $(VA_i - PC_i)$ can be interpreted as passenger(s) i's "surplus value" beyond the baseline price. The baseline price plays the role of reserve price defined in the literature (McAfee, 1993; Jehiel, 1999; Hartline and Roughgarden, 2009). In the auction design theory, buyers bid for a good with a price starting from the reserve price, which is set by the seller. In fact, the social welfare in the auction with reserve prices is buy s' accumulative surplus value beyond the reserve price (McAfee, 1993; Jehiel, 1999; Hartline and Roughgarden, 2009). Thus, this objective function (Formula 16) can be interpreted as the "surplus social welfare", which is defined as passengers' cumulative surplus values minus the service provider's transportation cost. We have the following reason to use this

objective function.

The baseline price (PC_i) in the objective function of "surplus social welfare" maximization plays an important role in differentiating passenger requests with identical maximum willing-to-pay prices but in different locations and/or with different numbers of passengers in the requests. For example, two passengers in two different locations send two requests. They have identical maximum willing-to-pay prices ($VA_1 = VA_2$). The first passenger's location is farther away from the transit hub than the second passenger's location. Thus, the first passenger's baseline price is greater than the second passenger's baseline price ($PC_1 > PC_2$). Intuitively, the second passenger is more valuable than the first passenger. This can be reflected by passengers' surplus values: we have $VA_1 - PC_1 < VA_2 - PC_2$, indicating that the second passenger has a larger surplus value and is more valuable. Similarly, passenger requests in the same location with identical maximum willing-to-pay prices but with different numbers of passengers in the requests are treated as differently valuable requests. For example, in the same location, the first request has one passenger ($np_1 = 1$), and the second request has two passengers ($np_2 = 2$). The mechanism can set $PC_1 < PC_2$ since the second request has one more passenger. Then, we have $VA_1 - PC_1 > VA_2 - PC_2$, indicating that the first request has a larger surplus value and is more valuable.

Formulas (6-15) are the constraints of model Md_0. Formula (6) ensures that if passenger(s) j is picked up by vehicle k, vehicle k must come from one location, either the vehicle departure location or the last passenger(s) location. Formula (7) demonstrates that if passenger(s) i is picked up by vehicle k, vehicle k must travel to the next location, either the destination (transit hub) or the location of the next passenger(s). Formula (8) ensures that each vehicle should be dispatched at most once in each time slice. Formula (9)

represents that each passenger(s) will either be picked up by one vehicle or not be served by any vehicles. Formula (10) is the vehicle capacity constraint. Constrained by Formula (11), in which "*M*" is a large enough number, each vehicle, after it is available, must be able to arrive at the transit hub before arrival deadlines of all passengers served by this vehicle. Formula (12) formulates all passengers' in-vehicle travel times, as well as prohibits illegal sub-tours. Formula (13) guarantees the non-negativity of each passenger's in-vehicle travel time. Formula (14) obtains all passengers' values. If passenger(s) *i* is served by a vehicle, the value equals $V_i^{max} - \alpha_i(IVT_i - t_{i0})$. Otherwise, the passenger's value is zero. Formula (15) means that x_{ij}^k, y_i^k, z_i^k, are w_i^k are binary variables.

In this model, only the Formulas (12) and (14) are nonlinear, which can be reformulated as linear constraints.

For Formula (12), we introduce a new variable u_{ij}^k. We use Formulas (17) and (18) to ensure that $u_{ij}^k = x_{ij}^k IVT_j$ for all $i, j \in P, k \in V$.

$$0 \le u_{ij}^k \le IVT_j \text{ for all } i, j \in P, k \in V \tag{17}$$

$$IVT_j - (1 - x_{ij}^k)M \le u_{ij}^k \le x_{ij}^k M, \text{ for all } i, j \in P, k \in V \tag{18}$$

where "*M*" is an enough large positive number.

Then Formula (12) can be linearized to Formula (19).

$$IVT_i = \sum_{k \in V} \sum_{j \in P} \left(u_{ij}^k + x_{ij}^k t_{ij} \right) + \sum_{k \in V} w_i^k t_{i0} \text{ for all } i \in P \tag{19}$$

Formula (14) can be reformulated as Formulas (20) and (21), because $\sum_{k \in V} y_i^k$ is

equal to either 0 or 1 for all $i \in P$ based on Formula (9).

$$0 \le VA_i \le V_i^{\max} - \alpha_i \cdot \left(IVT_i - t_{i0} \right) \quad \text{for all } i \in P \tag{20}$$

$$V_i^{\max} - \alpha_i \cdot \left(IVT_i - t_{i0} \right) - \left(V_i^{\max} + \alpha_i t_{i0} \right) \left(1 - \sum_{k \in V} y_i^k \right) \le VA_i \le V_i^{\max} \sum_{k \in V} y_i^k, \text{ for all } i \in P \tag{21}$$

Formulas (20) and (21) ensure that if passenger(s) i is served ($\sum_{k \in V} y_i^k = 1$), his value equals $V_i^{\max} - \alpha_i (IVT_i - t_{i0})$; otherwise, his value equals 0.

After reformulation, the constraints are Formulas (6-11, 13, 15, 17-21). Then optimization model Md_0 is a mixed integer linear programming, which can be exactly solved by a commercial solver CPLEX using a branch and bound algorithm.

5.2.2 The pricing scheme

Before introducing the pricing scheme, we newly define a set of optimization models, Md_g, $g \in P$. Note that models Md_g ($g \in P$) are used to calculate the prices, and do not affect the matching and routing plan.

Objective function:

Formula (5): $\max f(X) = \sum_{i \in P} VA_i(X) - TC(X) + \sum_{i \in P} PC_i \left(1 - \sum_{k \in V} y_i^k \right)$

Constraints:

Formulas (6-11, 13, 15, 17-21) and Formula (22)

$$y_g^k = 0, \quad \text{for all } k \in V \tag{22}$$

The practical meaning of model Md_g is that passenger(s) g is rejected by the service and the remaining passengers' matching and routing plan is optimized with the same objective function of model Md_0.

Let $f(X)$ denote the objective function of models Md_0 and Md_g. Let $X^*_{Md_0}$ and $X^*_{Md_g}$ denote the optimal solutions of models Md_0 and Md_g, respectively. The price is given by

$$p_g = f\left(X^*_{Md_g}\right) - f\left(X^*_{Md_0}\right) + VA_g\left(X^*_{Md_0}\right) \tag{23}$$

In practice, the price is determined when the passenger's request is accepted and will not change if there is no deliberate detour. However, if the driver deliberately detours, the price will decrease. After the matching and routing plan is determined, the first two parts in Formula (23) "$f\left(X^*_{Md_g}\right) - f\left(X^*_{Md_0}\right)$" are determined and will not change any more. The third part "$VA_g\left(X^*_{Md_0}\right)$", which is the passenger's value, is determined by the actual routing and may change due to extra detour. Therefore, in practice, the pricing scheme can be formulated as $p_g = f\left(X^*_{Md_g}\right) - f\left(X^*_{Md_0}\right) + VA_g\left(X_{actual}\right)$, where X_{actual} is the actual route adopted by all dispatched vehicles. If all dispatched vehicles implement the routing plan exactly as specified by $X^*_{Md_0}$, then $X_{actual} = X^*_{Md_0}$ and all passengers' prices will not change after the plan is determined. However, if the vehicle serving passenger(s) g deliberately detours, causing extra in-vehicle travel time for the passenger, passenger(s) g's value will decrease: $VA_g\left(X_{actual}\right) < VA_g\left(X^*_{Md_0}\right)$, and the price decreases as well. This

indicates that the driver will lose money due to deliberate detour. Thus, this mechanism can prevent drivers' deliberate detour.

Figure 5.4 uses the same example in Figure 5.2 to demonstrate the pricing scheme of the MPMBPC mechanism. Take Passenger 1 as an example. Passenger 1's price is

$$PC_1 + VA_2\left(X^*_{Md_1}\right) + VA_3\left(X^*_{Md_1}\right) - TC\left(X^*_{Md_1}\right) - \left(VA_2\left(X^*_{Md_0}\right) + VA_3\left(X^*_{Md_0}\right) - TC\left(X^*_{Md_0}\right)\right) = PC_1 + 6 + 5 - 3.5 - (6 + 5 - 4) = PC_1 + 0.5.$$

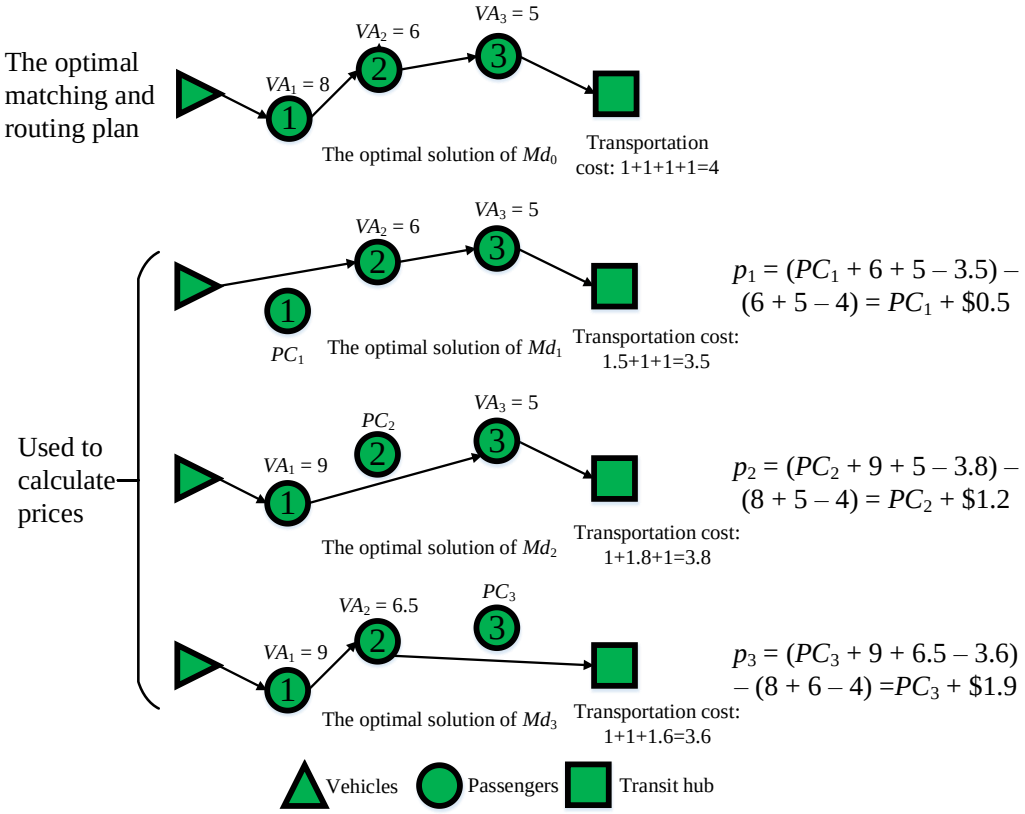

Figure 5.4 A Simple Example to Calculate MPMBPC Prices

Note that this pricing scheme is not simply the VCG price plus the baseline price. We use another example to show the difference between the proposed pricing scheme and

the VCG price plus the baseline price and to demonstrate the advantage of the proposed mechanism (Appendix B.1)

Finally, Algorithm 1 presents the pseudocode to obtain the MPMBPC mechanism design solutions.

Algorithm 1 obtaining the MPMBPC mechanism $\boldsymbol{M}\left(X^*_{Md_0}, \mathbf{p}\right)$

Input all parameters.

Solve the optimization model Md_0 and get the optimal solution $X^*_{Md_0}$, the optimal objective function value $f\left(X^*_{Md_0}\right)$, and each passenger's value $VA_g\left(X^*_{Md_0}\right)$.

For g = 1:n

Solve the optimization model Md_g, and get the optimal objective function value $f\left(X^*_{Md_g}\right)$.

Calculate passenger(s) g's price $p_g = f\left(X^*_{Md_g}\right) - f\left(X^*_{Md_0}\right) + VA_g\left(X^*_{Md_0}\right)$.

End for

Output the mechanism $\boldsymbol{M}\left(X^*_{Md_0}, \mathbf{p}\right)$.

5.5.3 Theoretical Analysis

Theoretical analysis is used to prove that the proposed MPMBPC mechanism can ensure important mechanism design properties, including "individual rationality", "incentive compatibility", "price controllability", and "detour-discounting reasonability".

Definition 1. Individual rationality. A mechanism is individual rational if all passengers' values are greater than or equal to the actual price paid (the utility is always non-negative, Formula 24).

$$U_g = VA_g - p_g \geq 0 \text{ for any } g \in P \tag{24}$$

Proposition 2 The mechanism $\boldsymbol{M}(X^*_{Md_0}, \mathbf{p})$ is individual rational.

$$U_g\left(X^*_{Md_0}, p_g\right) = VA_g\left(X^*_{Md_0}\right) - p_g \geq 0 \quad \text{for any passenger(s) } g \in P$$

Proof:

$$\begin{aligned} U_g\left(X^*_{Md_0}, p_g\right) &= VA_g\left(X^*_{Md_0}\right) - p_g \\ &= f\left(X^*_{Md_0}\right) - f\left(X^*_{Md_g}\right) \end{aligned}$$

Compared with model Md_0, the model Md_g has one more constraint (Formula 22). Thus the constraints of model Md_g are stricter than those of model Md_0, and thus the optimal objective function value of model Md_0 is greater than or equal to that of Md_g. That is

$$f\left(X^*_{Md_0}\right) - f\left(X^*_{Md_g}\right) \geq 0$$

Thus,

$$U_g\left(X^*_{Md_0}, p_g\right) = VA_g\left(X^*_{Md_0}\right) - p_g \geq 0$$

□

Definition 2. Incentive compatibility. A mechanism is incentive compatible if truthfully reporting the arrival deadline, non-detour value, and detour discounting rate is optimal for any passenger regardless of other passengers' reporting strategies.

$$U_g{}' \leq U_g, \text{ for any } g \in P \tag{25}$$

where $U_g{}'$ is passenger(s) g's utility if he misreports DL_g, $V_g^{\max}$, and/or α_g, and U_g is passenger(s) g's utility if he truthfully reports DL_g, $V_g^{\max}$, and α_g.

Proposition 3 The mechanism $\boldsymbol{M}(X^*_{Md_0}, \mathbf{p})$ is incentive compatible.

Proof:

We assume that if any passenger(s) g misreports DL_g, V_g^{max}, and/or α_g, the optimal vehicle-passenger matching and vehicle routing plan (i.e. the optimal solution of model Md_0) becomes $Y^*_{Md_0}$. The system will mistake passenger(s) g's actual value ($VA_g\left(Y^*_{Md_0}\right)$) for $VA'_g\left(Y^*_{Md_0}\right)$. Note that the system uses all passengers' reported information as input data to calculate the prices regardless of the truthfulness.

It can be easily proved that the optimal solution $X^*_{Md_g}$ of model Md_g remains

constant no matter what passenger(s) g reports. This is because in model Md_g, passenger(s) g is not served by any vehicle, and thus the model Md_g is independent of passenger(s) g's reported values. Then the price is

$$p'_g = f\left(X^*_{Md_g}\right) - f'\left(Y^*_{Md_0}\right) + VA'_g\left(Y^*_{Md_0}\right)$$

where $f'\left(Y^*_{Md_0}\right) = \sum_{i\in P, i\neq g} VA_i\left(Y^*_{Md_0}\right) + VA'_g\left(Y^*_{Md_0}\right) + \sum_{i\in P} PC_i\left(1 - \sum_{k\in V} y_i^k\right) - TC\left(Y^*_{Md_0}\right)$.

We discuss two subcases:

1) Passenger(s) g is unable to arrive at the transit hub before the actual arrival deadline given the matching and routing plan $Y^*_{Md_0}$. Thus, passenger(s) g's requirement is not satisfied while he could have arrived at the transit hub in time if he had truthfully reported the deadline. Truthful report is the best strategy for this case.

2) Passenger(s) g can arrive at the transit hub before the actual arrival deadline given the plan $Y^*_{Md_0}$. For this case, $Y^*_{Md_0}$ is a feasible solution of model Md_0. Given the misreported information, passenger(s) g's utility is

$$\begin{aligned} U_g\left(Y^*_{Md_0}, p'_g\right) &= VA_g\left(Y^*_{Md_0}\right) - p'_g \\ &= f'\left(Y^*_{Md_0}\right) - VA'_g\left(Y^*_{Md_0}\right) + VA_g\left(Y^*_{Md_0}\right) - f\left(X^*_{Md_g}\right) \\ &= f\left(Y^*_{Md_0}\right) - f\left(X^*_{Md_g}\right) \end{aligned}$$

In this case, $Y^*_{Md_0}$ is a feasible solution but not necessarily the optimal solution of

model Md_0 while $X^*_{Md_0}$ is the optimal solution of model Md_0 if passenger(s) g truthfully reports his value. Thus,

$$f\left(Y^*_{Md_0}\right) \le f\left(X^*_{Md_0}\right).$$

Thus, we have

$$U_g\left(Y^*_{Md_0}, p_g'\right) = f\left(Y^*_{Md_0}\right) - f\left(X^*_{Md_g}\right) \le f\left(X^*_{Md_0}\right) - f\left(X^*_{Md_g}\right) = U_g\left(X^*_{Md_0}, p_g\right)$$

This indicates that truthfully reporting the mobility preference is passenger(s) g's weakly dominant strategy regardless of other passengers' reporting strategies.

□

Definition 3. Price controllability. A mechanism is price controllable if the following condition is satisfied. If any passenger(s) g is served by a vehicle, the price is greater than or equal to the baseline price PC_g; otherwise, the price is zero.

$$p_g \begin{cases} =0, \text{ if passenger(s) } g \text{ is not served} \\ \ge PC_g, \text{ if passenger(s) } g \text{ is served} \end{cases} \tag{26}$$

Before proving that the mechanism has the property of price controllability, we define the concept of "transition solution", which will be used in the proof of price controllability.

Definition 4. Transition solution. $Y_g = TS_g(X)$ is the g^{th} transition solution from a feasible solution X of the model Md_0 to the corresponding feasible solution Y_g of the model Md_g if the transition process is given by Algorithm 2.

Algorithm 2 Obtain the transition solutions $Y_g = TS_g(X)$

Input a solution $X = \{x_{ij}^k, y_i^k, z_i^k, w_i^k\}$;

Let $Y_g = X$;

If $\sum_{k \in V} y_g^k = 1$

Find k that $y_g^k = 1$;

If $z_g^k = 0$ or $w_g^k = 0$

If $z_g^k = 1$

Find j that $x_{gj}^k = 1$ and let $x_{gj}^k = 0$;

Let $z_j^k = 1$;

Else

If $w_g^k = 1$

Find i that $x_{ig}^k = 1$ and let $x_{ig}^k = 0$;

Let $w_i^k = 1$;

Else

Find i that $x_{ig}^k = 1$ and let $x_{ig}^k = 0$;

Find j that $x_{gj}^k = 1$ and let $x_{gj}^k = 0$;

Let $x_{ij}^k = 1$;

End if

End if

Let $y_g^k = 0, z_g^k = 0, w_g^k = 0$;

End if

Output Y_g.

Transition solution can be described as follows. If passenger(s) g is not served by any vehicle in solution X, the gth transition solution of X is identical with X. If passenger(s) g is served by a vehicle in solution X (shown in Figure 5.5), in the transition solution $TS_g(X)$, the vehicle gets rid of passenger(s) g and the remaining routing plan keeps unchanged.

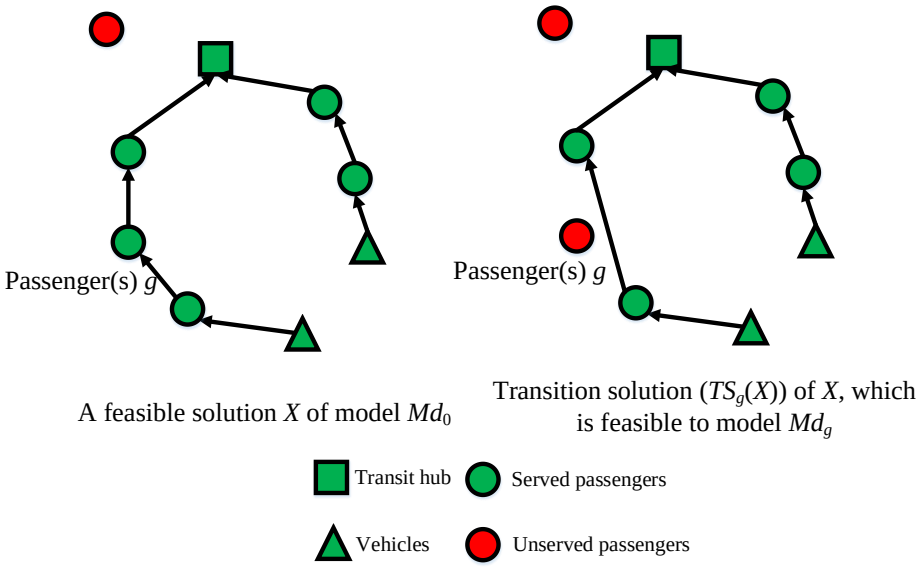

Figure 5.5 An Example of Transition Solution

Proposition 4 If $Y_g = TS_g(X)$, for any $g \in P$, the transportation cost $TC(Y_g) \leq TC(X)$. The proof is shown in Appendix A.

Proposition 4 will be used in the proof of Proposition 6.

Proposition 5 If $Y_g = TS_g(X)$, for any $g \in P$, $\sum_{i \in P \setminus g} VA_i(X) \le \sum_{i \in P} VA_i\left(Y_g\right)$.

The proof is presented in Appendix A.

Proposition 5 will be used in the proof of Proposition 6.

Proposition 6 The proposed mechanism is price controllable.

Proof:

If passenger(s) g is not served in the plan $X^*_{Md_0}$, $VA_g\left(X^*_{Md_0}\right) = 0$ and it is obvious that $X^*_{Md_0} = X^*_{Md_g}$. Then

$$p_g = f\left(X^*_{Md_g}\right) - f\left(X^*_{Md_0}\right) + VA_g\left(X^*_{Md_0}\right) = 0.$$

Now we consider that passenger(s) g is served in the plan $X^*_{Md_0}$. Let Y_g^* be the gth transition solution of $X^*_{Md_0}$, i.e. $Y_g^* = TS_g\left(X^*_{Md_0}\right)$. Since Y_g^* is a feasible solution of model Md_g while $X^*_{Md_g}$ is the optimal solution of model Md_g, we have $f\left(X^*_{Md_g}\right) \ge f\left(Y_g^*\right)$.

$$\begin{aligned}
p_g &= f\left(X^*_{Md_g}\right) - f\left(X^*_{Md_0}\right) + VA_g\left(X^*_{Md_0}\right) \\
&\ge f\left(Y_g^*\right) - f\left(X^*_{Md_0}\right) + VA_g\left(X^*_{Md_0}\right) \\
&= PC_g + \left(\sum_{i \in P} VA_i\left(Y_g^*\right) - \sum_{i \in P \setminus g} VA_i\left(X^*_{Md_0}\right)\right) + \left(TC\left(X^*_{Md_0}\right) - TC\left(Y_g^*\right)\right)
\end{aligned}$$

Based on Propositions 4 and 5, respectively, we have

$$TC\left(X^*_{Md_0}\right) - TC\left(Y^*_g\right) \geq 0$$

and

$$\sum_{i \in P} VA_i\left(Y^*_g\right) - \sum_{i \in P \setminus g} VA_i\left(X^*_{Md_0}\right) \geq 0.$$

Thus, we have

$$p_g \geq PC_g .$$

□

Definition 5. Detour-discounting reasonable. The mechanism is detour-discounting reasonable if the following condition is satisfied. If passenger(s) g (for any $g \in P$) places a stricter requirement on detour (i.e. α_g is increased), as long as this passenger(s) is still served by a vehicle, then

1) this passenger(s)' extra in-vehicle travel time will either remain constant or decrease, and

2) the price will either remain constant or increase.

Using mathematical expression: when $\alpha_g = \alpha_g^-$, the optimal vehicle-passenger matching and vehicle routing plan is X^- and the price is p^-, and when $\alpha_g = \alpha_g^+$, the optimal vehicle-passenger matching and vehicle routing plan is X^+ and the price is p^+. If $\alpha_g^+ > \alpha_g^-$, $EIVT_g(X^-) \geq EIVT_g(X^+)$ and $p^- \leq p^+$.

Proposition 7 The mechanism $\boldsymbol{M}(X^*_{Md_0}, \mathbf{p})$ is detour-discounting reasonable

Proof:

There exists a set $\{\alpha_g^1, \ldots, \alpha_g^k, \ldots, \alpha_g^K\}$, where $\alpha_g^K > \alpha_g^{K-1} > \ldots > \alpha_g^1$ are transition points of passenger(s) g's detour discounting rate α_g, through which the optimal matching and routing plan changes (Note that we only consider the situation in which passengers are still served by one vehicle according to Definition 5). When α_g is varying within the range $[\alpha_g^k, \alpha_g^{k+1}]$ for any k, the optimal plan of model Md_0 does not change. When α_g is varying beyond the range $[\alpha_g^k, \alpha_g^{k+1}]$, the optimal plan changes.

Assume that passenger(s) g (for any $g \in P$) increases α_g from α_g^- to α_g^+. We only need to prove two sub-propositions below, and then Proposition 7 can be proved.

1) If both α_g^+ and α_g^- belong to $[\alpha_g^k, \alpha_g^{k+1}]$, for any $k = 1, 2, \ldots, K-1$, passenger(s) g's extra in-vehicle travel time and price do not change.

2) If $\alpha_g^- \in [\alpha_g^{k-1}, \alpha_g^k]$ and $\alpha_g^+ \in [\alpha_g^k, \alpha_g^{k+1}]$, for any $k = 2, \ldots, K-1$, passenger(s) g's extra in-vehicle travel time is non-increasing and his price is non-decreasing.

For the first situation, since the optimal matching and routing plan does not change, passenger(s) g's extra in-vehicle travel time does not change as well. In the price calculation $p_g = f\left(X^*_{Md_g}\right) - f\left(X^*_{Md_0}\right) + VA_g\left(X^*_{Md_0}\right)$, $f\left(X^*_{Md_g}\right)$ is independent of passenger(s) g's reported detour discounting rate α_g. Thus $f\left(X^*_{Md_g}\right)$ remains constant. Moreover, $f\left(X^*_{Md_0}\right) - VA_g\left(X^*_{Md_0}\right) = \sum_{i \in P \setminus g} VA_i - TC + \sum_{i \in P} PC_i \left(1 - \sum_{k \in V} y_i^k\right)$ also remains constant because all other elements do not change due to the constant of the optimal plan. Thus, the price remains constant.

Let us prove the second situation. Let $F^-(\alpha_g) = f(X^{-*}, \alpha_g)$ denote the objective

function value of model Md_0 given that X^{-*} is the optimal plan when $\alpha_g = \alpha_g^- \in [\alpha_g^{k-1}, \alpha_g^k]$. Let $F^+(\alpha_g) = f(X^{+*}, \alpha_g)$ denote the objective function value of model Md_0 given that X^{+*} is the optimal plan when $\alpha_g = \alpha_g^+ \in [\alpha_g^k, \alpha_g^{k+1}]$. Both $F^-(\alpha_g)$ and $F^+(\alpha_g)$ are denoted as functions of α_g. Based on Formulas (1) and (5), we have

$$\frac{dF^-(\alpha_g)}{d\alpha_g} = -EVIT(X^{-*}), \text{ and}$$

$$\frac{dF^+(\alpha_g)}{d\alpha_g} = -EVIT(X^{+*})$$

Let $\alpha_g^+ = \alpha_g^k + \Delta\alpha_g$ ($\Delta\alpha_g > 0$). Then

$$F^+(\alpha_g^+) = F^+(\alpha_g^k + \Delta\alpha_g) = F^+(\alpha_g^k) - \Delta\alpha_g EIVT_g(X^{+*})$$
$$F^-(\alpha_g^+) = F^-(\alpha_g^k + \Delta\alpha_g) = F^-(\alpha_g^k) - \Delta\alpha_g EIVT_g(X^{-*})$$

Since

$$F^+(\alpha_g^+) = f(X^{+*}, \alpha_g^+) \geq f(X^{-*}, \alpha_g^+) = F^-(\alpha_g^+)$$

thus,

$$F^+(\alpha_g^k) - \Delta\alpha_g EIVT_g(X^{+*}) \geq F^-(\alpha_g^k) - \Delta\alpha_g EIVT_g(X^{-*})$$

It is obvious that $F^{+}(\alpha_g^k) = F^{-}(\alpha_g^k)$ because α_g^k is the transition point of passenger(s) g's detour discounting rate α_g, through which the optimal matching and routing plan changes. Thus

$$EIVT_g(X^{+*}) \le EIVT_g(X^{-*})$$

Let p_g^{k+} represent passenger g's price when his detour discounting rate $\alpha_g = \alpha_g^k$ and the optimal plan is X^{+*}. Since when α_g^{+} belongs to $[\alpha_g^k, \alpha_g^{k+1}]$, the price, denoted as p_g^{+}, remains constant if the optimal plan X^{+*} does not change as we proved in the first situation, then

$$p_g^{+} = p_g^{k+} = f\left(X_{Md_g}^{*}\right) - f\left(X^{+*}, \alpha_g^k\right) + VA_g\left(X^{+*}, \alpha_g^k\right)$$

Let p_g^{k-} represent passenger g's price when his detour discounting rate $\alpha_g = \alpha_g^k$ and the optimal plan is X^{-*}. Since when α_g^{-} belongs to $[\alpha_g^{k-1}, \alpha_g^k]$, the price, denoted as p_g^{-}, remains constant if the optimal plan X^{-*} does not change, then

$$p_g^{-} = p_g^{k-} = f\left(X_{Md_g}^{*}\right) - f\left(X^{-*}, \alpha_g^k\right) + VA_g\left(X^{-*}, \alpha_g^k\right)$$

Based on Formula (1), $VA_g\left(X^{-*}, \alpha_g^k\right) \le VA_g\left(X^{+*}, \alpha_g^k\right)$ since $EIVT_g(X^{+*}) \le EIVT_g(X^{-*})$. Moreover, it is obvious that $f\left(X^{-*}, \alpha_g^k\right) = f\left(X^{+*}, \alpha_g^k\right)$. Thus,

$$p_g^+ = f\left(X^*_{Md_g}\right) - f\left(X^{+*}, \alpha_g^k\right) + VA_g\left(X^{+*}, \alpha_g^k\right) \geq f\left(X^*_{Md_g}\right) - f\left(X^{-*}, \alpha_g^k\right) + VA_g\left(X^{-*}, \alpha_g^k\right) = p_g^-$$

□

Finally, our mechanism can ensure that different requests with identical mobility preferences (i.e. arrival deadlines, non-detour values, and detour disvalues) sent from the same location within the same time slice can have the same service and are charged with identical prices if they are all served by the same vehicle. This property can be mathematically represented by Proposition 8.

Proposition 8 We have $p_i = p_j$ for any two passengers i and j, satisfying that $DL_i = DL_j$, $V_i^{\max} = V_j^{\max}$, $\alpha_i = \alpha_j$, $L_i = L_j$, and rt_i and $rt_j \in TS_h$, and there exists a vehicle k that $y_i^k = y_j^k = 1$, where L_i and L_j are passengers i's and j's locations, respectively, rt_i and rt_j, passengers i's and j's request times, are within the same time slice TS_h.

The proof is presented in Appendix A.

However, we cannot easily tell whether two passengers in the same origin with different mobility preferences will be charged with the same or different prices. We use two examples for demonstration (see Appendix B.2).

5.6 Solution Approaches

This section proposes solution approaches for small-scale and large-scale problems, respectively. The optimization models, including Md_0 and Md_g for all $g \in P$, have already been reformulated as mixed integer linear programming (MILP). When the problem scale is small, the models can be solved exactly by the commercial solver "CPLEX" in the software AIMMS using a Branch and Bound algorithm.

However, because these models are all NP-hard, exact algorithms are unable to

solve these models in polynomial time. Thus, we design an efficient heuristic algorithm, solution pooling approach (SPA), to solve large-scale on-demand ridesharing problems. SPA is originally proposed by our previous work (Bian and Liu, 2019b) for solving the scheduled ridesharing mechanism design problem. In this chapter, we adapt the original SPA algorithm to the on-demand scenario. We will theoretically prove that SPA is able to sustain the properties of "individual rationality", "incentive compatibility", and "detour-discounting reasonability" in the following sections. In comparison, other traditional heuristic algorithms may not sustain these properties. Note that SPA can simultaneously handle the n+1 optimization models (one model Md_0 and n models Md_g) in the designed mechanism, where n is the number of passenger requests in a time slice, whereas traditional heuristic algorithms have to solve these models one by one. Therefore, it is expected that the SPA is more computationally efficient than traditional heuristic algorithms.

The basic idea of SPA is to pre-generate solution pools for the corresponding models and select the best solution from each solution pool. We denote the solution pools of models Md_0 and Md_g as $Xpool_{Md_0}$ and $Xpool_{Md_g}$, respectively. The method to generate solution pools $Xpool_{Md_0}$ and $Xpool_{Md_g}$ can be described as follows. First, SPA generates an initial solution pool $Xpool$ for the optimization model Md_0 (see Algorithm 3). Second, Algorithm 2 is used to generate gth (for all $g \in P$) transition solutions of each solution in $Xpool$. These transition solutions form the solution pool $Xpool_{Md_g}$ for each $g \in P$. Finally, all solutions in $Xpool_{Md_g}$ for all $g \in P$ are combined into the initial pool $Xpool$ to form a new solution pool $Xpool_{Md_0}$ of model Md_0.

All solution pools should be pre-generated and passengers' reported arrival deadlines (DL_i),

non-detour values V_i^{max}, and detour discounting rates α_i do not influence the generation of the solution pools. Accordingly, the generation of solution pools $Xpool_{Md_g}$ (for all $g \in P$) and $Xpool_{Md_0}$ is independent of passenger(s) g's report of the mobility preference. In this way, the mechanism obtained by SPA is incentive compatible (please refer to the proof of the incentive compatibility proposition, Proposition 10, of the SPA). The generated solutions in each solution pool can satisfy all constraints except the arrival deadline constraint (Formula 11) since we do not use passengers' reported arrival deadlines as input data. The generated solutions may be infeasible to their corresponding models. Thus, we select the best feasible solution $XP_{Md_0}^*$ from $Xpool_{Md_0}$ which is adopted as the matching and routing plan. Similarly, the best feasible solutions $XP_{Md_g}^*$ are then selected from the solution pools $Xpool_{Md_g}$ for all $g \in P$ to calculate all passengers' prices (Formula 27). Figure 5.6 shows the logic flow of the SPA to obtain the mechanism.

$$p_g = \begin{cases} f\left(XP_{Md_g}^*\right) - f\left(XP_{Md_0}^*\right) + VA_g\left(XP_{Md_0}^*\right), \text{passenger(s) } g \text{ is served} \\ 0, \text{ passenger(s) } g\text{'s request is rejected} \end{cases} \quad (27)$$

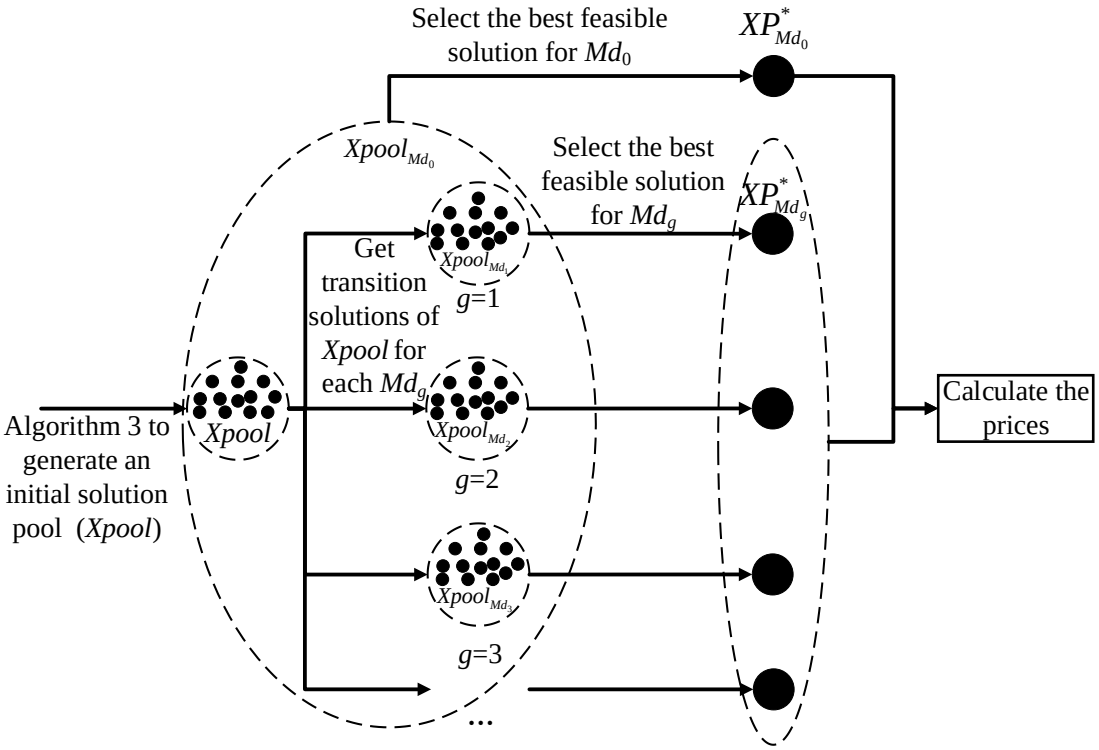

Figure 5.6 Flow Chart of SPA in Obtaining the Mechanism

We propose two strategies to improve the quality of the selected solution from the obtained solution pool of Md_0: 1) generate a large enough number of solutions in the solution pool *Xpool*; 2) randomly and periodically simulate virtual parameters (DL_i, V_i^{max}, and α_i) that are used to direct wide-range generation of the solutions. This simulation strategy is inspired by our previous work (Bian and Liu, 2018b). Algorithm 3 gives the pseudocode of the solution pool generation algorithm.

Algorithm 3 Generation of solution pool *Xpool*
Input the total number of iterations (*NI*), number of iterations in each period (*NIP*) for updating DL_i, V_i^{max}, and α_i, number of candidate solutions (*CN*), number of

solutions (*NS*) assigned into the solution pool for each iteration, and all other parameters of the problem;

Initialize a feasible solution X_0 to the model Md_0 as the current solution $X_{current}$, the virtual values of DL_i, V_i^{max}, and α_i, $it = 0$ (current number of iterations), $pit = 0$ (current number of iterations in one period), and the empty solution pool *Xpool*;

Do while $it < NI$

If $pit > NIP$

$pit = 0$;

Randomly re-generate virtual values of DL_i, V_i^{max}, and α_i;

End if

Generate *CN* candidate solutions $\{X_1, X_2, \ldots, X_{CN}\}$ of $X_{current}$'s neighbors;

Calculate $\{\Delta f(X_1), \Delta f(X_2), \ldots, \Delta f(X_{CN})\}$ ($\Delta f(X_i) = f(X_i) - f(X_{current})$) and record the subscript *opt*, where $\Delta f(X_{opt}) = \max\{\Delta f(X_1), \Delta f(X_2), \ldots, \Delta f(X_{CN})\}$;

Randomly select *NS* solutions from *CN* candidate solutions $\{X_1, X_2, \ldots, X_{CN}\}$ and put them into the solution pool *Xpool*;

Do while X_{opt} is in tabu list

Select the suboptimal solution as X_{opt} from $\{X_1, X_2, \ldots, X_{CN}\}$;

End do

$X_{current} = X_{opt}$;

Update the tabu list;

$it = it + 1$;

$pit = pit + 1$;

End do

Output *Xpool*.

Finally, we use Algorithm 4 to get the mechanism, including the optimal matching and routing plan and all passengers' prices.

Algorithm 4 SPA to the mechanism

Input the solution pool *Xpool* obtained by Algorithm 3 and all parameters of the problem;

For $g = 1{:}n$

Use Algorithm 2 to get the gth transition solutions of all the solutions in *Xpool* as the solution pool of Md_g, $Xpool_{Md_g}$:

$Xpool_{Md_g} = \left\{ Y_g \middle| Y_g = TRS_g\left(X_i\right), \text{ for all } X_i \in Xpool \right\}$;

End for

Put all $Xpool_{Md_g}$ into $Xpool_{Md_0}$: $Xpool_{Md_0} = \left\{ Xpool, Xpool_{Md_g} (\text{for all } g \in P) \right\}$;

Select the best feasible solution $XP^*_{Md_0}$ from $Xpool_{Md_0}$ that

$XP^*_{Md_0} = \arg\max f\left(X\right),\ X \in Xpool_{Md_0}$ and satisfying arrival deadline constraint (Formula 11);

For $g = 1{:}n$

Select the best feasible solution $XP^*_{Md_g}$ from $Xpool_{Md_g}$ that

$XP^*_{Md_g} = \arg\max f\left(X\right),\ X \in Xpool_{Md_g}$ and satisfying arrival deadline constraint (Formula 11);

If $\sum_{k \in V} y_g^k = 0$

$p_g = 0;$

else

$p_g = f\left(XP_{Md_g}^*\right) - f\left(XP_{Md_0}^*\right) + VA_g\left(XP_{Md_0}^*\right);$

End if

End for

Output the optimal solution $XP_{Md_0}^*$ and all passengers' prices $\mathbf{p} = \{p_1, p_2, ..., p_n\}$.

Before conducting the theoretical analysis for SPA, we do the following reformulation for the SPA algorithm.

$XP_{Md_0}^*$ is the best feasible solution selected from the solution pool $Xpool_{Md_0}$, and thus $XP_{Md_0}^*$ can be defined as the optimal solution of the optimization model below. We denote this model as Mdp_0.

Objective function: Formula (5):

$$\max f(X) = \sum_{i \in P} VA_i(X) - TC(X) + \sum_{i \in P} PC_i\left(1 - \sum_{k \in V} y_i^k\right)$$

Subject to constraints: Formulas (6-11, 13, 15, 17-21) and Formula (28):

$$X \in Xpool_{Md_0} \tag{28}$$

We denote the region constrained by Formulas (6-11, 13, 15, 17-21) as C_0. Thus, a feasible solution X of model Mdp_0 can be represented by $X \in C_0 \bigcap Xpool_{Md_0}$.

Similarly, $XP^*_{Md_g}$ is the best feasible solution selected from $Xpool_{Md_g}$. It can be defined as the optimal solution of the model below (Mdp_g).

Objective function: Formula (5):

$$\max f(X) = \sum_{i \in P} VA_i(X) - TC(X) + \sum_{i \in P} PC_i \left(1 - \sum_{k \in V} y_i^k\right)$$

Subject to constraints: Formulas (6-11, 13, 15, 17-22), and Formula (29):

$$X \in Xpool_{Md_g} \tag{29}$$

We denote the region constrained by Formulas (6-11, 13, 15, 17-22) as C_g. Thus, a feasible solution X of model Mdp_g can be represented by $X \in C_g \bigcap Xpool_{Md_g}$.

Proposition 9 The mechanism $\boldsymbol{M}(XP^*_{Md_0}, \mathbf{p})$ obtained by SPA is individual rational.

The proof is presented in Appendix A.

Proposition 10 The mechanism $\boldsymbol{M}(XP^*_{Md_0}, \mathbf{p})$ obtained by SPA is incentive compatible.

The proof is presented in Appendix A.

Proposition 11 The mechanism $\boldsymbol{M}(XP^*_{Md_0}, \mathbf{p})$ obtained by SPA is detour-discounting reasonable.

The proof is presented in Appendix A.

If the mechanism is obtained by SPA, the price may be lower than the baseline price. The property "price controllability" may not necessarily be true for the SPA algorithm, and we use mathematical deduction to show the reason.

From the proof of Proposition 6 (price controllability), we can summarize that the proposition is valid because three conditions are satisfied: 1) $f\left(X^*_{Md_g}\right) \geq f\left(Y^*_g\right)$, where $X^*_{Md_g}$ is the optimal solution of model Md_g and Y_g^* is the gth transition solution of $X^*_{Md_0}$: $Y^*_g = TS_g\left(X^*_{Md_0}\right)$; 2) Proposition 4; and 3) Proposition 5. Proposition 4 and Proposition 5 are generalized and are always true, but the first condition is not necessarily valid if the mechanism is obtained by SPA. Let $XP^*_{Md_g}$ denote the optimal solution of model Mdp_g obtained by SPA, and $YP^*_g = TS_g\left(XP^*_{Md_0}\right)$, where $XP^*_{Md_0}$ is the optimal solution of model Mdp_0 obtained by SPA. The inequality $f\left(XP^*_{Md_g}\right) \geq f\left(YP^*_g\right)$ is not necessarily true, because although $XP^*_{Md_g}$ is the best feasible solution selected from solution pool $Xpool_{Md_g}$, YP^*_g is not necessarily in the solution pool $Xpool_{Md_g}$. Thus we cannot guarantee that $XP^*_{Md_g}$ is superior to YP^*_g. Even so, it can be easily proved that $p_g \geq PC_g + f\left(XP^*_{Md_g}\right) - f\left(YP^*_g\right)$. Generally, even if $f\left(XP^*_{Md_g}\right) - f\left(YP^*_g\right)$ is possible to be negative, it is very close to zero, and the price will not be significantly smaller than the baseline price, as shown in Section 7 via the numerical examples.

We use a simple example to straightforwardly show why the price controllability may not hold (see Appendix B.3).

5.7 Numerical Examples

5.7.1 Experimental Setup

We use the solver CPLEX in the software of AIMMS (https://aimms.com/english/developers/resources/solvers/) to solve the mixed integer linear programming. The CPLEX solver uses the branch and bound algorithm to solve mixed integer linear programming. It can obtain the exact solution when the problem scale is small. We also use our developed SPA to solve both small- and large-scale problems and compare the results with CPLEX.

Besides CPLEX, we also compare SPA with another heuristic algorithms, Hybrid Simulated Annealing and Tabu Search (HSATS), which has been shown to outperform many other heuristic algorithms (e.g. simulated annealing, tabu search, genetic algorithm, ant colony optimization, and particle swarm optimization), for solving routing problems (Lin et al., 2016). The numerical analysis is run on a Dell computer with processor Intel(R) Core(TM) i7-4790 CPU @ 3.60GHz and 8 GB RAM.

5.7.2 An Illustrative Example

This section develops an illustrative example via computer simulation to interpret the mechanism results.

7.2.1 Data setting

Since the rolling horizon planning approach continually processes passengers' requests, we use one hour (e.g. from 8:00 am to 9:00 am) to present mechanism design results. In this numerical example, we start to simulate 60 passengers' requests after 8:00 am. The locations of all passenger requests are randomly and uniformly generated in an

annular region. The radius of inner circle of the annular region is set to one mile, $r = 1$, indicating a walking distance. The radius of outer circle of the annular region is set to 6 miles. Passengers' requesting times are uniformly generated between 8:00 am and $DL_i - t_{i0} - pt - 20$ minutes, where DL_i is passenger i's arrival deadline, t_{i0} is the shortest travel time to the transit hub, pt is the anticipated pickup time span, and the "20 minutes" is a buffer time within which passengers are waiting to be picked up (Figure 5.7). Passengers' arrival deadlines are randomly and uniformly simulated within the time interval from 8:40 am to 9:00 am. The maximum response time span is set to 2 minutes. Note that these values are used for illustrative purpose. They can be adapted to different practical scenarios.

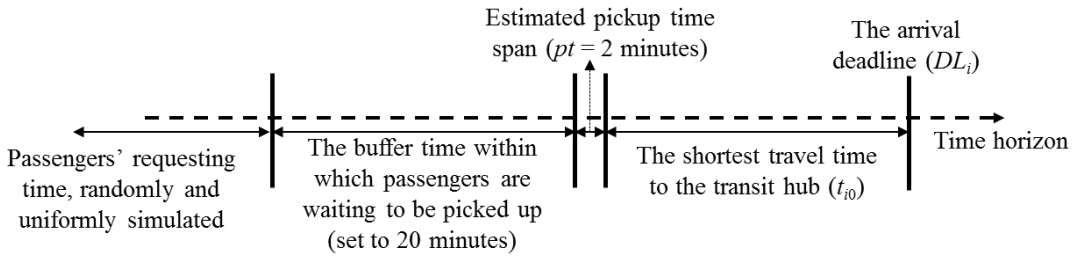

Figure 5.7 Set of Passengers' Requests

After the simulation of passengers' requests, the rolling horizon planning approach determines 9 time slices automatically based on the occurrence of these passenger requests. The information of the 9 time slices is presented in Table 5.2. The number of available vehicles (m) at the end of each time slice is randomly generated from a uniform distribution within the interval [2, 6]. The vehicle locations are randomly and uniformly generated in the same annular region as well. Note that the mechanism is not based on the assumption that available vehicles are randomly distributed. Only in the numerical example, we use

simulation to randomly generate the available vehicles in order to demonstrate that our mechanism can determine the matching and routing plan as well as the prices wherever the available vehicles are. Among the *m* vehicles, $\lceil rand \times 1/3 \times m \rceil$ vehicles are not available immediately, but will be available $10 \times rand$ minutes after the end of each time slice, where "*rand*" is a number uniformly distributed within (0, 1), and the bracket "⌈ ⌉" gets the minimum integer greater than or equal to the number in this bracket. The rest of the vehicles are available immediately at the end of the time slice.

Table 5.2 Time Slice Information

The information of each time slice	Time slices								
	1	2	3	4	5	6	7	8	9
Start time	8:00:10	8:02:18	8:04:54	8:06:57	8:09:10	8:11:39	8:13:49	8:15:49	8:18:32
End time	8:02:10	8:04:18	8:06:54	8:08:57	8:11:10	8:13:39	8:15:49	8:17:49	8:20:32
Number of passenger requests	7	10	6	9	4	6	6	5	7
Number of available vehicles	4	5	6	4	3	6	2	6	5

The coordinate of the transit hub is (0, 0), located in the center. For convenience but without losing generality, the travel distance between two locations is set to the Euclidean distance in miles. The transportation cost between two locations is proportional to the Euclidean distance ($c_{ij} = 0.5d_{ij}$, $i \in P \bigcup V$ and $j \in P \bigcup H$). Note that this numerical example uses Euclidean distance only for illustrative simplification in order to illustrate

how the mechanism is obtained. Our mechanism design model is suitable for any type of distance, which does not depend on the Euclidean distance assumption.

The travel time between two locations is not necessarily proportional to the distance. Thus, we use a different method to generate travel time between two locations. Virtual coordinates (xv_i, yv_i) of locations are generated, which satisfy $xv_i = x_i + \varepsilon$ and $yv_i = y_i + \varepsilon$, where (x_i, y_i) is the real coordinates of passenger locations, vehicle locations, and the transit hub. ε is normally distributed with the mean of "0" and variance of "0.1". ε is randomly generated by the computer. The travel time between i and j is set to $t_{ij} = 2.5\sqrt{\left(xv_i - xv_j\right)^2 + \left(yv_i - yv_j\right)^2} + 2$. "2.5" represents that the vehicle needs approximately 2.5 minutes to travel per mile. The pickup time span, which is set to 2 minutes, is included in the travel time, and thus the travel time is added by "2".

For simplicity, we assume that each request has only one passenger ($np_i = 1$, for all $i \in P$). All vehicles can pick up at most 4 passengers ($Q = 4$). Passengers' maximum willing-to-pay prices for direct shipment (non-detour values) are determined by $V_i^{\max} = 2c_{i0} + \varepsilon_i$, where ε_i is randomly generated from a normal distribution with the mean of "4" and variance of "1". Passengers' detour discounting rate α_i is randomly generated from a uniform distribution within the range of [0, 0.5]. The constant initial fee in the baseline price (PC_i) is set to 1.5 dollars (cf = \$1.5), and the distance rate is 0.5 dollar per mile (dr = 0.5 dollar/mile), so $PC_i = 1.5 + 0.5 \times d_{i0}$. Note that our methodology is not limited to the input data of this numerical example, and other values can be used as well.

7.2.2 Results of the mechanism

Table 5.3 presents the results of the three solution approaches, CPLEX, HSATS,

and SPA. The results of the mechanism obtained by HSATS and SPA are entirely identical with those obtained by the exact solver CPLEX, including the optimal matching and routing plan (identical objective functions values of model Md_0) and all passengers' prices, for the initial small-scale problem.

Table 5.4 presents the computing times of CPLEX, HSATS, and SPA. Except for the second time slice with the relatively largest-scale problem (10 passengers and 5 vehicles), CPLEX can solve the mechanism design problem very fast because the scales of all these problems are small. SPA and HSATS do not have superiority over the commercial solver CPLEX in solving small-scale problems in terms of computational efficiency. However, as we will show in Section 7.3, the SPA can solve large-scale problems much faster than the CPLEX solver and HSATS.

Table 5.3 Results of CPLEX (Branch and Bound Algorithm), HSATS, and SPA, for Small-Scale Problem

Time slices	Objective function values of model Md_0			Percentages of identical prices, compared with CPLEX branch and bound results	
	CPLEX (branch and bound)	HSATS	SPA (our algorithm)	HSATS	SPA (our algorithm)
1	38.00	38.00	38.00	100%	100%
2	59.35	59.35	59.35	100%	100%
3	31.13	31.13	31.13	100%	100%
4	60.00	60.00	60.00	100%	100%
5	17.38	17.38	17.38	100%	100%

6	28.69	28.69	28.69	100%	100%
7	32.86	32.86	32.86	100%	100%
8	25.39	25.39	25.39	100%	100%
9	32.23	32.23	32.23	100%	100%

Percentages of identical prices: Percentage of the number of prices obtained by HSATS and SPA identical with those obtained by CPLEX in the total number of passenger requests.

Table 5.4 Computing Time of CPLEX, HSATS, and SPA

Time slices	Problems scales		Total computing time, including optimization time and price calculating time (seconds)		
	Number of passengers	Number of vehicles	CPLEX	HSATS	SPA (our algorithm)
1	7	4	1.94	4.73	1.17
2	10	5	24.62	9.23	1.73
3	6	6	1.82	4.04	1.15
4	9	4	2.47	7.38	1.39
5	4	3	<0.01	1.65	0.50
6	6	6	1.69	4.30	1.14
7	6	2	<0.01	2.55	0.57
8	5	6	0.01	3.51	0.97
9	7	5	2.29	5.17	1.18

Figure 5.8 presents the results of the mechanism, including optimal vehicle-passenger matching and vehicle routing plans and passengers' prices, for the nine time slices. There exist two phenomena in these figures that need to be explained.

1) Most passengers are served by vehicles, with only a few passengers being rejected by the service. There are three possible reasons for service rejection: a) the

passenger's value (maximum willingness-to-pay price) is so low that the passenger is unwilling to pay the charged price if he is served by any vehicle; b) available vehicles might be so far away from the passenger location so that there is no enough time for any vehicle to drive the passenger to the transit hub before the arrival deadline; and c) there are no enough available vehicles to drive all passengers to the transit hub and thus some passengers have to be rejected. We use Figure 5.8 (f) (time slice 6) to demonstrate the first reason. For example, if Passenger 6 is served by Vehicle 6, his price will be \$8.41 based on Formula (23) ($p_6 = PC_6 + c_{6,6} + c_{6,0} = 4.10 + 1.71 + 2.60 = \$8.41$), greater than his maximum willing-to-pay price \$8.26. Thus, he is unwilling to pay the price and is rejected to have the service. Figure 5.8 (h) (time slice 8) can illustrate the second reason. The closest available vehicle to Passenger 3 is Vehicle 5. Vehicle 5 can drive Passenger 3 to the transit hub by 8:49 pm as earliest, but Passenger 3's preferred arrival deadline is 8:47 pm. Thus, available vehicles do not have enough time to drive Passenger 3 to the transit hub before his arrival deadline and the passenger is rejected to take the service. The third reason can be inferred from Figure 5.8 (d). Passenger 1 is not served because no vehicles are available to drive him to the transit hub. In practice, these unserved passenger' requests can be transmitted into the next time slice for re-matching and some vehicles may be available to serve them.

2) There exist some cross routes that do not achieve the minimization of transportation cost. This is because passengers' detour tolerances (α_i) affect the optimization of vehicle routing. Take Figure 5.8 (b) as an example. The route of Vehicle 5 is "Vehicle 5 → Passenger 8 → Passenger 1 → the transit hub", in which "Vehicle 5 → Passenger 8" crosses over "Passenger 1 → the transit hub". It is obvious that another

route "Vehicle 5 → Passenger 1 → Passenger 8 → the transit hub" is shorter and thus has less transportation cost (in our numerical example, the transportation cost is proportional to the travel distance). Vehicle 5 does not adopt the route with less transportation cost because Passenger 1 dislikes detour much more than Passengers 8 does ($\alpha_1 = 0.40$, $\alpha_8 = 0.16$). The increased passengers' total value can compensate for the increased transportation cost when adopting the longer routing plan (Vehicle 5 → Passenger 8 → Passenger 1 → the transit hub) instead of the shorter routing plan (Vehicle 5 → Passenger 1 → Passenger 8 → the transit hub).

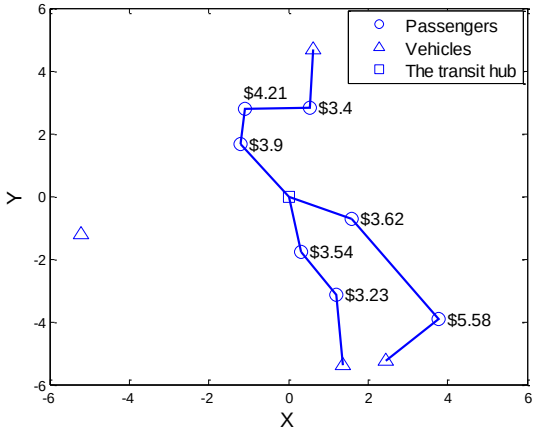

(a) Time slice 1

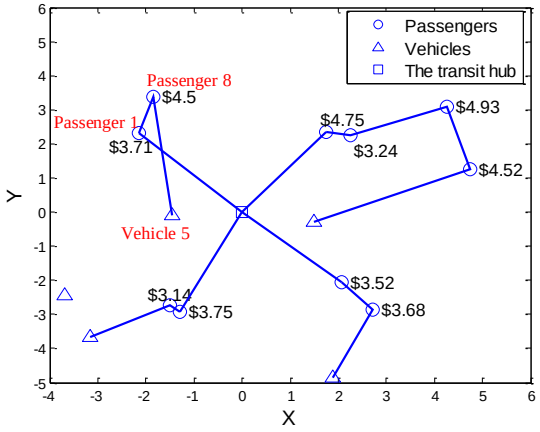

(b) Time slice 2

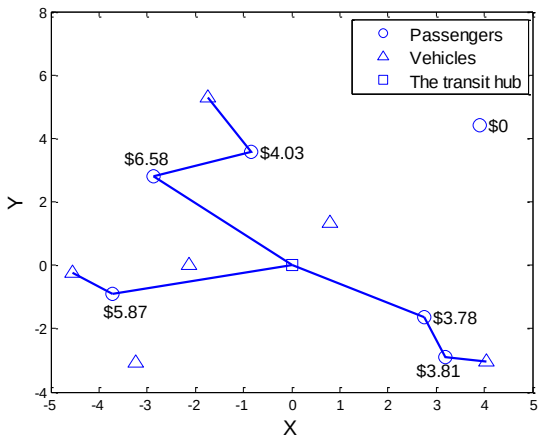

(c) Time slice 3

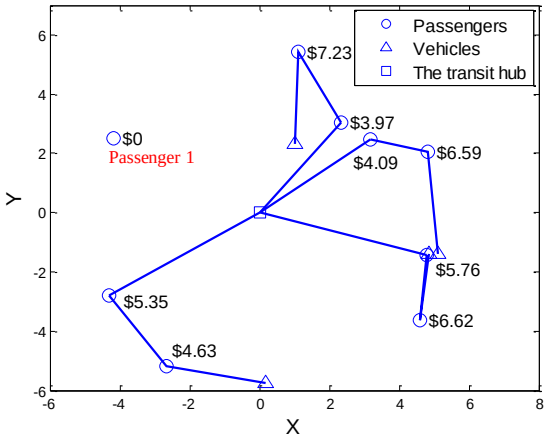

(d) Time slice 4

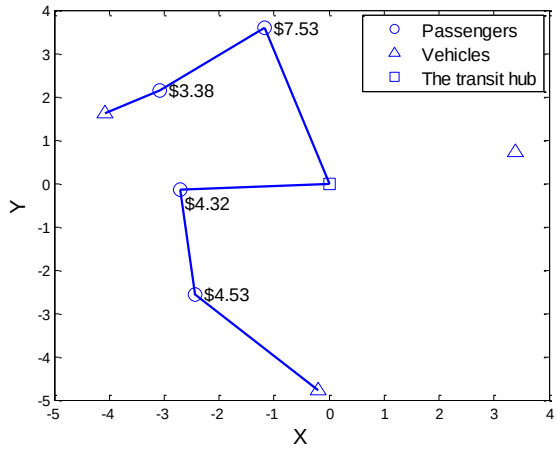

(e) Time slice 5

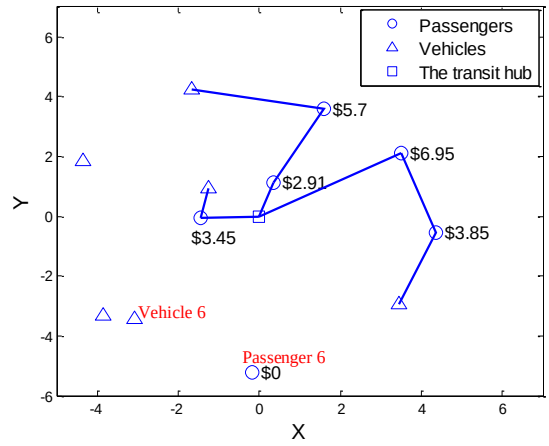

(f) Time slice 6

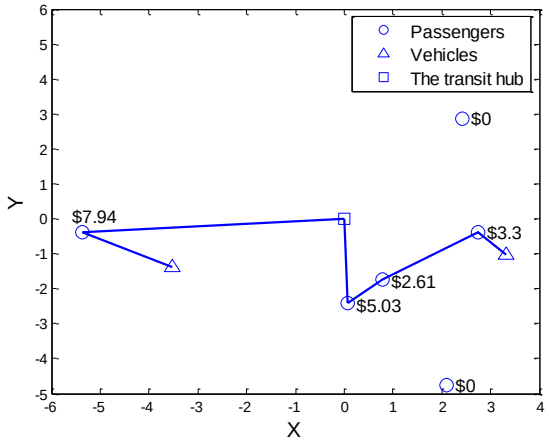

(g) Time slice 7

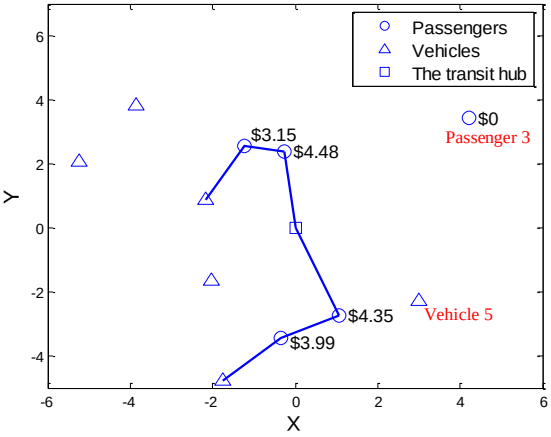

(h) Time slice 8

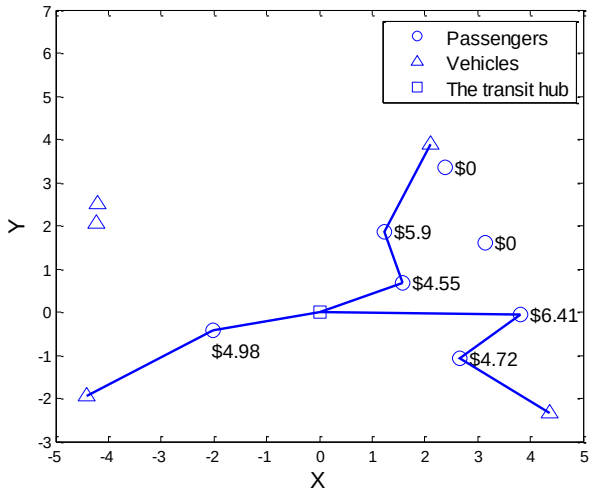

(i) Time slice 9

Figure 5.8 The Vehicle-Passenger Matching, Vehicle Routing Plan, and the Prices for All Time Slices

Table 5.5 summarizes the results of the mechanism. Only 26 vehicles are dispatched to drive 52 passengers to the transit hub. The total transportation cost is $93.07. In total, 239.58 dollars are collected from 52 passengers. On average, a passenger pays 239.58/52 = $4.61 and one vehicle collects 239.58/26 = $9.21. If all passengers take the taxi service without sharing the ride with others, 52 vehicles should be dispatched to drive the 52 passengers to the transit hub (assuming that each vehicle picks up one passenger). The ridesharing can save half of the vehicles dispatched. The total price collected from all passengers $239.58 can well cover the $93.07 transportation cost.

Table 5.5 Summary of the Mechanism Results

Time slices	1	2	3	4	5	6	7	8	9	Total

Number of passenger requests	7	10	6	9	4	6	6	5	7	60
Number of served passengers	7	10	5	8	4	5	4	4	5	52
Number of vehicle trips	3	4	3	4	2	3	2	2	3	26
Social welfare ($)	38.01	59.35	26.68	56.06	17.38	24.59	25.39	21.17	26.36	294.99
Total transportation cost ($)	9.93	15.20	9.20	19.63	7.81	9.56	7.08	5.88	8.78	93.07
Total collected price ($)	27.49	39.73	24.07	44.24	19.77	22.86	18.89	15.97	26.56	239.58
The net profit($)	17.56	24.53	14.87	24.61	11.96	13.30	11.81	10.09	17.79	146.52

Note that if we consider the vehicle availability dynamics and occurrence of potential passenger requests in our mechanism, we anticipate that the system will serve more passengers, provide passengers with more incentive, and achieve larger social welfare. We use an example (Appendix B.4) for demonstration.

Figure 5.9 presents served passengers' maximum willing-to-pay prices without detour (V_i^{max}), actual maximum wiling-to-pay prices (VA_i) given the optimal vehicle-passenger matching and vehicle routing plan, the actual paid prices (p_i), and the baseline prices (PC_i). In Proposition 2, we already proved that the mechanism is individual rational. This is reflected in Figure 5.9. The red line is below the blue line, indicating that all passengers' actual paid prices are lower than or equal to their maximum willing-to-pay

prices. Recall that Proposition 6 indicates that passengers' actual prices are always greater than or equal to the baseline prices if the passengers are served (for price control purpose to avoid service deficit). Figure 5.9 can also validate this (actual price versus baseline price).

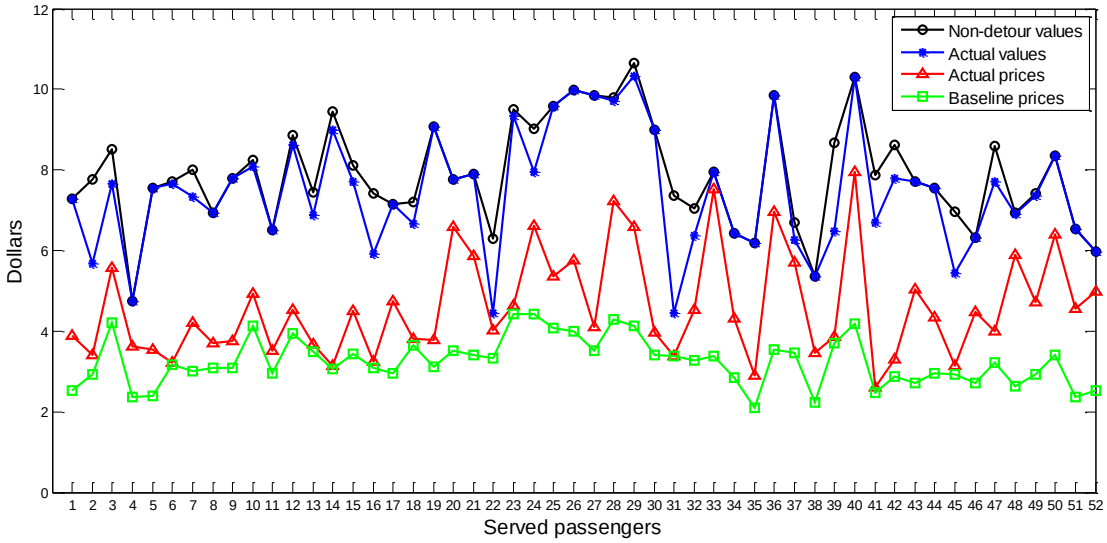

Figure 5.9 All Served Passengers' Non-Detour Values, Actual Values, Actual Paid Prices, and the Baseline Prices

Figure 5.10 demonstrates the property of "incentive compatibility" (Definition 2). We select Passenger 9 in time slice 2 as an example (Figure 5.10a) to show that truthfully report non-detour value and detour discounting rate is a passenger's best strategy. Passenger 9's truthful non-detour value is \$7.42 ($V_9^{\max} = 7.42$) and his truthful detour discounting rate is 0.46 ($\alpha_9 = 0.46$). If he intentionally decreases the non-detour value, his utility initially remains constant and then decreases to zero. This is because initially the price does not change, and then the passenger is rejected by the service and the utility drops to zero when the non-detour value decreases to an enough low value. Similarly, Passenger

9's truthful acceptable detour discounting rate is 0.46 (α_9 = 0.46). If he intentionally increases the detour discounting rate, his utility initially remains constant and then decreases. Initially the price does not change. When the detour discounting rate increases to large enough, Passenger 9 has less detour and thus the price increases, leading to the decrease of his utility. In Figure 5.10(b), we take Passenger 1 in time slice 9 as an example to show that truthfully reporting the arrival deadline is also a passenger's best strategy. If Passenger 1 misreports an earlier arrival deadline (< 8:40 am) instead of the true one (8:40 am), the price will either remain constant or increase, and thus his utility either remains constant or decreases. When the passenger misreports a very early arrival deadline, there is no enough time for any vehicle to drive him to the transit hub. The request will be rejected and his utility drops to zero, but he could have been served if he had truthfully reported the arrival deadline. If the misreported arrival deadline is later than the true one (> 8:40 am), the passenger may be unable to arrive at the transit hub before his actual arrival deadline. We deem that the passenger's maximum willing-to-pay price is zero if his requirement is not satisfied, but he still has to pay a positive price. Thus, his utility is negative. Therefore, misreporting can never help this passenger to obtain a larger utility than the truthful reporting. This property is valid for all of the other passengers as proved in Proposition 3.

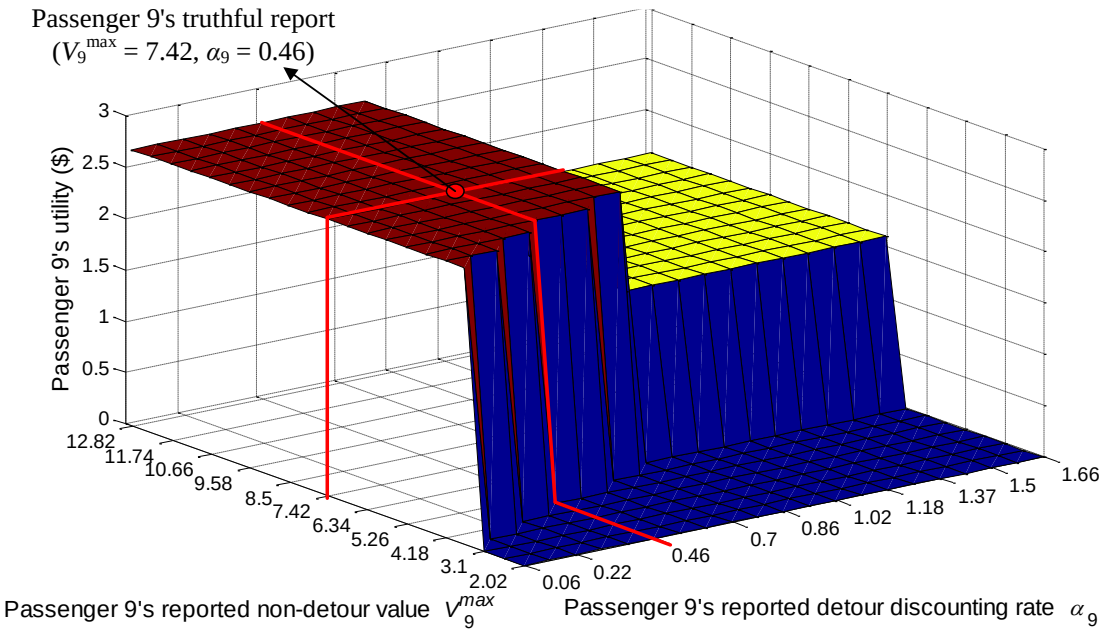

(a)

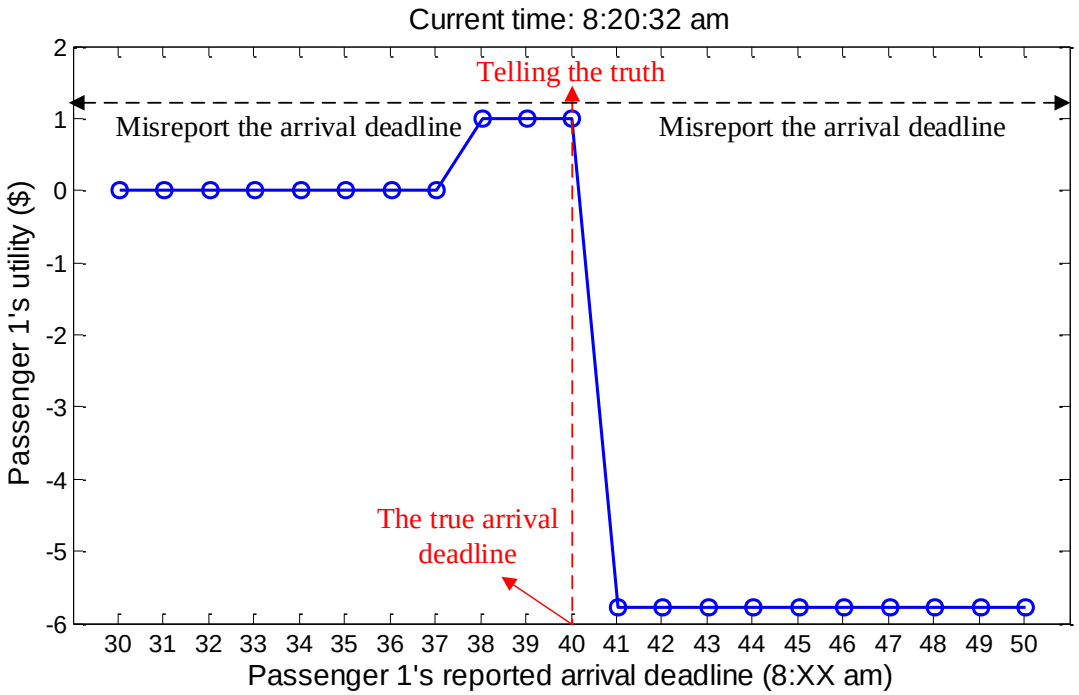

(b)

Figure 5.10 Demonstration of the Property of "Incentive Compatibility"

Figure 5.11 and Figure 5.12 demonstrate "detour-discounting reasonability" property (Definition 5). We use time slice 2 (the largest scale among the nine time slices) as an example to show this property. As passengers are less tolerant of detour (i.e. they increase the detour discounting rate α_g), all passengers' in-vehicle travel times either remain constant or decrease as their α_g increase. Figure 5.12 shows that passengers' prices are non-decreasing as the passengers are less tolerant of detouring. Note that Passengers 3 and 5 are rejected by the service as their α_g increase to large enough, causing their prices to drop to zero.

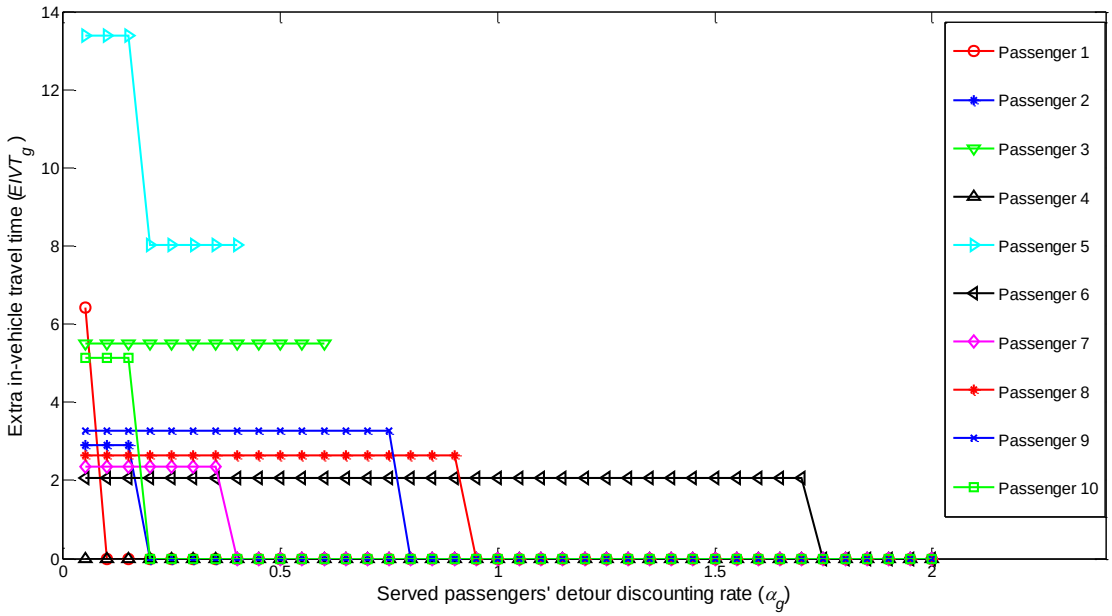

Figure 5.11 Changing Extra In-Vehicle Travel Time as Passengers Become Less Tolerable of Detour

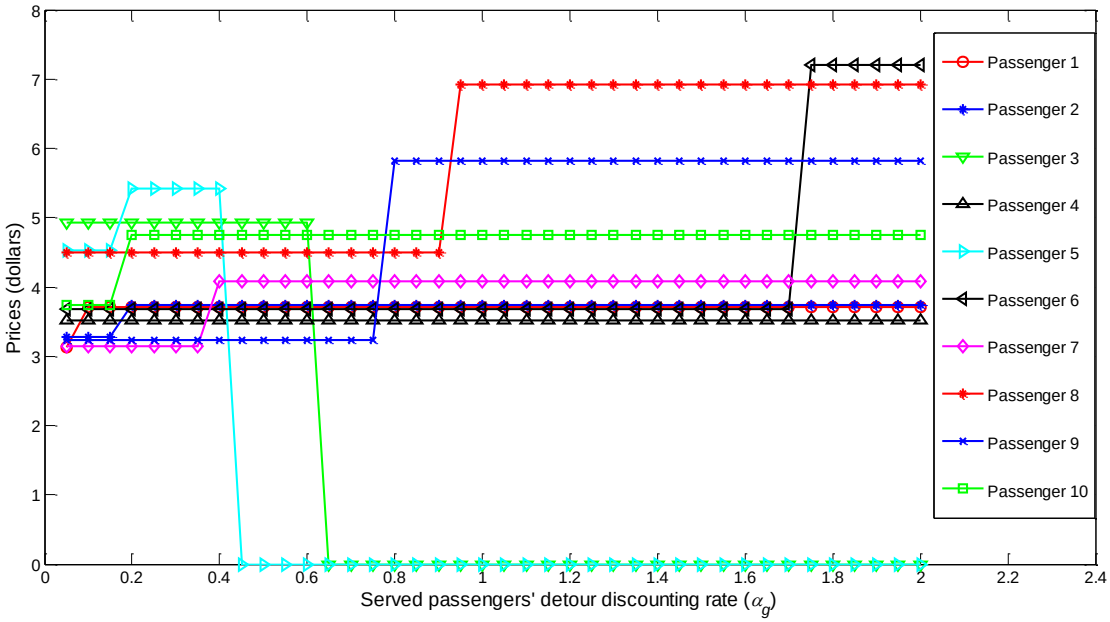

Figure 5.12 Changing Prices as Passengers Become Less Tolerable of Detour

7.2.3 Comparison of MPMBPC with traditional VCG mechanism

This section makes a comparison between the traditional VCG mechanism and the proposed MPMBPC mechanism. Table 5.6 presents the comparison results using the designed numerical example.

- From the results, VCG mechanism serves 55 passengers, slightly more than the MPMBPC mechanism does (52 passengers). In VCG mechanism, as long as a passenger can contribute to the increase of social welfare (summation of passengers' values minus the service provider's transportation cost), this passenger will be served. In contrast, with the baseline price control component, some passengers with unreasonably low values can be rejected by the MPMBPC mechanism.

- The VCG mechanism dispatches 28 vehicles and the MPMBPC mechanism dispatches 26 vehicles. The transportation cost of the VCG mechanism is $102.97, which

is slightly larger than that of the MPMBPC mechanism ($93.07). This result indicates that MPMBPC may reduce transportation cost for the service provider and dispatch fewer vehicles to the transit hub compared with the VCG mechanism.

- The VCG mechanism can only receive 90.07 dollars from all 55 passengers, leading to a $12.90 deficit. In contrast, the collected prices ($239.58) in MPMBPC mechanism can cover the cost ($93.07), indicating that MPMBPC mechanism is financially sustainable without external investment due to the incorporation of baseline pricing component.

- Since the MPMBPC mechanism includes a baseline price control component in the objective function, it is not necessarily efficient (i.e. the social welfare may not be maximized). The last row in Table 5.6 compares the social welfare of the MPMBPC mechanism with that of the VCG mechanism. The largest gap between MPMBPC and VCG among the nine time slices is 13.84% (time slice 6). The average gap for the nine time slices is 1 – 294.99/304.30 = 3.06%.

Table 5.6 Comparison between VCG Mechanism and MPMBPC Mechanism

Time slices		1	2	3	4	5	6	7	8	9	Total
Number of passenger requests		7	10	6	9	4	6	6	5	7	60
Number of served passengers	VCG	7	10	6	8	4	6	4	4	6	55
	MPMBPC	7	10	5	8	4	5	4	4	5	52
Number of vehicle trips	VCG	3	4	4	4	2	4	2	2	3	28
	MPMBPC	3	4	3	4	2	3	2	2	3	26
Total transportation cost ($)	VCG	9.93	15.20	14.35	19.63	7.81	13.87	7.08	5.88	9.22	102.97
	MPMBPC	9.93	15.20	9.20	19.63	7.81	9.56	7.08	5.88	8.78	93.07
	VCG	6.09	6.48	12.19	14.03	5.77	11.77	9.67	4.16	19.91	90.07

Total collected price ($)	MPMBPC	27.49	39.73	24.07	44.24	19.77	22.86	18.89	15.97	26.56	239.58
The net profit ($)	VCG	-3.84	-8.72	-2.16	-5.60	-2.04	-2.10	2.59	-1.72	10.69	-12.90
	MPMBPC	17.56	24.53	14.87	24.61	11.96	13.30	11.81	10.09	17.79	146.52
Social welfare ($)	VCG	38.01	59.35	29.30	56.06	17.38	28.54	25.39	21.17	29.10	304.30
	MPMBPC	38.01	59.35	26.68	56.06	17.38	24.59	25.39	21.17	26.36	294.99

Figure 5.13 compares the VCG mechanism with MPMBPC mechanism. The MPMBPC mechanism can avoid unreasonable low prices because of the baseline prices (the prices in the brackets in the figure, which are calculated by Formula 4). Note that the matching and routing plan of VCG is not necessarily always identical with that of MPMBPC in all scenarios and Figure 5.13 just shows a coincidence.

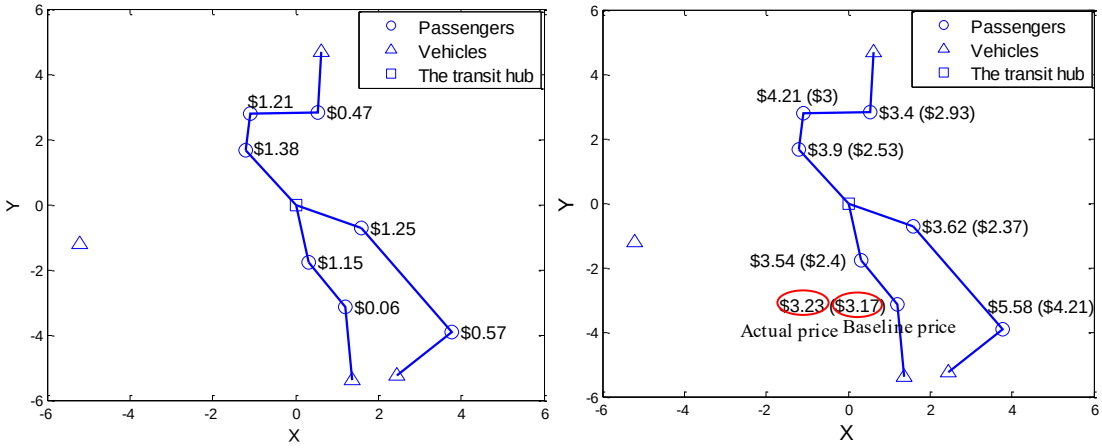

(a) the VCG mechanism (b) the MPMBPC mechanism

Figure 5.13 The Matching and Routing Plan and the Prices of the VCG Mechanism and the MPMBPC Mechanism (Time Slice 1)

5.7.3 Large-Scale Numerical Examples

In this section, we extend the numerical analysis to a larger scale with more passengers and vehicles. In some regions with high population density (e.g. Manhattan in New York City), it is possible that many passengers will send requests for the first-mile ridesharing service within a short time interval in peak hours (e.g. 8:00 am - 9:00 am on weekdays). The mechanism design problem in each time slice is similar, so we only show the result of one time slice for illustrative convenience.

The basic rule of parameter setting is to generate the parameters as randomly as possible so that the results can demonstrate the adaptability of the proposed mechanism in a variety of real-world scenarios. We design eight numerical examples with the number of passenger requests increasing from 15 to 50 by the interval of 5. It is based on the NYC taxi data that we determine the example with 50 passengers as the largest scale. We find that an average of 8555 taxis traveled to the New York Penn Station (one of the busiest stations in the U.S.) every day. If there are 4 peak hours in one day and we assume that all taxis traveling to the Penn Station are within the peak hours, then there are 36 trips to the Penn Station on average within each minute. Considering fluctuation of the trip number, we set 50 passengers as the largest scale. In order to simulate the short supply of vehicles in practice, the number of available vehicles is set to half of the number of passenger requests. We use "N_x_y" to denote a numerical example, where "x" is the number of passenger requests and "y" is the number of vehicles. In real-world scenarios, it is possible that passengers' and vehicles' locations are distributed near the transit hub with high randomness. Thus, in this experiment, both passengers' and vehicles' locations are randomly and uniformly generated in an annular region with a one-mile-radius inner circle

and a 7-mile-radius outer circle. All vehicles are available at the end of the time slice. The remaining time for driving all passengers to the transit hub is set to 30 minutes for all numerical examples, which is reasonably long for passengers to achieve the first-mile travel after sending the requests. The methods of generating other data, including the location of the transit hub, travel distance, travel time, transportation cost, vehicle capacity, passengers' non-detour values and detour discounting rates, and baseline pricing, are identical with those in the small-scale numerical example in Section 7.2. Some of these parameters are randomly generated to demonstrate that the mechanism can be adapted for any random scenario in practice.

We apply the three solution approaches, CPLEX solver, HSATS, and SPA to solve the mechanism design problems. CPLEX solver can only solve the problem of the smallest-scale numerical example, N_15_8. The computing times to obtain the optimal matching and routing plan and to calculate all passengers' prices are 8.37 seconds and 109.84 seconds, respectively. The objective function value of model Md_0 obtained by CPLEX is 95.82, identical with those obtained by HSATS and SPA. However, the CPLEX solver is unable to solve larger-scale problems within a reasonable amount of time. Thus, Table 5.7 and Table 5.8 do not present the result of the CPLEX solver, and only present those of HSATS and SPA.

Table 5.7 compares the performances of HSATS and SPA in solving the matching and routing problem (model Md_0) and in sustaining the properties of "individual rationality", "detour-discounting reasonability", and "price controllability". Table 5.7 shows that when the problem scale is relatively small, the solution qualities obtained by HSATS and SPA are identical (numerical examples N_15_8 and N_20_10). When the

problem scale increases, the solution qualities of HSATS are slightly higher than those of SPA, except the numerical example "N_45_23". The largest difference between SPA and HSATS in solution quality among the eight numerical examples is only 1.69% (N_50_25).

We use the optimal social welfare produced by the VCG mechanism as a benchmark to compare with that produced by the MPMBPC mechanism obtained by SPA. The comparison result is also presented in Table 5.7. The largest gap of the social welfare between MPMBPC and VCG among the eight numerical examples is 8.18% (example N_20_10). The average gap of the social welfare for the eight numerical examples is only 1.86%. The small difference in social welfare between VCG and MPMBPC obtained by SPA indicates the effectiveness of the SPA in sustaining high social welfare for large-scale problems.

In order to compare the performance of the two algorithms in sustaining "individual rationality", Table 5.7 shows the percentages of the number of passenger requests with non-negative utilities. It shows that HSATS cannot ensure that all passengers' utilities are non-negative (see numerical examples N_25_13, N_40_20, N_45_23, and N_50_25 as counter cases), indicating that some passengers are unwilling to pay the prices. Thus, the mechanism obtained by HSATS is not necessarily individual rational. **In Section 6, we already proved that the mechanism obtained by SPA is always individual rational**, and thus all passengers' utilities are non-negative, which has also been verified in Table 5.7 as well.

Table 5.7 also compares the performance of the two algorithms in sustaining "price controllability". Neither HSATS nor SPA holds the property of "price controllability" and thus is able to ensure that the price is 100% controllable. Table 5.7 shows the percentages

of the number of served passengers whose prices are greater than or equal to the baseline prices in the total number of served passengers. SPA shows only two non-100% percentages, 82.35% and 91.84%, while HSATS shows six non-100% percentages. We also calculate the maximum difference between the baseline price and the actual paid price (max ($PC_i - p_i$)). In the mechanism results obtained by SPA, we find that the largest difference between the baseline price and the actual paid price is only \$0.81 (occurred in the numerical example "N_50_25") among all of the numerical examples. Except another numerical "N_20_10" with the positive value of max ($PC_i - p_i$) = \$0.38, all of the other numerical examples do not show any counter cases violating the property "price controllability", demonstrated by the result that the maximum differences between the baseline prices and the actual paid prices are all negative (max ($PC_i - p_i$) < 0). In the mechanism results obtained by HSATS, we find more positive values of "max ($PC_i - p_i$)". The largest "max ($PC_i - p_i$)" is \$2.38, much more than that obtained by SPA. Based on the results, we can conclude that the SPA has a stronger ability to sustain "price controllability" than HSATS does.

The "detour-discounting reasonability" is compared via the following method. Each time, a passenger's detour-discounting rate α_i is increased from 0.1 to 1 by 0.1. Other passengers' detour-discounting rates are unchanged. We obtain the mechanism results each time when α_i increases. We record the number of passenger requests whose mechanism changing processes are "reasonable", which means that the extra in-vehicle travel time is non-increasing and the price is non-decreasing. Then we calculate the percentage of this number in the total number of passenger requests. As shown in Table 5.7, HSATS cannot sustain "detour-discounting reasonability", indicating that if a passenger places a stricter

requirement on detour, he may have to stay in the vehicle for longer extra time and the price may decrease, which is counter-intuitive. By contrast, the SPA is able to ensure detour-discounting reasonability. This property of the SPA has been proved in Section 6. Note that the property "incentive compatibility" is not tested here because it is impossible to enumerate all combinations of passengers' reported values. However, the mechanism obtained by SPA has been proved to be incentive compatible (Proposition 10) while truthful mechanisms obtained by traditional heuristic algorithms are not necessarily incentive compatible (Nisan et al., 2007).

Table 5.7 Comparison between SPA and HSATS in Obtaining the MPMBPC Mechanism

Numerical examples	Objective function values of model Md_0				Social welfare		Individual rationality (%)		Price controllability (%)		Max (PC_i - p_i) ($)		Detour-discounting reasonability (%)	
	HSATS	SPA	VCG	SPA	HSATS	SPA	HSATS	SPA	HSATS	SPA	HSATS	SPA	HSATS	SPA
N_15_8	95.82	95.82	91.00	91.00	100.00	100 (proved)	92.86	100.00	0.55	< 0	73.33	100 (proved)		
N_20_10	114.19	114.19	112.45	103.25	100.00	100 (proved)	100.00	82.35	< 0	0.38	45.00	100 (proved)		
N_25_13	165.38	164.05	160.92	159.12	96.00	100 (proved)	95.83	100.00	0.20	< 0	52.00	100 (proved)		
N_30_15	193.10	189.88	185.65	181.71	100.00	100 (proved)	76.92	100.00	1.03	< 0	6.67	100 (proved)		
N_35_18	228.44	227.23	228.44	227.23	100.00	100 (proved)	96.97	100.00	0.59	< 0	8.57	100 (proved)		
N_40_20	268.97	267.35	269.68	267.35	97.50	100 (proved)	82.50	100.00	1.72	< 0	0.00	100 (proved)		

N_45_23	300.29	300.52	302.42	300.52	35.56	100 (proved)	100.00	100.00	< 0	< 0	0.00	100 (proved)
N_50_25	350.16	344.24	346.61	341.62	96.00	100 (proved)	68.00	91.84	2.38	0.81	0.00	100 (proved)

Mechanism design performance evaluation criteria:

1) Objective function value: Formula (5);
2) Social welfare: summation of passengers' cumulative values minus the transportation cost;
3) Individual rationality: percentage of the number of passenger requests with non-negative utilities;
4) Price controllability: percentage of the number of served passengers whose prices are greater than or equal to the baseline prices in the total number of served passengers;
5) Max (PC_i - p_i): the maximum difference between the baseline price and the actual price;
6) Detour-discounting reasonability: percentage of number of passenger requests with reasonable changing processes in the total number of passenger requests.

Table 5.8 presents the computing time of HSATS and SPA. Before running the two algorithms, we adjust the parameters of the two algorithms so that the computing time in solving the matching and routing problem (model Md_0) is less than 10 seconds for all numerical examples because the on-demand ridesharing service requires prompt determination of the matching and routing plan. Then, we record the computing time of HSATS and SPA to calculate prices and the total computing time to obtain the mechanism.

We find that the SPA is much faster than HSATS in calculating the prices. SPA needs less than 20 seconds to obtain the mechanism for all numerical examples. In contrast, HSATS needs more than 20 seconds for even the smallest-scale numerical example (N_15_8) and even more than 400 seconds for the largest-scale numerical example (N_50_25). From Figure 5.14, we observe that the computing time of HSATS increases much faster than that of SPA as the problem scale increases. Figure 5.15 shows the

mechanism results for the largest-scale numerical example (N_50_25), which is obtained by the SPA within a reasonable amount of time (19.84 seconds). The computational time can be further substantially reduced using parallel computation or better computational hardware.

Table 5.8 Computing Time of HSATS and SPA

Numerical examples	Computing time to obtain optimal matching and routing plan (seconds)		Computing time to calculate prices (seconds)		Total computing time (seconds)	
	HSATS	SPA	HSATS	SPA	HSATS	SPA
N_15_8	1.53	1.74	21.94	1.11	23.47	2.85
N_20_10	1.99	2.31	34.14	1.87	36.13	4.18
N_25_13	2.78	3.37	72.51	2.87	75.29	6.24
N_30_15	3.80	4.49	113.07	4.07	116.87	8.56
N_35_18	4.65	5.28	151.97	5.45	156.62	10.73
N_40_20	5.55	6.40	199.46	7.38	205.01	13.78
N_45_23	6.79	7.91	310.04	8.63	316.83	16.54
N_50_25	8.04	9.48	397.14	10.36	405.18	19.84

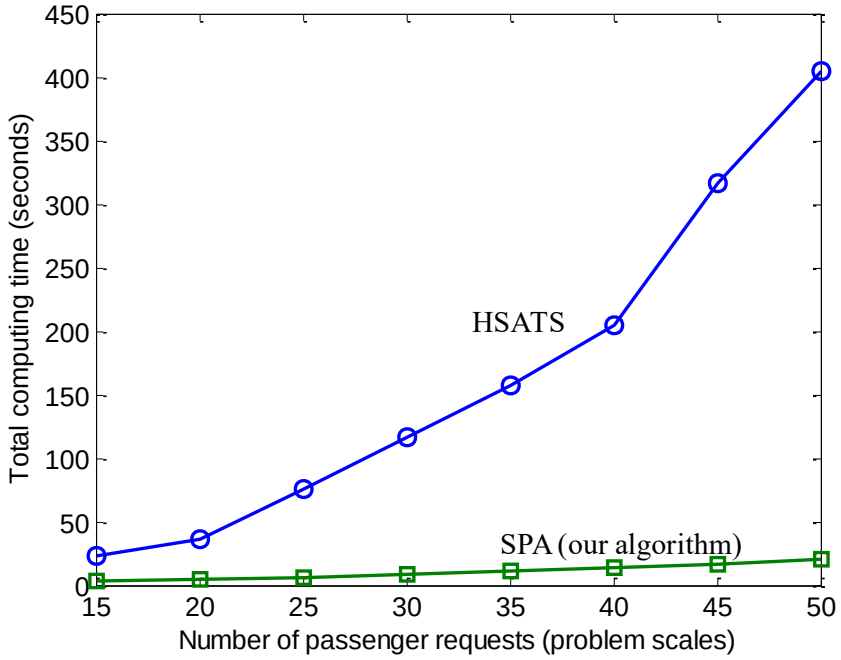

Figure 5.14 Computing Times of HSATS and SPA

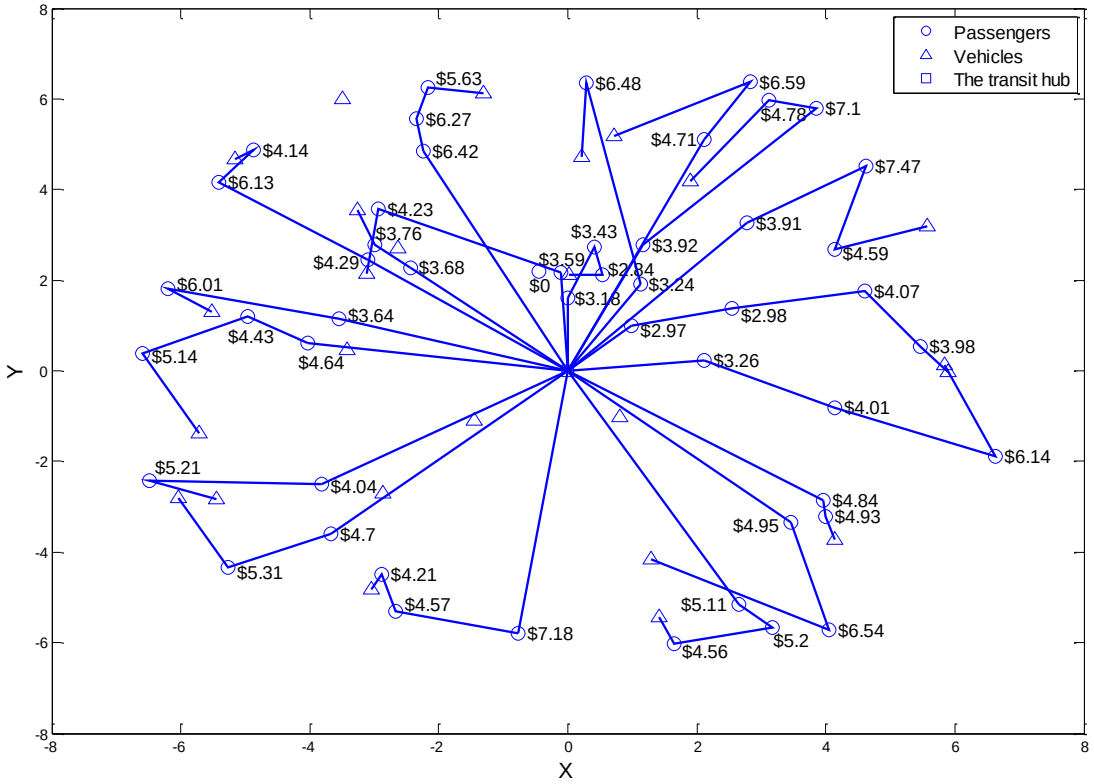

Figure 5.15 The Vehicle-Passenger Matching, Vehicle Routing Plan, and the Prices of the MPMBPC Mechanism Obtained by SPA (N_50_25)

Finally, we design a sufficiently large-scale numerical example with 300 passengers and 150 vehicles (denoted as N_300_150) to demonstrate the effectiveness of the proposed SPA algorithm. For the results, please see Appendix B.5.

5.8 Conclusions

This chapter studies the mechanism design problem for on-demand first-mile ridesharing. The traditional general-purpose VCG mechanism may sustain a financial deficit for ridesharing service providers. To address this challenge, we integrate a baseline price control component into the VCG mechanism, and propose a novel mobility-preference-based mechanism with baseline price control (MPMBPC). We prove an important property, named as "price controllability", which means that the served passengers' prices will never be lower than the baseline prices, enabling to avoid some passengers' unreasonably low prices and to prevent the service provider's deficit. Besides, the MPMBPC is proved to have the properties of "individual rationality" and "incentive compatibility". The "individual rationality" property ensures that all passengers will gain non-negative utilities and thus are willing to participate in the ridesharing service. The "incentive compatibility" property ensures that truthfully reporting one's mobility preference is the passenger's optimal strategy regardless of other passengers' reporting strategies. Another proved property, "detour-discounting reasonability", demonstrates that passengers can have customized mobility services: if passengers are less tolerant of detour,

they will have decreasing extra in-vehicle travel time but need to pay an increasing price if they are still served. Compared with the traditional VCG mechanism, our proposed MPMBPC mechanism can financially sustain the service without external investment. An efficient heuristic algorithm called Solution Pooling Approach (SPA) is developed to solve large-scale dynamic ridesharing problems. The SPA is theoretically proved to sustain the properties of "individual rationality", "incentive compatibility", and "detour discounting reasonability". Large-scale numerical examples show that SPA can quickly obtain the mechanism results with overall high-quality solutions. The theoretical modeling and the computational algorithms developed in this chapter might be useful for a variety of other relevant mechanism design problems in innovative shared mobility systems.

Appendix A. Proofs of Propositions

Proposition 1 Adding the baseline price control component in the objective function can ensure that if any passenger(s) *i*'s request is accepted, his value will never be smaller than PC_i; otherwise, this passenger request will be rejected.

Proof of Proposition 1:

Let *g* represent any passenger request accepted by the service. Let $X^*_{Md_0}$ represent the optimal matching and routing plan (the optimal solution of model Md_0) and $Y_g^* = TS_g(X^*_{Md_0})$ represent the *g*th transition solution (see Definition 4) of $X^*_{Md_0}$.

Based on Propositions 4 and 5, we have $TC(Y_g^*) \le TC(X^*_{Md_0})$ and $\sum_{i\in P\setminus g} VA_i\left(X^*_{Md_0}\right) \le \sum_{i\in P} VA_i\left(Y_g^*\right)$. Then

$$f(Y_g^*) = \sum_{i \in P} VA_i\left(Y_g^*\right) - TC(Y_g^*) + \sum_{i \in P} PC_i\left(1 - \sum_{k \in V} y_i^k\right)$$
$$\geq \sum_{i \in P \setminus g} VA_i\left(X_{Md_0}^*\right) - TC(X_{Md_0}^*) + \sum_{i \in P} PC_i\left(1 - \sum_{k \in V} y_i^k\right)$$

Since in $X_{Md_0}^*$, passenger request g is served, $1 - \sum_{k \in V} y_g^k = 0$. Then

$$f(X_{Md_0}^*) = \sum_{i \in P} VA_i\left(X_{Md_0}^*\right) - TC(X_{Md_0}^*) + \sum_{i \in P \setminus g} PC_i\left(1 - \sum_{k \in V} y_i^k\right)$$

Since Y_g^* is not necessarily the optimal solution of model Md_0, we have

$$f(X_{Md_0}^*) \geq f(Y_g^*)$$

Then

$$f(X_{Md_0}^*) = \sum_{i \in P} VA_i\left(X_{Md_0}^*\right) - TC(X_{Md_0}^*) + \sum_{i \in P \setminus g} PC_i\left(1 - \sum_{k \in V} y_i^k\right)$$
$$\geq f(Y_g^*)$$
$$\geq \sum_{i \in P \setminus g} VA_i\left(X_{Md_0}^*\right) - TC(X_{Md_0}^*) + \sum_{i \in P} PC_i\left(1 - \sum_{k \in V} y_i^k\right)$$

Thus

$$VA_g\left(X_{Md_0}^*\right) \geq PC_g$$

□

Proposition 4 If $Y_g = TS_g(X)$, for any $g \in P$, the transportation cost $TC(Y_g) \leq TC(X)$.

Proof of Proposition 4:

If $\sum_{k \in V} y_g^k = 0$ in X, $Y_g = X$, and thus

$$TC(Y_g) = TC(X).$$

If $\sum_{k \in V} y_g^k = 1$ in X, assume that we find k that $y_g{}^k = 1$. Then we discuss the four cases:

1) If we find i and j that $x_{ig}{}^k = 1$ and $x_{gj}{}^k = 1$, then $TC(X) - TC(Y_g) = c_{ig} + c_{gj} - c_{ij} \geq 0$ based on the triangle inequality.

2) If we find $w_g{}^k = 1$ and find i that $x_{ig}{}^k = 1$, then $TC(X) - TC(Y_g) = c_{ig} + c_{g0} - c_{i0} \geq 0$ based on the triangle inequality.

3) If we find $z_g{}^k = 1$ and find j that $x_{gj}{}^k = 1$, then $TC(X) - TC(Y_g) = c_{kg} + c_{gj} - c_{kj} \geq 0$ based on the triangle inequality.

4) If we find $z_g{}^k = 1$ and $w_g{}^k = 1$, then $TC(X) - TC(Y_g) = c_{kg} + c_{g0} > 0$.

Thus,

$$TC(Y_g) \leq TC(X).$$

□

Proposition 5 If $Y_g = TS_g(X)$, for any $g \in P$, $\sum_{i \in P \setminus g} VA_i(X) \leq \sum_{i \in P} VA_i(Y_g)$.

Proof of Proposition 5:

If $\sum_{k \in V} y_g^k = 0$, $Y_g = X$. $\sum_{i \in P} VA_i(X) = \sum_{i \in P} VA_i(Y_g)$ and $VA_g(X) = 0$. Thus

$$\sum_{i \in P \setminus g} VA_i(X) = \sum_{i \in P} VA_i(Y_g).$$

If $\sum_{k \in V} y_g^k = 1$ in X, we assume that passenger(s) g is picked up by vehicle k, i.e. $y_g^k = 1$. We only need to compare the values of passengers served by vehicle k, because other vehicles' routing plans do not change and the same passengers have identical values in X and Y_g. Since the passenger(s) g is not served in Y_g (see Figure 5.5), the extra in-vehicle travel times of other passengers served by vehicle k either decrease or remain constant. That is $EIVT_i(Y_g) \leq EIVT_i(X)$ for any passenger(s) i served by vehicle k. Based on Formula (1), we have $VA_i(Y_g) \geq VA_i(X)$, for any passenger(s) i served by vehicle k. Thus we have

$$\sum_{i \in P \setminus g} VA_i(X) \leq \sum_{i \in P} VA_i(Y_g).$$

□

Proposition 8 We have $p_i = p_j$ for any two passengers i and j, satisfying that $DL_i = DL_j$, $V_i^{\max} = V_j^{\max}$, $\alpha_i = \alpha_j$, $L_i = L_j$, rt_i and $rt_j \in TS_h$, and there exists a vehicle k that $y_i^k = y_j^k = 1$, where L_i and L_j are passengers i's and j's locations, respectively, rt_i and rt_j, passengers i's and j's request times, are within the same time slice TS_h.

Proof of Proposition 8:

In the optimal matching and routing plan $X^*_{Md_0}$, it is deemed that passengers *i* and *j* are picked up at the same time ($t_{ij} = 0$) because they are waiting at the same location ($L_i = L_j$) ready to be picked up. Thus, they have identical extra in-vehicle time travel time $EIVT_i = EIVT_j$. In addition, $V_i^{\max} = V_j^{\max}$. Based on the value function (Formula 1), we have $VA_i\left(X^*_{Md_0}\right) = VA_j\left(X^*_{Md_0}\right)$. Moreover, the optimal solutions of models Md_i and Md_j are entirely the same because requests *i* and *j* have identical parameters ($DL_i = DL_j$, $V_i^{\max} = V_j^{\max}$, $\alpha_i = \alpha_j$, $PC_i = PC_j$, and $L_i = L_j$). Thus, we have $f\left(X^*_{Md_i}\right) = f\left(X^*_{Md_j}\right)$. Then, based on Formula (23), we have

$$p_i = f\left(X^*_{Md_i}\right) - f\left(X^*_{Md_0}\right) + VA_i\left(X^*_{Md_0}\right) = f\left(X^*_{Md_j}\right) - f\left(X^*_{Md_0}\right) + VA_j\left(X^*_{Md_0}\right) = p_j$$

Thus, the two passengers *i* and *j* have identical prices.

□

Proposition 9 The mechanism ***M***($XP^*_{Md_0}$, **p**) obtained by SPA is individual rational.

Proof of Proposition 9:

Based on Formula (27), if passenger(s) *g*'s request is rejected, his price is "0" and his utility is "0" as well. If passenger(s) *g* is served, his price is given by

$$p_g = f\left(XP^*_{Md_g}\right) - \left(f\left(XP^*_{Md_0}\right) - VA_g\left(XP^*_{Md_0}\right)\right)$$

Then passenger(s) g's utility is

$$U_g\left(XP^*_{Md_0}, p_g\right) = VA_g\left(XP^*_{Md_0}\right) - p_g$$
$$= f\left(XP^*_{Md_0}\right) - f\left(XP^*_{Md_g}\right)$$

Based on Proposition 12 (see Appendix A), since $XP^*_{Md_g}$ is a feasible solution of model Mdp_g, it is a feasible solution of model Mdp_0 as well. $XP^*_{Md_0}$ is the optimal solution of model Mdp_0. Thus, we have

$$U_g\left(XP^*_{Md_0}, p_g\right) = f\left(XP^*_{Md_0}\right) - f\left(XP^*_{Md_g}\right) \geq 0$$

□

Proposition 10 The mechanism $\boldsymbol{M}(\ XP^*_{Md_0}\ ,\ \mathbf{p})$ obtained by SPA is incentive compatible.

Proof of Proposition 10:

We assume that if passenger(s) g misreports DL_g, V_g^{max}, and/or α_g, the optimal plan will be $YP^*_{Md_0}$ instead of $XP^*_{Md_0}$. The system will mistake passenger(s) g's actual value ($VA_g\left(YP^*_{Md_0}\right)$) for $VA'_g\left(YP^*_{Md_0}\right)$. Passenger(s) g is charged with the price p'_g instead of p_g.

We discuss three cases.

1) Passenger(s) g's request is rejected by the service in the plan $YP^*_{Md_0}$. Then, $VA_g\left(YP^*_{Md_0}\right) = 0$ and $p'_g = 0$ based on Formula (27), and $U_g\left(YP^*_{Md_0}, p'_g\right) = VA_g\left(YP^*_{Md_0}\right)$

$-p'_g = 0$. Based on Proposition 9, $U_g\left(XP^*_{Md_0}, p_g\right) \geq 0$ if passenger(s) g tells the truth. Thus, we have $U_g\left(YP^*_{Md_0}, p'_g\right) \leq U_g\left(XP^*_{Md_0}, p_g\right)$.

2) Passenger(s) g is served but is unable to arrive at the transit hub before the actual arrival deadline given the matching and routing plan $YP^*_{Md_0}$. Thus, passenger(s) g's requirement is not satisfied while he could have arrived at the transit hub in time given the plan $XP^*_{Md_0}$ if he had truthfully reported the deadline. Truthful report is the best strategy for this case.

3) Passenger(s) g is served and he can arrive at the transit hub before the actual arrival deadline given the plan $YP^*_{Md_0}$. Since the generation of solution pool $Xpool_{Md_g}$ is independent of passenger(s) g's report based on the SPA algorithm, the constraint of Formula (29) of model Mdp_g remains constant. In model Mdp_g, the constraints of Formulas (6-10, 13, 15, 17-22) are always constant regardless of passenger(s) g's report because these constraints do not involve any mobility preferences. Only Formula (11) has an arrival deadline constraint for model Mdp_g. However, in model Mdp_g, passenger(s) g's value is always zero regardless of passenger(s) g's report because he is not served based on Formula (22). Thus, the constraint region C_g (Formulas 6-11, 13, 15, 17-22) is always constant regardless of passenger(s) g's report.

Thus, the feasible region ($C_g \cap Xpool_{Md_g}$) of model Mdp_g is constant. Moreover, the objective function of model Mdp_g is independent of passenger(s) g's report. In conclusion, model Mdp_g and the optimal objective function value of model Mdp_g ($f\left(XP^*_{Md_g}\right)$) remain constant regardless of passenger(s) g's report. Thus, for this case,

passenger(s) g's price is

$$p'_g = f\left(XP^*_{Md_g}\right) - f'\left(YP^*_{Md_0}\right) + VA'_g\left(YP^*_{Md_0}\right)$$

where

$$f'\left(YP^*_{Md_0}\right) = \sum_{i\in P, i\neq g} VA_i\left(YP^*_{Md_0}\right) + VA'_g\left(YP^*_{Md_0}\right) + \sum_{i\in P} PC_i\left(1 - \sum_{k\in V} y_i^k\right) - TC\left(YP^*_{Md_0}\right)$$

For this case, $YP^*_{Md_0}$ is a feasible solution of model Mdp_0 because passenger(s) g can arrive at the transit hub before the actual arrival deadline and $YP^*_{Md_0}$ is selected from the pool $Xpool_{Md_0}$: $YP^*_{Md_0} \in C_0 \bigcap Xpool_{Md_0}$. Given the misreported information, passenger(s) g's utility is

$$\begin{aligned} &U_g\left(YP^*_{Md_0}, p'_g\right) = VA_g\left(YP^*_{Md_0}\right) - p'_g \\ &= f'\left(YP^*_{Md_0}\right) - VA'_g\left(YP^*_{Md_0}\right) + VA_g\left(YP^*_{Md_0}\right) - f\left(XP^*_{Md_g}\right) \\ &= f\left(YP^*_{Md_0}\right) - f\left(XP^*_{Md_g}\right) \end{aligned}$$

$YP^*_{Md_0}$ is not necessarily the optimal solution of model Mdp_0 while $XP^*_{Md_0}$ is the optimal solution of model Mdp_0 if passenger(s) g truthfully reports his value. Thus,

$$f\left(YP^*_{Md_0}\right) \leq f\left(XP^*_{Md_0}\right).$$

Thus, we have

$$U_g\left(YP^*_{Md_0}, p'_g\right) = f\left(YP^*_{Md_0}\right) - f\left(XP^*_{Md_g}\right) \le f\left(XP^*_{Md_0}\right) - f\left(XP^*_{Md_g}\right) = U_g\left(XP^*_{Md_0}, p_g\right)$$

From the results of the three cases, we can conclude that the mechanism obtained by SPA is incentive compatible.

□

Proposition 11 The mechanism ***M***($XP^*_{Md_0}$, **p**) obtained by SPA is detour-discounting reasonable.

Proof Proposition 11:

Similarly, we only need to prove the two sub-propositions in Proposition 7.

For the first situation, the optimal matching and routing plan $XP^*_{Md_0}$ does not change, and thus passenger(s) g's extra in-vehicle travel time does not change. In the price calculation $p_g = f\left(XP^*_{Md_g}\right) - \left(f\left(XP^*_{Md_0}\right) - VA_g\left(XP^*_{Md_0}\right)\right)$, $f\left(XP^*_{Md_g}\right)$ remains constant because model Md_g does not change regardless of passenger(s) g's reported α_g. Moreover, $f\left(XP^*_{Md_0}\right) - VA_g\left(XP^*_{Md_0}\right) = \sum_{i\in P\setminus g} VA_i\left(XP^*_{Md_0}\right) - TC\left(XP^*_{Md_0}\right) + \sum_{i\in P} PC_i\left(1 - \sum_{k\in V} y_i^k\right)$ also remains constant because all other elements do not change due to the constant of the optimal plan. Thus, the price remains constant.

For the second proposition, the detailed proof is entirely identical with that in Proposition 6.

□

Proposition 12 If X is a feasible solution of model Mdp_g, then X must be a feasible solution of model Mdp_0 as well.

Proof of Proposition 12:

Based on Algorithm 4, $Xpool_{Md_g} \subset Xpool_{Md_0}$, for all $g \in P$. Moreover, the constraint set C_g has one more constraint (Formula 22) compared with the constraint set C_0. Therefore, $C_g \subseteq C_0$. Let X be any one feasible solution of model Mdp_g, $X \in C_g \bigcap Xpool_{Md_g}$. Since $Xpool_{Md_g} \subset Xpool_{Md_0}$, $X \in Xpool_{Md_0}$. Similarly, since $C_g \subseteq C_0$, $X \in C_0$. Then, for any $X \in C_g \bigcap Xpool_{Md_g}$, we have $X \in C_0 \bigcap Xpool_{Md_0}$ as well. Thus, X is a feasible solution of model Mdp_0 as well.

□

Appendix B. Additional demonstration of the MPMBPC mechanism and the SPA algorithm

B.1 Demonstration of the Difference between the MPMBPC Price and the VCG Price Plus the Baseline Price

Figure 5.16 shows the difference between the proposed MPMBPC pricing scheme and the VCG price plus the baseline price and demonstrates the advantage of the MPMBPC mechanism. If the price equals VCG price plus baseline price, the important property "individual rationality" no longer holds. Figure 5.16 (a) is the optimal plan for the VCG mechanism with the price equaling VCG price plus baseline price. We find that both Passengers 2 and 3's prices ($9 and $2) exceed their maximum willing-to-pay prices ($6

and $0). Thus, the property "individual rationality" does not hold. MPMBPC mechanism is proved to hold the property of "individual rationality"; thus both Passengers 2 and 3's prices ($0 and $4) do not exceed their maximum willing-to-pay prices ($0 and $5), as shown in Figure 5.16 (b).

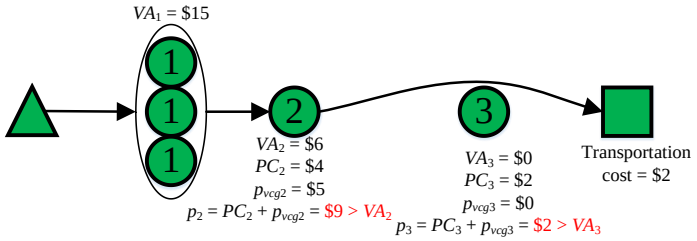

(a) Optimal plan for VCG mechanism

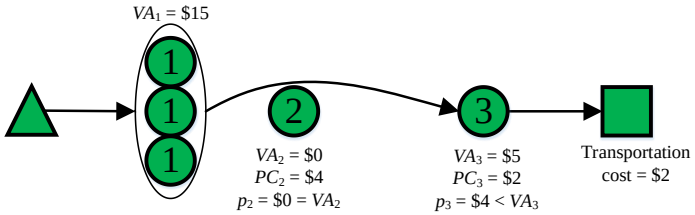

(b) Optimal plan for MPMBPC mechanism

Figure 5.16 The Difference between the MPMBPC Price and the VCG Price Plus the Baseline Price

B.2 Prices of Passengers in the Same Origin with Different Mobility Preferences

We cannot easily tell whether two passengers in the same origin with different mobility preferences will be charged with the same or different prices. We use two examples for demonstration.

Let us see the first example in Figure 5.17, demonstrating that riders are charged with the same price even if the mobility preferences are different. Passenger 1 and Passenger 2 are in the same origin, but they have different mobility preferences. Passenger

1's value (non-detour value – detour disvalue) is \$8, higher than Passenger 2's value (\$6). In the optimal routing plan, Passenger 1 and Passenger 2 share the ride and are picked up at the same time. Then we calculate the two passengers' prices: $p_1 = PC_1 + 0.2$ and $p_2 = PC_2 + 0.2$. Since the two passengers are in the same origin, the baseline prices are identical: $PC_1 = PC_2$. Thus, the two passengers' prices are the same: $p_1 = p_2$.

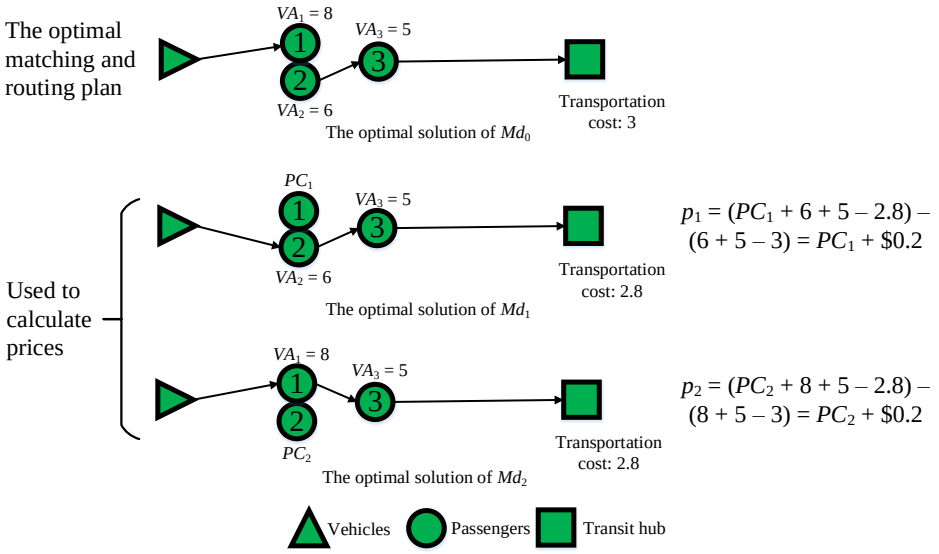

Figure 5.17 Riders in the Same Origin Charged with the Same Price

Let us see the second example in Figure 5.18, demonstrating that riders are charged with different prices when the mobility preferences are different. Passenger 1 and Passenger 2 are in the same origin. Passenger 2's arrival deadline is much earlier than Passenger 1. If Passenger 2 waits for Vehicle 1 to pick him up, he will arrive at the transit hub later than the deadline. Thus, a closer vehicle (Vehicle 2) is dispatched to pick up Passenger 2 and drive him to the transit hub directly. At this time, Passenger 1 is charged

with $PC_1 + 0.8$ and Passenger 2 is charged with $PC_2 + 2$. Since $PC_1 = PC_2$, then $p_1 = PC_1 + 0.8 < p_2 = PC_2 + 2$. The prices are different.

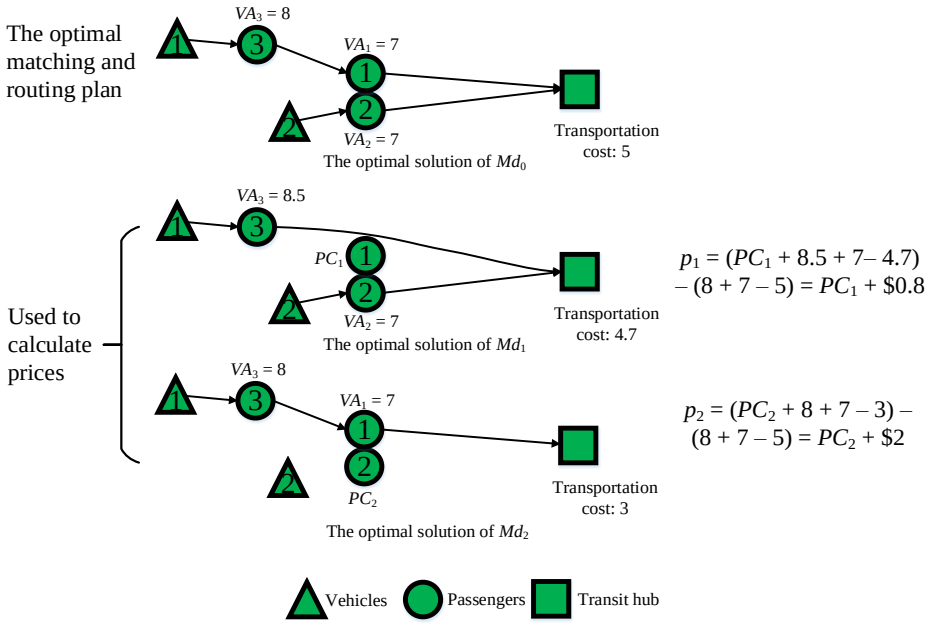

Figure 5.18 Riders in the Same Origin Charged with Different Prices

B.3 Demonstration of SPA Violating the Property of "Price Controllability"

We use a simple example (Figure 5.19) to straightforwardly show why the price controllability may not hold. In Figure 5.19, $XP^*_{Md_1}$ is the best solution selected from the pool $Xpool_{Md_1}$ and $YP_1{}^*$ is the transition solution of $XP^*_{Md_0}$ (the best solution in $Xpool_{Md_0}$). If the condition $f\left(XP^*_{Md_1}\right) \geq f\left(YP^*_1\right)$ can be satisfied, the property holds. However, we find that the objective function value of $XP^*_{Md_1}$ (14.6) is smaller than that of $YP_1{}^*$ (15.3). This is because $YP_1{}^*$ is not in the pool $Xpool_{Md_1}$. Due to this reason $f\left(XP^*_{Md_1}\right) < f\left(YP^*_1\right)$, the final price is less than the baseline price: $p_1 = PC_1 - 0.4 < PC_1$.

If $X^*_{Md_1}$ is the exact optimal solution of the model Md_1, it is impossible that $f(X^*_{Md_1}) < f(Y_1^*)$, where Y_1^* is the transition solution of $X^*_{Md_0}$ (the exact optimal solution of model Md_0). This is because Y_1^* is a just feasible solution of model Md_1 while $X^*_{Md_1}$ is the optimal solution of model Md_1. Thus, if we use an exact algorithm to obtain $X^*_{Md_1}$, the property of "price controllability" can always hold, but SPA cannot guarantee the optimality of $XP^*_{Md_1}$ and thus is possible to violate the property.

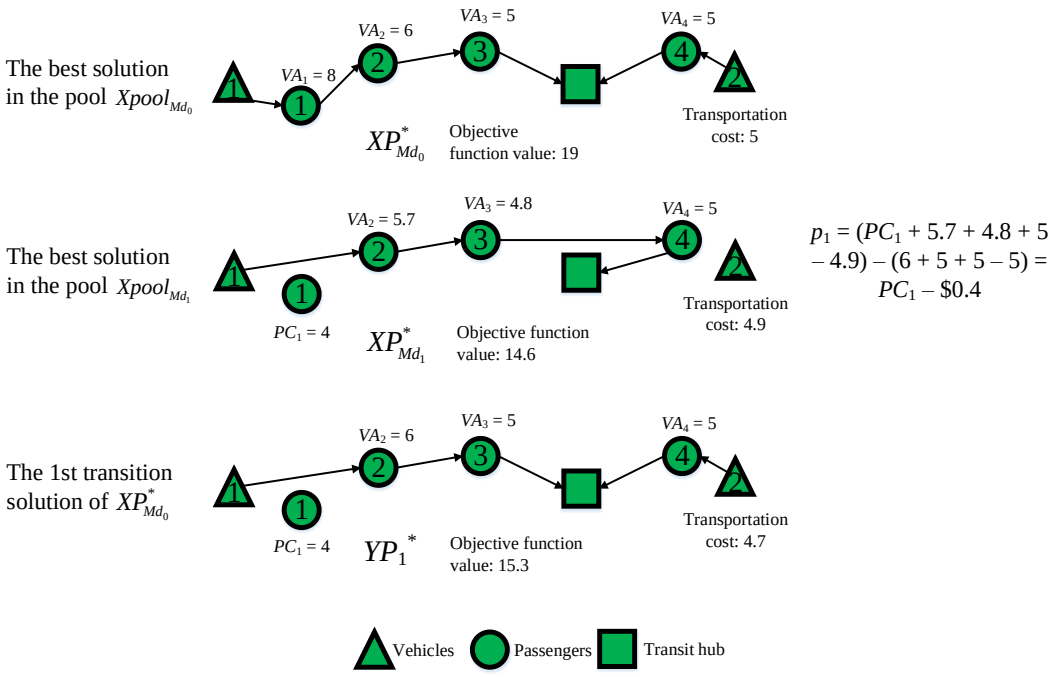

Figure 5.19 A Counter Case Violating the Property "Price Controllability"

B.4 Potential Impact of Considering the Vehicle Availability Dynamics and Predicting Occurrence of Passenger Requests

If we consider the vehicle availability dynamics and occurrence of potential passenger requests in our mechanism, we anticipate that the system will serve more passengers, provide passengers with more incentive, and achieve larger social welfare. We use the following example (Figure 5.20) for demonstration. As Figure 5.20(a) shows, if we do not consider potential passengers in the next several minutes, the optimal matching and routing plan is "Vehicle 1 → Passenger 1 → Passenger 2 → Passenger 3 → the transit hub". However, if we can predict that Passengers 4 and 5 (e.g. commuters taking ridesharing service routinely) will have a very large probability to send requests (Figure 5.20b), then the previous matching and routing plan is no longer optimal. This is because Vehicle 1 is no longer available if it is dispatched, Vehicle 2 is too far away to serve these two passengers, and thus these two passengers may not be served in time if no other vehicles become available nearby within the next few minutes. The mechanism thus can dispatch Vehicle 2 to serve Passengers 1, 2, and 3, and let Vehicle 1 wait to serve Passengers 4 and 5, as Figure 5.20(c) shows. We can achieve better optimization by predicting available vehicle locations and potential passenger requests in the next few minutes based on historical data. However, designing such more advanced mechanisms needs plenty of historical data to predict where and when vehicles will be available and where, when, and how likely potential passenger requests will occur. We may consider this in our future work.

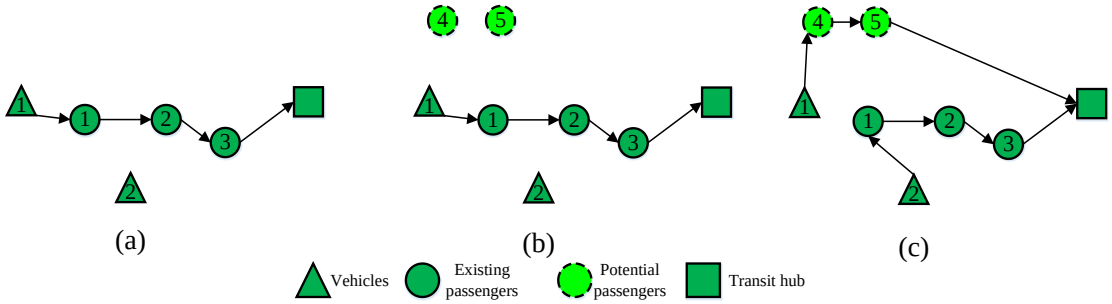

Figure 5.20 Optimization of Matching and Routing Considering Vehicle Availability Dynamics and Potential Passenger Occurrence

B.5 Mechanism Results for the Large-Scale Example N_300_150

We use the SPA to solve the mechanism design problem for the numerical example N_300_150. Table 5.9 and Figure 5.21 show the results of the SPA algorithm.

Table 5.9 The Output Results of the SPA Algorithm for N_300_150

Output performances	Values
Objective function value (SPA)	2095.71
Objective function value (HSATS)	2182.16
The gap of SPA from HSATS in objective function value	3.96%
Total collected prices ($)	1366.35
Total transportation cost ($)	396.71
Total profit ($)	969.64
Price controllability (%)	100%
Number of passengers served	300
Number of vehicles dispatched	118
Vehicle occupancy rate	63.56%

Computing time (seconds)	148.92

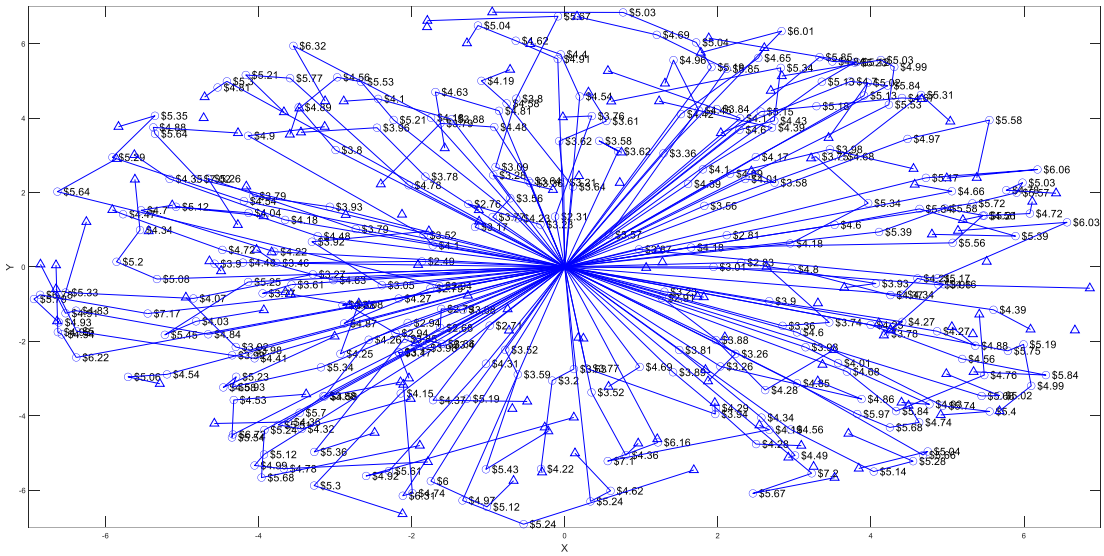

Figure 5.21 The Vehicle-Passenger Matching, Vehicle Routing Plan, and the Prices of the MPMBPC Mechanism Obtained by SPA (N_300_150)

From the results presented in Table 5.9 and Figure 5.21, we can conclude that the SPA algorithm still has a high performance in solving the extremely large-scale problem. The gap of SPA from HSATS in the objective function value is only 3.96%. The total collected price is \$1366.35, which can cover the 396.71-dollar transportation cost. The profit made by the service provider is \$969.64. In this example, the SPA sustains the property of price controllability (100% of the prices are no less than the baseline prices). All passengers are served. The number of dispatched vehicles is 118 with the vehicle seat occupancy rate of 63.56%.

We admit that the computing time (148.92 seconds = 2.48 minutes) of the SPA

algorithm for the numerical example N_300_150 is not prompt enough for on-demand ridesharing. However, our SPA algorithm can be implemented for parallel computation and the computer hardware is not so advanced. Thus, the computational time can be further substantially reduced using parallel computation and better computer hardware. Our future work will improve the SPA algorithm by seeking the tradeoff among validity of mechanism design properties, solution qualities, and computational speed.

CHAPTER 6 CONCLUSIONS AND FUTURE WORK

6.1 Conclusions

This dissertation studies the mechanism problem for both scheduled and on-demand ridesharing service. The designed mechanisms aim to optimize the passenger-vehicle matching and vehicle routing as well as to design a pricing scheme with multiple incentive objectives. The designed mechanisms are able to promote passengers to participate in the ridesharing service by satisfying their mobility preferences via the property of "individual rationality", promote passengers to truthfully report their mobility preference via the property of "individual rationality", and incentivize the service provider to provide the service via the properties like "price controllability". In addition, the mechanisms can also offset passengers' inconvenience cost considering their mobility preferences or requirements, and can prevent drivers from deliberately detouring. In order to obtain the mechanism results for large-scale problems, this dissertation develops an efficient heuristic algorithm, called Solution Pooling Approach (SPA). The SPA algorithm is successfully used to solve the mechanism design problems for both scheduled and on-demand first-mile ridesharing. The SPA can sustain the two mechanism design properties, "individual rationality" and "incentive compatibility". From the experimental results, SPA is much more efficient in solving large-scale problems compared with the commercial solver (e.g. Branch and Bound) and traditional heuristic algorithms (e.g. hybrid simulated annealing and tabu search) from the literature. The designed mechanisms and the SPA algorithm can be adapted for similar problems in shared mobility.

6.2 Future Work

Upon completing this dissertation, I find a lot of future work can be studied in depth.

- In our current mechanism, once the vehicle-passenger matching, vehicle routing plan, and passengers' payments are determined, the plan and payments will not change. In the future, we will develop an online mechanism allowing to change the vehicle-passenger matching, vehicle routing, and pricing in real time.

- Our future work will study how taking vehicle dynamics into consideration can achieve better optimization of matching and routing plan by predicting vehicle locations in the next few minutes based on historical data.

- I will consider developing another incentive mechanism that aims to direct vehicles to undersupplied locations.

- Furthermore, in this dissertation, the travel time between two locations are assumed to be deterministic. Travel time uncertainty and reliability will be considered for the mechanism design in our future work.

- Also, in the future if more people use the first-mile ridesharing service, which will account for a large portion of the transportation network, we will use game-theoretic model to determine the travel time depending on the assignment of ridesharing vehicles to different roads in equilibrium.

- I will design mechanisms for on-demand first-mile ridesharing system involving multiple transit hubs instead of one hub.

- Mixed scheduled and on-demand passenger requests will be considered in the future. I will develop a hybrid mechanism for this mixed scheduled and on-demand first-mile ridesharing to incentivize passengers to early schedule the service.

- Last but not least, I will adapt the designed mechanism to other shared mobility modes, including carsharing, bikesharing, vanpooling, etc.

REFERENCES

[1] Agatz, N., et al. *The Value of Optimization in Dynamic Ride-Sharing: a Simulation Study in Metro Atlanta, Research paper, Erasmus Research Institute of Management (ERIM), Report No*. ERS-2010-034-LIS. 2010, Retrieved from: http://hdl. handle. net/1765/20456.

[2] Agatz, Niels, et al. "Dynamic ride-sharing: A simulation study in metro Atlanta." *Procedia-Social and Behavioral Sciences* 17 (2011): 532-550.

[3] Agussurja, Lucas, Shih-Fen Cheng, and Hoong Chuin Lau. "A state aggregation approach for stochastic multi-period last-mile ride-sharing problems." *Transportation Science* (2018).

[4] Alemi, Farzad, and Caroline Rodier. *Simulation of Ridesourcing Using Agent-Based Demand and Supply Regional Models: Potential Market Demand for First-Mile Transit Travel and Reduction in Vehicle Miles Traveled in the San Francisco Bay Area*. No. NCST-20161200. 2016

[5] American Public Transportation Association (2016) http://www.apta.com/mediacenter/ptbenefits/Pages/default.aspx

[6] Amey, A., J. Attanucci, and R. Mishalani. "'Real-Time' Ridesharing – The Opportunities and Challenges of Utilizing Mobile Phone Technology to Improve Rideshare Services." *TRB Annual Meeting*, 2011.

[7] Amirgholy, Mahyar, and Eric J. Gonzales. "Demand responsive transit systems with time-dependent demand: user equilibrium, system optimum, and management strategy." *Transportation Research Part B: Methodological*92 (2016): 234-252.

[8] Amirian, Pouria, Anahid Basiri, and Jeremy Morley. "Predictive analytics for enhancing travel time estimation in navigation apps of Apple, Google, and Microsoft." *Proceedings of the 9th ACM SIGSPATIAL International Workshop on Computational Transportation Science*. ACM, 2016.

[9] Arentze, Theo A. "Adaptive personalized travel information systems: A Bayesian method to learn users' personal preferences in multimodal transport networks." *IEEE Transactions on intelligent transportation systems* 14.4 (2013): 1957-1966.

[10] Armant, Vincent, and Kenneth N. Brown. "Minimizing the driving distance in ride sharing systems." *Tools with Artificial Intelligence (ICTAI), 2014 IEEE 26th International Conference on*. IEEE (2014).

[11] Asghari, Mohammad, et al. "Price-aware real-time ride-sharing at scale: an auction-based approach." *Proceedings of the 24th ACM SIGSPATIAL International Conference on Advances in Geographic Information Systems*. ACM, 2016.

[12] Asghari, Mohammad, and Cyrus Shahabi. "An on-line truthful and individually rational pricing mechanism for ride-sharing." *Proceedings of the 25th ACM SIGSPATIAL International Conference on Advances in Geographic Information Systems*. ACM, 2017.

[13] Baldacci, Roberto, Vittorio Maniezzo, and Aristide Mingozzi. "An exact method for the car pooling problem based on lagrangean column generation." *Operations Research* 52.3 (2004): 422-439.

[14] Banerjee, Siddhartha, Carlos Riquelme, and Ramesh Johari. "Pricing in Ride-share Platforms: A Queueing-Theoretic Approach." (2015)

"https://papers.ssrn.com/sol3/papers.cfm?abstract_id=2568258".

[15] BBC news 2016: http://www.bbc.co.uk/newsbeat/article/37219411/uber-detours-and-how-to-fight-them

[16] Ben-Akiva, Moshe E., and Steven R. Lerman. *Discrete choice analysis: theory and application to travel demand*. Vol. 9. MIT press, 1985.

[17] Bian, Zheyong, and Xiang Liu. "Planning the Ridesharing Route for the First-Mile Service Linking to Railway Passenger Transportation." *2017 Joint Rail Conference*. American Society of Mechanical Engineers, 2017.

[18] Bian, Zheyong, and Xiang Liu. "A Detour-based Pricing Mechanism for First-mile Ridesharing in Connection with Rail Public Transit." *2018 Joint Rail Conference*. American Society of Mechanical Engineers (2018a).

[19] Bian, Zheyong, and Xiang Liu. "A real-time adjustment strategy for the operational level stochastic orienteering problem: A simulation-aided optimization approach." *Transportation Research Part E: Logistics and Transportation Review* 115 (2018b): 246-266.

[20] Bian, Zheyong, and Xiang Liu. "Mechanism design for first-mile ridesharing based on personalized requirements part I: Theoretical analysis in generalized scenarios." *Transportation Research Part B: Methodological* 120 (2019a): 147-171.

[21] Bian, Zheyong, and Xiang Liu. "Mechanism design for first-mile ridesharing based on personalized requirements part II: Solution algorithm for large-scale problems." *Transportation Research Part B: Methodological* 120 (2019b): 172-192.

[22] Bimpikis, Kostas, Ozan Candogan, and Daniela Saban. "Spatial pricing in ride-sharing networks." *Operations Research* (2019): Vol. 67, No. 3.

[23] Bistaffa, Filippo, et al. "Recommending fair payments for large-scale social ridesharing." *Proceedings of the 9th ACM Conference on Recommender Systems*. ACM, 2015.

[24] Biswas, Arpita, et al. "Impact of Detour-Aware Policies on Maximizing Profit in Ridesharing." *arXiv preprint arXiv:1706.02682* (2017a).

[25] Biswas, Arpita, et al. "Profit optimization in commercial ridesharing." *Proceedings of the 16th Conference on Autonomous Agents and MultiAgent Systems*. International Foundation for Autonomous Agents and Multiagent Systems, 2017b.

[26] Bussieck, Michael R., and Stefan Vigerske. "MINLP solver software." *Wiley encyclopedia of operations research and management science* (2010): 1-12.

[27] Calvo, Roberto Wolfler, Fabio de Luigi, Palle Haastrup, and Vittorio Maniezzo. "A distributed geographic information system for the daily car pooling problem." *Computers & Operations Research* 31.13 (2004): 2263-2278.

[28] Chao, Xiuli, et al. "Approximation algorithms for capacitated perishable inventory systems with positive lead times." *Management Science* (2017).

[29] Chen, Lu, et al. "Price-and-time-aware dynamic ridesharing." *2018 IEEE 34th International Conference on Data Engineering (ICDE)*. IEEE, 2018.

[30] Chen, Mengjing, et al. "Dispatching Through Pricing: Modeling Ride-Sharing and Designing Dynamic Prices." 2019, iiis.tsinghua.edu.cn.

[31] Chen, Yiwei, and Hai Wang. "Pricing for a last-mile transportation system." *Transportation Research Part B: Methodological* 107 (2018): 57-69.

[32] Cheng, Shih-Fen, Duc Thien Nguyen, and Hoong Chuin Lau. "A Mechanism for Organizing Last-Mile Service Using Non-Dedicated Fleet." *Web Intelligence and*

Intelligent Agent Technology (WI-IAT), 2012 IEEE/WIC/ACM International Conferences on. Vol. 2. IEEE, 2012.

[33] Cheng, Shih-Fen, Duc Thien Nguyen, and Hoong Chuin Lau. "Mechanisms for arranging ride sharing and fare splitting for last-mile travel demands." *Proceedings of the 2014 international conference on Autonomous agents and multi-agent systems*. International Foundation for Autonomous Agents and Multiagent Systems, 2014.

[34] Chou, Sheng-Kai, Ming-Kai Jiau, and Shih-Chia Huang. "Stochastic set-based particle swarm optimization based on local exploration for solving the carpool service problem." *IEEE transactions on cybernetics* 46.8 (2016): 1771-1783.

[35] Cici, Blerim, et al. "Assessing the potential of ride-sharing using mobile and social data: a tale of four cities." *Proceedings of the 2014 ACM International Joint Conference on Pervasive and Ubiquitous Computing*. ACM, 2014.

[36] Clarke, Edward H. "Multipart pricing of public goods." *Public choice* 11.1 (1971): 17-33.

[37] Dobzinski, Shahar, Noam Nisan, and Michael Schapira. "Approximation algorithms for combinatorial auctions with complement-free bidders." *Mathematics of Operations Research* 35.1 (2010): 1-13.

[38] Fang, Zhixuan, Longbo Huang, and Adam Wierman. "Prices and Subsidies in the Sharing Economy: Profit versus Welfare." https://www.semanticscholar.org/paper/Prices-and-Subsidies-in-the-Sharing-Economy%3A-Profit-Fang-Huang/695c0c9db8d22bf9cf25129565af5e8c8d911837

[39] Friedman, Eric J., and David C. Parkes. "Pricing wifi at starbucks: issues in online mechanism design." *Proceedings of the 4th ACM conference on Electronic commerce*. ACM, 2003.

[40] Di Febbraro, A., E. Gattorna, and N. Sacco. "Optimization of dynamic ridesharing systems." *Transportation Research Record: Journal of the Transportation Research Board* 2359 (2013): 44-50.

[41] Fan, Jing, et al. "URoad: An Efficient Algorithm for Large-Scale Dynamic Ridesharing Service." *2018 IEEE International Conference on Web Services (ICWS)*. IEEE, 2018.

[42] Frisk, Mikael, et al. "Cost allocation in collaborative forest transportation." *European Journal of Operational Research* 205.2 (2010): 448-458.

[43] Furuhata, Masabumi, et al. "Ridesharing: The state-of-the-art and future directions." *Transportation Research Part B: Methodological* 57 (2013): 28-46.

[44] Geisberger, Robert, et al. "Fast detour computation for ride sharing." *arXiv preprint arXiv:0907.5269* (2009).

[45] Gendreau, Michel, et al. "Parallel tabu search for real-time vehicle routing and dispatching." *Transportation science* 33.4 (1999): 381-390.

[46] Gendreau, Michel, Alain Hertz, and Gilbert Laporte. "A tabu search heuristic for the vehicle routing problem." *Management science* 40.10 (1994): 1276-1290.

[47] Ghoseiri, Keivan, Ali Ebadollahzadeh Haghani, and Masoud Hamedi. Real-time rideshare matching problem. *Berkeley: Mid-Atlantic Universities Transportation Center* (2011).

[48] Golledge, Reginald G., Mei-Po Kwan, and Tommy Garling. "Computational-process modelling of household travel decisions using a geographical information system." *University of California Transportation Center* (1994).

[49] Gopalakrishnan, Ragavendran, Koyel Mukherjee, and Theja Tulabandhula. "The Costs and Benefits of Ridesharing: Sequential Individual Rationality and Sequential Fairness." *arXiv preprint arXiv:1607.07306* (2016).

[50] Groves, Theodore. "Incentives in teams." *Econometrica: Journal of the Econometric Society* (1973): 617-631.

[51] Gupta, Anupam, Viswanath Nagarajan, and R. Ravi. "Approximation algorithms for optimal decision trees and adaptive TSP problems." *Mathematics of Operations Research* 42.3 (2017): 876-896.

[52] Hajibabai, Leila, Yun Bai, and Yanfeng Ouyang. "Joint optimization of freight facility location and pavement infrastructure rehabilitation under network traffic equilibrium." *Transportation Research Part B: Methodological* 63 (2014): 38-52.

[53] Hall, Jonathan, Cory Kendrick, and Chris Nosko. "The effects of Uber's surge pricing: A case study." *The University of Chicago Booth School of Business* (2015).

[54] Hara, Yusuke, and Eiji Hato. "A car sharing auction with temporal-spatial OD connection conditions." *Transportation research procedia* 23 (2017): 22-40.

[55] Hara, Yusuke. "Behavioral mechanism design for transportation services: Laboratory experiments and preference elicitation cost." *Transportation Research Part B: Methodological* 115 (2018): 231-245.

[56] Hartline, Jason D., and Tim Roughgarden. "Simple versus optimal mechanisms." *Proceedings of the 10th ACM conference on Electronic commerce*. ACM, 2009.

[57] Hou, Liwen, Dong Li, and Dali Zhang. "Ride-matching and routing optimisation: Models and a large neighbourhood search heuristic." *Transportation Research Part E: Logistics and Transportation Review* 118 (2018): 143-162.

[58] Hsieh, Fu-Shiung, Fu-Min Zhan, and Yi-Hong Guo. "A solution methodology for carpooling systems based on double auctions and cooperative coevolutionary particle swarms." *Applied Intelligence* (2018): 1-23.

[59] Hsieh, Fu-Shiung. "Optimization of Monetary Incentive in Ridesharing Systems." *International Conference on Industrial, Engineering and Other Applications of Applied Intelligent Systems*. Springer, Cham, 2019.

[60] Hsieh, Fu-Shiung, Fu-Min Zhan, and Yi-Hong Guo. "A solution methodology for carpooling systems based on double auctions and cooperative coevolutionary particle swarms." *Applied Intelligence* 49.2 (2019): 741-763.

[61] Huang, Shih-Chia, Ming-Kai Jiau, and Chih-Hsiang Lin. "A genetic-algorithm-based approach to solve carpool service problems in cloud computing." *IEEE Transactions on Intelligent Transportation Systems* 16.1 (2015): 352-364.

[62] Huang, Shih-Chia, Ming-Kai Jiau, and Ka-Hou Chong. "A heuristic multi-objective optimization algorithm for solving the carpool services problem featuring high-occupancy-vehicle itineraries." *IEEE Transactions on Intelligent Transportation Systems* (2017).

[63] Huang, Shih-Chia, Ming-Kai Jiau, and Yu-Ping Liu. "An ant path-oriented carpooling allocation approach to optimize the carpool service problem with time windows." *IEEE Systems Journal* (2018).

[64] Hurwicz, Leonid, and Stanley Reiter. *Designing economic mechanisms*. Cambridge University Press, 2006.

[65] Jehiel, Philippe, Benny Moldovanu, and Ennio Stacchetti. "Multidimensional

mechanism design for auctions with externalities." *Journal of economic theory* 85.2 (1999): 258-293.

[66] Jiau, Ming-Kai, and Shih-Chia Huang. "Self-Organizing Neuroevolution for Solving Carpool Service Problem With Dynamic Capacity to Alternate Matches." *IEEE transactions on neural networks and learning systems* 99 (2018): 1-13.

[67] Jung, Jaeyoung, R. Jayakrishnan, and Ji Young Park. "Dynamic shared-taxi dispatch algorithm with hybrid-simulated annealing." *Computer-Aided Civil and Infrastructure Engineering* 31.4 (2016): 275-291.

[68] Kamar, Ece, and Eric Horvitz. "Collaboration and Shared Plans in the Open World: Studies of Ridesharing." *IJCAI*. Vol. 9. 2009.

[69] Karamanis, Renos, et al. "Assignment and Pricing of Shared Rides in Ride-Sourcing using Combinatorial Double Auctions." *arXiv preprint arXiv:1909.08608* (2019).

[70] Kim, Changmo, et al. "Automated Sequence Selection and Cost Calculation for Maintenance and Rehabilitation in Highway Life-Cycle Cost Analysis (LCCA)." *International Journal of Transportation Science and Technology* 4.1 (2015): 61-75.

[71] Kleiner, Alexander, Bernhard Nebel, and Vittorio Amos Ziparo. "A mechanism for dynamic ride sharing based on parallel auctions." *Twenty-Second International Joint Conference on Artificial Intelligence*. 2011.

[72] Krygsman, Stephan, Martin Dijst, and Theo Arentze. "Multimodal public transport: an analysis of travel time elements and the interconnectivity ratio." *Transport Policy* 11.3 (2004): 265-275.

[73] Kuhr, James, et al. *Ridesharing & Public-Private Partnerships: Current Issues, A Proposed Framework and Benefits*. No. 17-04965. 2017.

[74] Lam, Albert YS. "Combinatorial auction-based pricing for multi-tenant autonomous vehicle public transportation system." *IEEE Transactions on Intelligent Transportation Systems* 17.3 (2016): 859-869.

[75] Lei, Chao, Zhoutong Jiang, and Yanfeng Ouyang. "Path-based dynamic pricing for vehicle allocation in ridesharing systems with fully compliant drivers." *Transportation Research Part B: Methodological* (2019).

[76] Lehmann, Daniel, Liadan Ita Oćallaghan, and Yoav Shoham. "Truth revelation in approximately efficient combinatorial auctions." *Journal of the ACM (JACM)* 49.5 (2002): 577-602.

[77] Lenstra, Jan Karel, and A. H. G. Kan. "Complexity of vehicle routing and scheduling problems." *Networks* 11.2 (1981): 221-227.

[78] Lesh, Matthew Curtis. "Innovative concepts in first-last mile connections to public transportation." *Urban Public Transportation Systems 2013*. 2013. 63-74.

[79] Levinger, Chaya, Noam Hazon, and Amos Azaria. "Fair Sharing: The Shapley Value for Ride-Sharing and Routing Games." *arXiv preprint arXiv:1909.04713* (2019).

[80] Li, Shu, et al. "A Dynamic Pricing Method for Carpooling Service Based on Coalitional Game Analysis." *High Performance Computing and Communications; IEEE 14th International Conference on Smart City; IEEE 2nd International Conference on Data Science and Systems (HPCC/SmartCity/DSS), 2016 IEEE 18th International Conference on*. IEEE, 2016.

[81] Lin, Yu, Zheyong Bian, and Xiang Liu. "Developing a dynamic neighborhood structure for an adaptive hybrid simulated annealing–tabu search algorithm to solve

the symmetrical traveling salesman problem." *Applied Soft Computing* 49 (2016): 937-952.

[82] Liu, Yang, and Yuanyuan Li. "Pricing scheme design of ridesharing program in morning commute problem." *Transportation Research Part C: Emerging Technologies* 79 (2017): 156-177.

[83] Lloret-Batlle, Roger, Neda Masoud, and Daisik Nam. *P2p Ridesharing with Ride-Back on Hov Lanes: Towards a Practical Alternative Mode for Daily Commuting*. No. 17-06253. 2017.

[84] Lu, Wei. *Optimization and Mechanism Design for Ridesharing Services*. No. SWUTC/14/600451-00034-1. 2014.

[85] Lu, Wei, and Luca Quadrifoglio. "Fair cost allocation for ridesharing services–modeling, mathematical programming and an algorithm to find the nucleolus." *Transportation Research Part B: Methodological* 121 (2019): 41-55.

[86] Luo, Peiyu, "A two-stage approach to ridesharing assignment and auction in a crowdsourcing collaborative transportation platform." (2019). *Electronic Theses and Dissertations.* Paper 3240.

[87] Ma, Hongyao, Fei Fang, and David C. Parkes. "Spatio-Temporal Pricing for Ridesharing Platforms." *arXiv preprint arXiv:1801.04015* (2018).

[88] Ma, Shuo, Yu Zheng, and Ouri Wolfson. "T-share: A large-scale dynamic taxi ridesharing service." *Data Engineering (ICDE), 2013 IEEE 29th International Conference on*. IEEE, 2013.

[89] Ma, Tai-Yu. "On-demand dynamic Bi-/multi-modal ride-sharing using optimal passenger-vehicle assignments." *Environment and Electrical Engineering and 2017 IEEE Industrial and Commercial Power Systems Europe (EEEIC/I&CPS Europe), 2017 IEEE International Conference on*. IEEE (2017).

[90] McAfee, R. Preston. "Mechanism design by competing sellers." *Econometrica: Journal of the econometric society*(1993): 1281-1312.

[91] Maskin, Eric S. "Mechanism design: How to implement social goals." *American Economic Review* 98.3 (2008): 567-76.

[92] Masoud, Neda, and Roger Lloret-Batlle. "Increasing Ridership and User Permanence in Ridesharing Systems Using a Novel Peer-to-Peer Exchange Mechanism." *95th Annual Meeting of the Transportation Research Board, Washington, DC*. 2016.

[93] Masoud, Neda, et al. "Promoting Peer-to-Peer Ridesharing Services as Transit System Feeders." *Transportation Research Record: Journal of the Transportation Research Board* 2650 (2017a): 74-83.

[94] Masoud, Neda, Roger Lloret-Batlle, and R. Jayakrishnan. "Using bilateral trading to increase ridership and user permanence in ridesharing systems." *Transportation Research Part E: Logistics and Transportation Review* 102 (2017b): 60-77.

[95] Masoud, Neda, and R. Jayakrishnan. "A real-time algorithm to solve the peer-to-peer ride-matching problem in a flexible ridesharing system." *Transportation Research Part B: Methodological* 106 (2017a): 218-236.

[96] Masoud, Neda, and R. Jayakrishnan. "A decomposition algorithm to solve the multi-hop Peer-to-Peer ride-matching problem." *Transportation Research Part B: Methodological* 99 (2017b): 1-29.

[97] Mishra, Debasis. "An introduction to mechanism design theory." *The Indian Economic Journal* 56.2 (2008): 137-165.

[98] Montemanni, Roberto, et al. "Ant colony system for a dynamic vehicle routing problem." *Journal of Combinatorial Optimization* 10.4 (2005): 327-343.
[99] Mu'Alem, Ahuva, and Noam Nisan. "Truthful approximation mechanisms for restricted combinatorial auctions." *Games and Economic Behavior* 64.2 (2008): 612-631.
[100] Myerson, Roger B. "Incentive compatibility and the bargaining problem." *Econometrica: journal of the Econometric Society* (1979): 61-73.
[101] New York City Taxi, & Limousine Commission http://www.nyc.gov/html/tlc/html/about/trip_record_data.shtml (2018).
[102] Nguyen, Duc Thien. "Fair Cost Sharing Auction Mechanisms in Last Mile Ridesharing." (2013).
[103] Nisan, Noam, et al., eds. *Algorithmic game theory*. Cambridge University Press, 2007.
[104] Nisan, Noam, and Amir Ronen. "Computationally Feasible VCG Mechanisms." *J. Artif. Intell. Res.(JAIR)* 29 (2007): 19-47.
[105] Ozkan, Erhun, and Amy R. Ward. "Dynamic matching for real-time ridesharing." (2016).
[106] Pandit, Vivek Nagraj, et al. "Pricing in Ride Sharing Platforms: Static vs Dynamic Strategies." *2019 11th International Conference on Communication Systems & Networks (COMSNETS)*. IEEE, 2019.
[107] Parkes, David C., Jayant R. Kalagnanam, and Marta Eso. "Achieving budget-balance with Vickrey-based payment schemes in exchanges." (2001). "https://dash.harvard.edu/handle/1/4101693"
[108] Pelzer, Dominik, et al. "A partition-based match making algorithm for dynamic ridesharing." *IEEE Transactions on Intelligent Transportation Systems* 16.5 (2015): 2587-2598.
[109] Peng, Zixuan, et al. "Stable ride-sharing matching for the commuters with payment design." *Transportation* (2018): 1-21.
[110] Qian, Xinwu, and Satish V. Ukkusuri. "Taxi market equilibrium with third-party hailing service." *Transportation Research Part B: Methodological* 100 (2017): 43-63.
[111] Qian, Xinwu, et al. "Optimal assignment and incentive design in the taxi group ride problem." *Transportation Research Part B: Methodological* 103 (2017): 208-226.
[112] Rietveld, Piet. "The accessibility of railway stations: the role of the bicycle in The Netherlands." *Transportation Research Part D: Transport and Environment* 5.1 (2000): 71-75.
[113] Samadi, Pedram, et al. "Advanced demand side management for the future smart grid using mechanism design." *IEEE Transactions on Smart Grid* 3.3 (2012): 1170-1180.
[114] Santos, Douglas O., and Eduardo C. Xavier. "Taxi and ride sharing: A dynamic dial-a-ride problem with money as an incentive." *Expert Systems with Applications* 42.19 (2015): 6728-6737.
[115] Shaheen, Susan, and Nelson Chan. "Mobility and the Sharing Economy: Potential to Facilitate the First-and Last-Mile Public Transit Connections." *Built Environment* 42.4 (2016): 573-588.
[116] Shelton 2016: http://www.govtech.com/transportation/How-Can-Ride-Sharing-Companies-Partner-with-Public-Transit.html

[117] Shen, Wen, Cristina V. Lopes, and Jacob W. Crandall. "An Online Mechanism for Ridesharing in Autonomous Mobility-on-Demand Systems." *arXiv preprint arXiv:1603.02208* (2016).
[118] SMARTRAIL WORLD 2018: https://www.smartrailworld.com/its-not-just-cars-anymore.-uber-adds-public-transport-to-app-with-new-masabi-partnership
[119] Stiglic, Mitja, Niels Agatz, Martin Savelsbergh, and Mirko Gradisar. "Enhancing urban mobility: Integrating ride-sharing and public transit." *Computers & Operations Research* 90 (2018): 12-21.
[120] Taxi calculator 2018: https://www.taxi-calculator.com/taxi-fare-new%20york%20city/259
[121] Vickrey, William. "Counterspeculation, auctions, and competitive sealed tenders." *The Journal of finance* 16.1 (1961): 8-37.
[122] Wang, Fahui, and Yanqing Xu. "Estimating O–D travel time matrix by Google Maps API: implementation, advantages, and implications." *Annals of GIS* 17.4 (2011): 199-209.
[123] Wang, Hai, and Hai Yang. "Ridesourcing systems: A framework and review." *Transportation Research Part B: Methodological* 129 (2019): 122-155.
[124] Wang, Jing-Peng, Xuegang Jeff Ban, and Hai-Jun Huang. "Dynamic ridesharing with variable-ratio charging-compensation scheme for morning commute." *Transportation Research Part B: Methodological* 122 (2019): 390-415.
[125] Wang, Jiquan, et al. "Multi-offspring genetic algorithm and its application to the traveling salesman problem." *Applied Soft Computing* 43 (2016): 415-423.
[126] Wang, Xiaolei, Hai Yang, and Daoli Zhu. "Driver-Rider Cost-Sharing Strategies and Equilibria in a Ridesharing Program." *Transportation Science* (2018).
[127] Wang, Lilong, et al. "A Personalized Taxi Matching Algorithm for Ridesharing." *2018 International Conference on Network Infrastructure and Digital Content (IC-NIDC)*. IEEE, 2018b.
[128] Wang, Xing, Niels Agatz, and Alan Erera. "Stable matching for dynamic ride-sharing systems." *Transportation Science* (2017).
[129] Wang, Yong. "The hybrid genetic algorithm with two local optimization strategies for traveling salesman problem." *Computers & Industrial Engineering* 70 (2014): 124-133.
[130] Witt, Alice, Nicolas Suzor, and Patrik Wikström. "Regulating ride-sharing in the peer economy." *Communication Research and Practice* 1.2 (2015): 174-190.
[131] Xiao, Haohan, Meng Xu, and Ziyou Gao. "Shared parking problem: A novel truthful double auction mechanism approach." *Transportation Research Part B: Methodological*109 (2018): 40-69.
[132] Xu, Su Xiu, and George Q. Huang. "Efficient auctions for distributed transportation procurement." *Transportation Research Part B: Methodological* 65 (2014): 47-64.
[133] Yan, Shangyao, and Chun-Ying Chen. "An optimization model and a solution algorithm for the many-to-many car pooling problem." *Annals of Operations Research* 191.1 (2011): 37-71.
[134] Yang, Hai, Sze Chun Wong, and K. I. Wong. "Demand–supply equilibrium of taxi services in a network under competition and regulation." *Transportation Research Part B: Methodological* 36.9 (2002): 799-819.
[135] Yang, Hai, et al. "Integrated Reward Scheme and Surge Pricing in a Ride-Sourcing

Market." (2018).
[136] Zha, Liteng, Yafeng Yin, and Yuchuan Du. "Surge pricing and labor supply in the ride-sourcing market." *Transportation Research Procedia* 23 (2017): 2-21.
[137] Zhang, Jie, Ding Wen, and Shuai Zeng. "A Discounted Trade Reduction Mechanism for Dynamic Ridesharing Pricing." *IEEE Transactions on Intelligent Transportation Systems* 17.6 (2016): 1586-1595.
[138] Zhang, Wenbo, and Satish V. Ukkusuri. "Optimal fleet size and fare setting in emerging taxi markets with stochastic demand." *Computer-Aided Civil and Infrastructure Engineering* 31.9 (2016): 647-660.
[139] Zhang, Chaoli, et al. "Online Auctions with Dynamic Costs for Ridesharing." *Parallel and Distributed Systems (ICPADS), 2017 IEEE 23rd International Conference on*. IEEE, 2017.
[140] Zhang, Chaoli, Fan Wu, and Xiaohui Bei. "An Efficient Auction with Variable Reserve Prices for Ridesourcing." *Pacific Rim International Conference on Artificial Intelligence*. Springer, Cham, 2018.
[141] Zhang, Chaoli, et al. "Pricing and allocation algorithm designs in dynamic ridesharing system." *Theoretical Computer Science* (2019).
[142] Zhao, Dengji, et al. "Incentives in ridesharing with deficit control." *Proceedings of the 2014 international conference on Autonomous agents and multi-agent systems*. International Foundation for Autonomous Agents and Multiagent Systems, 2014.
[143] Zhao, Dengji, Sarvapali D. Ramchurn, and Nicholas R. Jennings. "Incentive Design for Ridesharing with Uncertainty." *arXiv preprint arXiv:1505.01617* (2015).
[144] Zheng, Libin, Peng Cheng, and Lei Chen. "Auction-based order dispatch and pricing in ridesharing." *2019 IEEE 35th International Conference on Data Engineering (ICDE)*. IEEE, 2019.
[145] Zou, Bo, et al. "A mechanism design based approach to solving parking slot assignment in the information era." *Transportation Research Part B: Methodological* 81 (2015): 631-653.